PHARMACOKINETIC PROPERTIES OF MEPROBAMATE IN THE DOG—AN EXAMPLE OF DOSE-DEPENDENCY IN ELIMINATION KINETICS

by

LEO MARTIS

A dissertation submitted in partial fulfillment
of the requirements for the degree of

DOCTOR OF PHILOSOPHY

UNIVERSITY OF WASHINGTON

1973

Approved by Renett Levy
(Chairman of Supervisory Committee)

Department Pharmaceutical Sciences
(Departmental Faculty sponsoring candidate)

Date 12/6/1973

UNIVERSITY OF WASHINGTON

Date: November 21, 1973

We have carefully read the dissertation entitled Pharmacokinetic Properties of Meprobamate in the Dog - An Example of Dose-Dependency in Elimination Kinetics submitted by Leo Martis in partial fulfillment of the requirements of the degree of Doctor of Philosophy and recommend its acceptance. In support of this recommendation we present the following joint statement of evaluation to be filed with the dissertation.

An investigation of the pharmacokinetics of meprobamate in the dog was conducted. A new analytical method for the determination of meprobamate in plasma and urine is presented. This method is tested and found to be specific and sensitive.

The pharmacokinetic properties of meprobamate in the dog are elucidated. It is found that the drug is extensively metabolized and that it is rapidly and completely absorbed after oral administration of an aqueous solution. A finding of significance is that meprobamate exhibits non-linear (dose-dependent) elimination kinetics. A pharmacokinetic model involving simultaneous first-order and capacity-limited elimination kinetics is proposed and experimentally tested. New mathematical relationships are developed to describe several useful properties of this model under single dose and multiple dosing conditions. Another significant contribution is found in the description of a new method of bioavailability calculations for drugs exhibiting simultaneous first-order and capacity-limited elimination kinetics.

The accomplishment of this work involved the use of gas-liquid chromatography, animal handling procedures and various advanced digital computer techniques.

The investigator demonstrated independent thinking and creativity in the interpretation of experimental results. The thesis is written in a logical and clear fashion.

DISSERTATION READING COMMITTEE: Rene H Levy

Donald P. Zorby

Nathan A. Hall

Doctoral Dissertation

In presenting this dissertation in partial fulfillment of the requirements for the doctoral degree at the University of Washington, I agree that the Library shall make its copies freely available for inspection. I further agree that extensive copying of this dissertation is allowable only for scholarly purposes. Requests for copying or reproduction of this dissertation may be referred to University Microfilms, 300 North Zeeb Road, Ann Arbor, Michigan 48106, to whom the author has granted "the right to reproduce and sell (a) copies of the manuscript in microform and/or (b) printed copies of the manuscript made from microform."

Signature 

Date Dec. 6, 1973

TABLE OF CONTENTS

CHAPTER PAGE

LIST OF FIGURES

LIST OF SCHEMES

LIST OF TABLES

GLOSSARY OF TERMS AND SYMBOLS

Term	Definition
AUC	Area under the plasma concentration-time curve
Compound I	2-methyl-2-ethyl-1, 3-propanediol
Compound II	2-methyl-2-n-propyl-1, 3-propanediol
Compound III	Trimethylsilyl derivatives of I
Compound IV	Trimethylsilyl derivative of II
GLC	Gas-liquid chromatography
I. V.	Intravenous
PCT	Plasma concentration-time

Symbol	
A_e	Amount of drug eliminated upto time t
A_m	Amount of drug metabolized upto time t
A_m^∞	Total amount of drug metabolized
A_t	Amount absorbed from gastro-intestinal tract upto time t
A_u	Amount of drug excreted unchanged upto time t
A_u^∞	Total amount of drug excreted unchanged in urine
a_o, a_1, a_2	Coefficients of a second degree polynomial
C	Concentration of drug in plasma at any time t
C_o	Concentration of drug in plasma at time 0
C_{max}	Maximum effective concentration of the drug in plasma
C_{min}	Minimum effective concentration of the drug in plasma
C^*	Steady-state concentration of the drug in plasma during continuous zero-order infusion

$\bar{C}$	Average concentration of the drug during fixed dose-fixed time schedule
D	Amount of drug in the gastro-intestinal tract
D_o	Dose
F	Fraction (as in fraction of the dose absorbed)
F_t	Fraction remaining to be absorbed from the gastro-intestinal tract upto time t
f	Any function (as in $f(t, \theta)$)
K	Constant of integration
K_a	Absorption rate constant
K_e	First-order rate constant for excretion of unchanged drug
K_m	Michaelis-Menten constant
K_1	Overall apparent first-order rate constant of an elimination process operating in parallel with a capacity-limited process
K_2	A quantity equal to $K_1K_m + V_m$
m_1	Amount of metabolite formed by the capacity-limited process in plasma at time t
m_2	Amount of m_1 that is found in urine at time t
p	Number of parameters
R_o	Infusion rate
$T_{\frac{1}{2}}$	Half-life of elimination
t	time
t'	time to reach the steady-state
t'_f	time to reach a fraction of the steady-state during continuous zero-order I. V. infusion
V	Volume of a one compartment model

V_m	Maximum velocity of Michaelis-Menten raction
X	$R_o/V - K_1K_m - V_m$
θ	Any pharmacokinetic parameter
ϵ	$4 R_o K_1 K_m/V$
τ	Dosing interval

ACKNOWLEDGMENTS

The author wishes to express his sincere gratitude to the following persons:

To René H. Levy, my research advisor for his constant and enthusiastic guidance, encouragement and inspiration throughout the course of the research presented in this dissertation. I am also thankful for our many thought provoking discussions and for his invaluable teachings which have immensely helped me in learning sound approaches and attitudes in scientific research.

To Dr. Nathan A. Hall and Dr. Donald L. Sorby, members of my thesis committee for their many helpful suggestions in preparing this manuscript. To Dr. Nathan A. Hall, I owe a special debt of gratitude for his encouragement and guidance during my early graduate career at the University of Washington.

To Dr. Donald C. Martin, Associate Professor of Biostatistics, for his discussions on the computer programming part of this research.

To Bruce A. Holland and Hardy Cowen for their assistance in animal work.

To my fellow graduate students for their friendship and many helpful discussions.

To Dean Jack E. Orr, Public Health Service and the Rubenstein Memorial Fellowship Fund for generous financial support during my graduate education.

TO MY PARENTS

CHAPTER I

INTRODUCTION

Meprobamate was first synthesized by Ludwig and Piech (1) in 1951 and intoduced for general medical use by Wallace Laboratories in 1955. It is widely used in the treatment of anxiety states and in other conditions in which anxiety and tension are associated with irritability. Because of its ability to produce muscular relaxation, the drug has been successfully employed in the treatment of musculoskeletal disorders. Meprobamate also has been used in certain neurological diseses such as petit mal epilepsy and tetanus (2, 3). The drug, however, is not effective in grand mal seizures (4).

Chemically meprobamate is 2-methyl-2-n-propyl-1, 3-propanediol dicarbamate with the following structural formula:

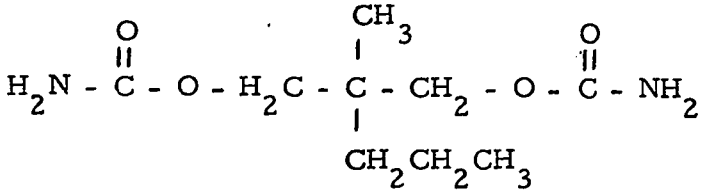

It is a white crystalline powder which melts without decomposition at 104-106° C. Meprobamate is soluble in water to the extent of 0.34 percent at 20° C and 0.79 percent at 37° C, and it is readily soluble in most organic solvents. It is stable in dilute acid and alkali and also in gastric or intestinal juices (5)

I-1 METABOLIC FATE

Early studies by Berger (5) on the fate of meprobamate in rat and man revealed that about 10 percent of an orally administered dose was

excreted unchanged in urine along with several metabolites including a glucuronide conjugate. Agranoff et al. (6) found similar results in man. They also showed that a glucuronide fraction was hydrolyzable with β-glucuronidase, and that the remainder could be split by chemical hydrolysis to give a meprobamate-like substance. Walkenstein (7) reported that about 60 percent of an orally administered dose of meprobamate was excreted by the dog as 2-hydroxymethyl-2-n-propyl-1,3-propanediol dicarbamate. However, a more extensive investigation by Ludwig et al. (8) established that the most abundant metabolite of meprobamate in man and dog was 2-(β-hydroxypropyl)-2-methyl-1,3-propanediol dicarbamate instead of the hydroxymethyl compound reported earlier by Walkenstein. Ludwig et al. (8) also presented evidence to show that the major conjugated metabolite of meprobamate in human urine was a glucosyluronide of unaltered meprobamate. The identity of this conjugate as the N-mono-β-D-glucopyranosiduronic acid of meprobamate has been reported by Tsukamoto et al. (9, 10). Indication for the occurence in the urine of experimental animals of other metabolic products such as an ether type glucuronide of hydroxy-meprobamate, the keto and carboxylic derivatives of meprobamate has been presented by Wiser and Siefter (11) and Yamamoto et al. (12, 13). Figure 3 in Chapter III (p. 27) lists all known metabolites of meprobamate in various species.

I-2 DRUG INTERACTIONS

A number of reports have appeared in the literature presenting evidence that the metabolism of meprobamate is altered by pretreatment with certain chemical compounds and by meprobamate itself. Conney and Burnes (14) first demonstrated that the administration of a number of drugs including phenobarbital barbital, phenylbutazone and aminopyrine shortened the duration of action of meprobamate in animals, and Kato (15) observed a similar effect due to chloropromazine. Rubin et al. (16) found that simultaneous administration of ethanol and meprobamate to humans resulted in a higher value for the elimination half-life of meprobamate. They proposed that there was inhibition of meprobamate metabolism by ethanol. Phillips et al. (17) observed that brain and blood concentrations of C^{14}-labeled meprobamate decreased at a more rapid rate in animals made tolerant by pretreatment with meprobamate for 35 days than in non-tolerant rats. Douglas et al. (18) in an investigation of the urinary excretion ratios of meprobamate and hydroxy-meprobamate found that human subjects receiving small doses of the drug over a period of at least 30 days excreted significantly larger proportion of hydroxy-meprobamate than did the subjects taking a single dose of the drug. The shift observed in the ratio of meprobamate urinary excretion products may be due to self induction of the hydroxylation reaction by meprobamate.

I-3 PHARMACOKINETICS

Inspite of the widespread use of meprobamate as a transquillizing agent and as a muscle relaxant, little attention has been paid to its pharmacokinetics. The first investigation on the pharmacokinetic properties of the drug was that of Walkenstein (7) who reported that meprobamate is absorbed rapidly from the gastro-intestinal tract of dogs, rats and humans. Heyman et al. (19) examined the effect of formulation variables on the absorption of meprobamate in humans and reported irregular absorption with large inter-subject variability. Extensive studies on the distribution of meprobamate were made by Van der Kleijn (20). Using whole-body autoradiographic study, it was found that shortly after either intravenous and/or oral administration of meprobamate-^{14}C to mice, the brain, thymus and body fat showed lower concentrations of radioactivity than the blood, lungs and skeletal muscles, while the myocardium, liver, hypophysis, and adrenal cortex showed a higher concentration. A slow penetration of meprobamate into the central nervous system was observed with maximum concentration of radioactivity occurring 10-15 min. after intravenous administration.

Hoffman and Ludwig (21) measured plasma levels of meprobamate in humans and reported that peak concentrations occur 1-2 hr. after oral administration of the drug. They estimated an elimination half-life of approximately 10 hr. from the post-absorptive phase of the plasma concentration-time curves. Hollister and Levy (22) measured the elimination

half-life of meprobamate in 12 healthy human volunteers after the oral administration of the drug and found the values ranging from 6.4 to 16.6 hr., indicating inter-subject variability in meprobamate elimination. In the same study, the authors reported that in two subjects who had received large doses for prolonged period of time, the drug exhibited considerably longer half-lives (24 and 48 hr.). To account for these differences, the authors suggested the possibility of dose-dependency in the kinetics of meprobamate elimination.

A review of the literature reveals that many pharmacokinetic properties of meprobamate such as volume of distribution, bioavailability, absorption rate constant, accumulation characteristics, etc. have not been elucidated in humans or in any other animal species.

I-4 THE PRESENT STUDY: PURPOSE AND APPROACH TO THE INVESTIGATION

4-a Purpose of the Investigation

The purpose of the present investigation is to study the pharmacokinetic properties of meprobamate with special emphasis on the dose-dependent aspects of its elimination. The need to know pharmacokinetic properties of meprobamate is of critical important for several reasons:

(a) the drug is used extensively as a tranquillizing agent and as a muscle relaxant

(b) it is administered in large doses (daily doses up to 6.4 gm.) (23)

(c) it can be easily abused because of its addictive properties (several hundred cases of suicidal attempts have been reported) (24-26) and

(d) it is extensively metabolized which increases the possibility of saturation of metabolizing enzyme systems.

Several drugs including alcohol, salicylate, diphenylhydantoin, amobarbital, sulfanilamide, phenylbutazone, etc. have been shown to exhibit dose-dependency in elimination kinetics. In spite of this large amount of experimental data, no detailed theory has been developed to relate various pharmacokinetic parameters and dose. Also, no method is presently available to enable bioavailability and/or dosage regimen calculations in such cases. Hence, if meprobamate exhibits dose-dependent kinetics a particular attempt will be made to develop theoretical approaches to the kinetic analysis of plasma concentration-time data of drugs showing non-linearity in elimination kinetics.

4-b Approach to the Investigation

(i) Quantitative Determination of Meprobamate in Biological Fluids: The first requirement in the pharmacokinetic analysis of a drug is to have an analytical procedure for the quantitative determination of the drug in biological fluids. Several methods for the determination of meprobamate have been reported in the literature. However, these methods lack the specificity and/or sensitivity needed for pharmacokinetic studies. Hence,

one of the initial goals in the present investigation is to develop an analytical method for the quantitative determination of the drug in biological fluids.

(ii) Animal Species: Dogs are used as the experimental subjects for the following reasons:

(a) Development of a complete pharmacokinetic profile for any drug requires that it can be administered both orally and intravenously across a wide range of doses. Meprobamate cannot be administered intravenously to humans due to the toxicity of the vehicle required to solubilize the drug.

(b) Administration of large quantities of meprobamate to humans to study the phenomenon of dose-dependency in elimination kinetics may produce toxicity and hence is not practical.

(c) Meprobamate is extensively metabolized (about 90 percent) in dogs as it is in humans.

(iii) Experimental Design: Four dogs are used to study the kinetics of absorption, distribution and elimination of meprobamate. The experimental design for single-dose studies includes administration of the drug both orally and intravenously at the doses of: 7, 10, 30 and 50 mg./kg. The protocol includes blood and urine collections at predetermined time intervals. Multiple dose studies are also planned.

CHAPTER II

EXPERIMENTAL

II - 1 MATERIALS

The following reagents were used: stock solutions of meprobamate[1] containing 5, 10, 15, 25 mcg./100μ l. and stock solution of internal standard (2-methyl-2-ethyl-1, 3-propanediol[2](I)) containing 75 mcg./ml. in water; sodium acetate buffer at pH 5.0 (sodium acetate 7.6 gm; glacial acetic acid 1.3 ml.; water q. s. 250 ml.); phosphate buffer at pH 7.2 (0.25 M K_2HPo_4); β-glucuronidase;[3] N, O-bis-(trimethylsilyl)-acetamide;[4] reagent grade anhydrous ether.

A commercially available[5] 8% $\frac{W}{V}$ solution of meprobamate (solvent—polyethylene glycol-400 65%; benzyl alcohol 2%; water 33%) was used for intravenous dosing to dogs. Appropriate doses for oral administration were prepared extemporaneously as solutions by wetting the appropriate amount of meprobamate (powder) with a few drops of ethanol and then dissolving it in approximately 80 ml. of warm water.

---

[1]Wyeth Laboratories, Inc., Philadelphia, Pa.

[2]K & K Laboratories, Inc., Hollywood, California.

[3]Calbiochem., Los Angeles, California.

[4]TRI-SIL/BSA, Pierce Chemical Co., Rockford, Ill.

[5]Intramuscular Miltown, Wallace Pharmaceuticals, Cranbury, N. J.

II - 2 INSTRUMENTATION

A Varian Model 1400 gas chromatograph[6] equipped with a hydrogen flame-ionization detector, a Varian A-25 recorder[7] and a glass column 5' X $\frac{1}{4}$" packed with 3% SE-30 on 80 to 100 mesh chromsorb W[6] was employed. A Finnigan Gas Chromatograph Peak Identifier[8] coupled to a visicorder[9] was used for the purpose of peak identification by mass spectroscopy.

II - 3 GLC OPERATING CONDITIONS

The following temperatures were used: column, 115°; injector, 175°; and detector, 175°. The gas flow rates were: carrier gas (helium), 50 ml./min., hydrogen, 30 ml./min., and air, 300 ml./min.

II - 4 SELECTION OF ANIMALS AND EXPERIMENTAL DESIGN

The animals used in this study were four healthy male mongrel dogs weighing about 10 kg. Table I gives the treatment plan. Four I. V. and four oral doses were selected and the assignment of treatments were made in a random fashion. At least one week was allowed between

---

[6]Varian Aerograph, Walnut Creek, California.

[7]Varian A-25, Walnut Creek, California.

[8]Finnigan Corporation, Sunnyvale, California.

[9]Honeywell, Denver, Colorado.

TABLE I

Treatment Schedule

Week No.	Dog # 510	970	1065	1122
1	7mg./Kg. -I. V.	10mg./Kg. -I. V.	10mg./KG. -oral	7mg./Kg. -I. V.
2	7mg./Kg. -oral	7mg./Kg. -I. V.	10mg./Kg. -I. V.	30mg./Kg. -I. V.
3	50mg./Kg. -I. V.	30mg./Kg. -oral	7mg./Kg. -I. V.	50mg./Kg. -I. V.
4	30mg./Kg. -oral	30mg./Kg. -I. V.	7mg./Kg. -oral	10mg./Kg. -I. V.
5	10mg./Kg. -I. V.	10mg./Kg. -oral	30mg./Kg. -I. V.	10mg./Kg. -oral
6	10mg./Kg. -oral	50mg./Kg. -oral	30mg./Kg. -oral	30mg./Kg. -oral
7	30mg./Kg. -oral	7mg./Kg. -oral	50mg./Kg. -I. V.	50mg./Kg. -oral
8	50mg./Kg. -oral	50mg./Kg. -I. V.	50mg./Kg. -oral	7mg./Kg. -oral

treatments so that the second treatment would not be affected by the first. Dogs were fasted for 20 hr. before drug administration.

II - 5 METHODS OF DRUG ADMINISTRATION

Intravenous administration of meprobamate was performed by injecting a bolus of the drug solution into the cephalic vein using a plastic syringe fitted with a 22 gauge 1 inch needle.[10] The doses used were 7, 10, 30 and 50 mg./kg. and the drug was injected over a period of 2-3 min. The concentration of meprobamate in the solution used for I. V. administration was 8% (W/V).

Oral administration of meprobamate was accomplished by introducing the drug solution directly into the stomach through a stomach tube. The tube was then rinsed with approximately 25 ml. of water, and the rinsings were also introduced into the stomach. The doses selected were the same as those used for I. V. dosing (7, 10, 30 and 50 mg./kg.).

II - 6 SAMPLE COLLECTION

Blood samples (2. 5 ml.) were obtained at predetermined time intervals from the cephalic vein (not used for dosing) with a 3 ml. plastic syringe fitted with a 23 gauge hypodermic needle.[10] Each sample was immediately transferred to a 5 ml. heparin-treated vacutainer tube,

---

[10] Becton, Dickinson and Company, Rutherford, N. J.

mixed and centrifuged at 2000 r. p. m. for 20 min. The plasma was then harvested and frozen until assayed.

Immediately following injection of the drug, the dogs were placed in metabolism cages to enable collection of urine for a 36 hr. period. Urine samples were also frozen until assayed.

11 - 7 QUANTITATION OF MEPROBAMATE IN BIOLOGICAL FLUIDS

7-a Plasma Standards

To 1 ml. of plasma were added 100 µ l. of aqueous meprobamate solution and 5 ml. of ether. The contents were shaken for 1 min. on the vortex mixer and centrifuged at 2000 r. p. m. for 5 min. Exactly 4 ml. of the organic layer was pipetted into a clean tube. The ether was evaporated at 40°, and 100 µl. of stock solution of internal standard and 1 ml. of 50% KOH were added to the dry tubes. The tubes were heated at 100° for 10 min. and were then cooled under running water. Three ml. of ether was added and the contents shaken for 1 min. on the vortex mixer, followed by centrifuging at 2000 r. p. m. for 5 min. About 2. 9 ml. of ether layer was transferred to a 12 ml. glass-stoppered centrifuge tube. The ether was evaporated at 40° and the residue was allowed to react with 25 µl. of silylating reagent for 10 min. at 60°. Approximately 1-2 µl. was injected into the gas chromatograph.

7-b Urine Standards

To 1 ml. of urine, were added 100 μ l. of aqueous meprobamate solution, 1 ml. of K_2HPO_4 buffer and 5 ml. of ether. The drug was extracted with ether and the remaining steps were the same as described above under plasma standards.

7-c Biological Samples from Drug-treated Dogs

Appropriate aliquots of dogs' plasma or urine samples were pipetted into 15 ml. tubes. The quantitative analysis of the samples was conducted as described under their respective standards except for the addition of meprobamate stock solution. Scheme 1, outlines the complete procedure for quantitative determination of meprobamate in plasma and urine.

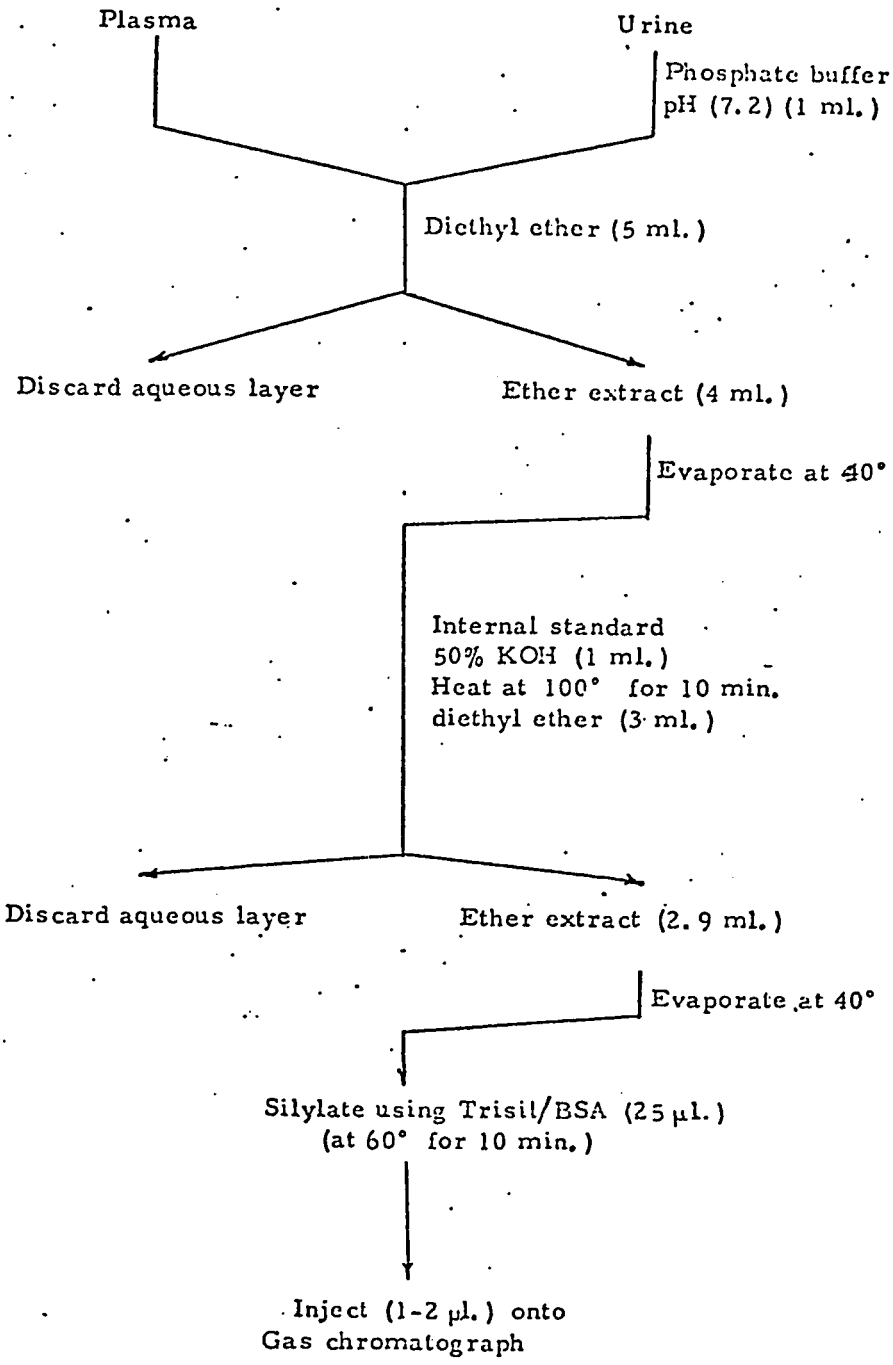

Scheme 1: Schematic Diagram for the Analysis of Meprobamate in Plasma and Urine.

CHAPTER III

RESULTS AND DISCUSSION

III - 1 GLC ASSAY FOR MEPROBAMATE IN PLASMA AND URINE

1-a Introduction

A variety of methods have been reported for the determination of meprobamate and most of them are either spectrophotometric (6, 21, 27-32) or gas-liquid chromatography (GLC) procedures (33-44). Many of the colorimetric methods seem adequate for the determination of the drug in dissolution studies but they lack sensitivity and specificity when applied to biological fluids. Agranoff, et al. (6) determined the amount of meprobamate by measuring the color resulting from the treatment of an extract of urine with H_2SO_4. Bedson (28) adapted this method to measure the concentration of meprobamate in blood. However, quantitation at therapeutic concentrations would be difficult using this method since the lowest measurable concentration shown in the calibration curves is 30 mcg./ml. Furthermore, the method is not specific because compounds related to meprobamate, such as 2-methyl-2-n-propyl-1, 3-propanediol (II) and 2-methyl-2-n-propyl-3-hydroxypropyl carbamate also react with sulfuric acid and thus interfere (6). Hoffman and Ludwig (21) described a colorimetric procedure based on the color which is formed by treatment of meprobamate with p-dimethyl-amino benzaldehyde and antimony trichloride in acetic anhydride. Several investigators have used this method with success for the determination of meprobamate in plasma samples (16, 22). However, when applied to urine samples, the method is not specific since a major metabolite of meprobamate, namely

2-methyl-2-(2-hydroxypropyl)-1,3-propanedial dicarbamate would interfere with measurement of color.

L-b Direct GLC of Meprobamate

Although colorimetric methods can be simple, rapid and sensitive, they are not always specific due to interference by compounds with cognate absorption characteristics. In such instances, interfering compounds may be separated by using procedures such as thin layer chromatography or solvent partition. These separation procedures can sometimes be tedious and lengthy, in which case the method becomes inconvenient for routine analysis of biological samples. Hence, GLC procedures have become more popular for the quantitative analysis of drugs in biological fluids. Several reports can be found (33-37, 39) where direct GLC has been used for the measurement of meprobamate levels in biological fluids. However, numerous reports (34, 35,39-41, 43, 45) have appeared in the literature documenting the variable decomposition of the drug during direct GLC. Consequently, before attempting to use direct GLC for the determination of meprobamate in biological fluids, it was decided to examine the approach of direct GLC for quantitation of meprobamate in an aqueous medium.

USP XVIII(46) had specified a GLC procedure for the determination of the meprobamate in dissolution medium, therefore it was decided to use the USP method to quantitate the drug in water. The USP recommendation read, ". . . . the amount in solution being determined by means

of gas chromatography, the internal standard consisting of a solution of dibutyl phthalate in anhydrous ether containing 0.4 mg. per ml." but it did not specify any GLC operating conditions. Since the USP's GLC procedure is very similar to that proposed by Douglas et al. (37) in that both utilize direct GLC of meprobamate as well as quantitation with dibutyl phthalate as an internal standard, it appeared reasonable to use the conditions of Douglas et al (37): glass column (3.8% UC-W 98 methyl silicone on 80 to 100 mesh Diataport S[6]) at 180°, injection port at 275°. A typical chromatogram (Figure 1) shows three peaks, A, B, and C were peak C corresponds to the internal standard. From the preliminary studies done on the effect of the injection port temperature on meprobamate breakdown, it became apparent that peaks B and A correspond respectively to unchanged meprobamate and a decomposition product. It consistently was found that a decrease in injection port temperature was accompanied by a concommitant increase in B/A peak height ratios (PHR's). Further investigation of this phenomenon showed that the B/A PHR is dependent on the injection rate, the slower injections always yielding larger ratios. As an example, a rapid (1 sec.) followed by a slow (3 sec.) injection of an ether extract of a 50 μg./ml. aqueous solution gave a B/A PHR's of 0.609 and 0.257, respectively. As pointed out also by Holch and Gjaldbaek (39), these results suggest that reaction with the injection needle plays an important role in the observed decomposition. As seen in Figure 1, the decomposition product has a very short retention time (50-60 sec.) relative to the internal standard

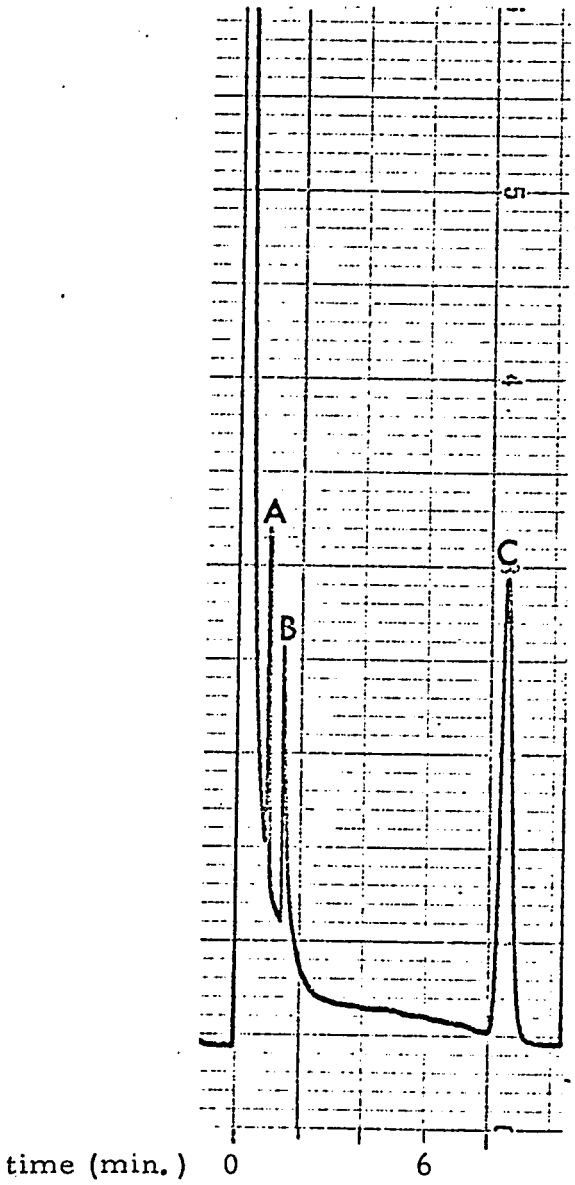

Figure 1. Chromatogram of meprobamate (50μg.) after injection of an ether extract. Peak A = decomposition product, Peak B = meprobamate, Peak C = dibutyl phthalate.

(6 min.). Thus under different GLC conditions such as higher column temperature and/or a larger solvent front, peak A can merge with the solvent peak and decomposition can be overlooked.

Several attempts to establish a suitable calibration curve proved unsuccessful. Table II shows the B/A and B/C PHR's obtained with various amounts of meprobamate, after repeated injections of the ether

TABLE II

Determination of Meprobamate by Direct GLC: B/A (meprobamate/decomposition product) and B/C (meprobamate/internal standard) Peak Height Ratios at Various Amounts of Meprobamate

Amount of Meprobamate (μg)	Number of Injections	B/A PHR (Mean ± SD)	B/C PHR (Mean ± SD)
50	7	0.771 ± 0.203(26.33)[a]	0.544 ± 0.149(27.4)[a]
100	7	1.226 ± 0.249(20.30)[a]	1.067 ± 0.219(20.5)[a]
200	7	2.755 ± 0.573(20.8)[a]	2.522 ± 0.356(14.1)[a]
400	7	6.121 ± 1.172(19.1)[a]	5.885 ± 0.622(10.6)[a]

[a]Corresponding coefficient of variation in per cent.

extracts (care was taken to maintain the injection rate as constant as possible). A plot of B/C PHR's versus drug amount is not linear but parabolic. Furthermore, the coefficients of variation on repeated injections at each concentrations ranged from 10.6% to 27.4%. Although the coefficients of variation decreased at the higher concentrations, they are still too high to allow an accurate determination of meprobamate.

The thermal decomposition of meprobamate at the injection port has been extensively documented in the past eight years (35, 36, 40, 41, 45).

Goldbaum and Domanski (34) found a marked increase in the meprobamate breakdown product peak when injection port temperature was raised from 250° to 320° (5% SE-30 on Gas Chrom. Q). Finkle (35) reported that the meprobamate breakdown product peak becomes significant at temperatures greater than 230° (2.5% SE-30 on chromosorb G). Cardini et al. (45) stated that due to decomposition they were not able to use their GLC method for quantitative analysis. Interestingly enough the first supplement to USP XVIII (47) has revised the analytical procedure in dissolution studies of meprobamate. The present method for quantitation of meprobamate in dissolution medium is a colorimetric procedure.

1-c Determination of Meprobamate Using Hydrolysis Followed by Silylation of the Hydrolysis Product

Holch and Gjaldbaek (39) found that the main breakdown products of meprobamate during GLC analysis are 2-methyl-2-propyl-1,3-propanediol (II) and 2-methyl-2-propyl-1,3-propanediol monocarbamate. Hence, the decomposition of meprobamate can be overcome if it is converted to II before injecting into the gas chromatograph. However, II is a very polar compound and when chromatographed directly, variable losses occur due to adsorption to the solid support. This was found in several glass columns packed with 3.8% UC-98 on chrom W, 5% UCW-98 on chrom W, 3% Carbowax on chrom W and 3% SE-30 on chrom W. In every case, the coefficient of variation on repeated injections (five) of the same sample varied from 5 to 8%. The method proposed by Skinner

(40) involved direct hydrolysis of meprobamate without extraction of unchanged drug from the biological sample. Therefore, any metabolite of meprobamate which, upon hydrolysis (as discussed later), gives II, would interfere with the assay. The hydrolysis approach was also used by Cerri (41), but his studies were limited to determination of meprobamate in water at relatively high concentrations.

The principle of the method selected for this research is shown in Scheme 2. This procedure involves extraction of the unchanged drug from the biological fluid, alkaline hydrolysis to give II followed by silylation of II with N, O-bis (trimethylsilyl) acetamide; I is added directly to the sample prior to the hydrolysis. After hydrolysis, ether extraction, and evaporation, the residue is allowed to react with N, O-bis (trimethylsilyl) acetamide whereby I and II are converted to the corresponding trimethylsilyl ethers, III and IV. The latter yield symmetrical peaks as shown in Figure 2, where peak A corresponds to III and peak B corresponds to IV. Peaks C, D and E are foreign peaks which are probably due to traces of moisture present in the sample. The height of the foreign peaks is time dependent. When the samples are allowed to stand at room temperature for 3-5 hr. after the addition of silylating reagent, peaks C and D decrease and finally disappear without any measurable change in PHR of IV to III.

(i) Specificity of the Method: Since the proposed method involves the formation of derivatives of meprobamate and the internal standard (in order to overcome problems associated with direct GLC), it is

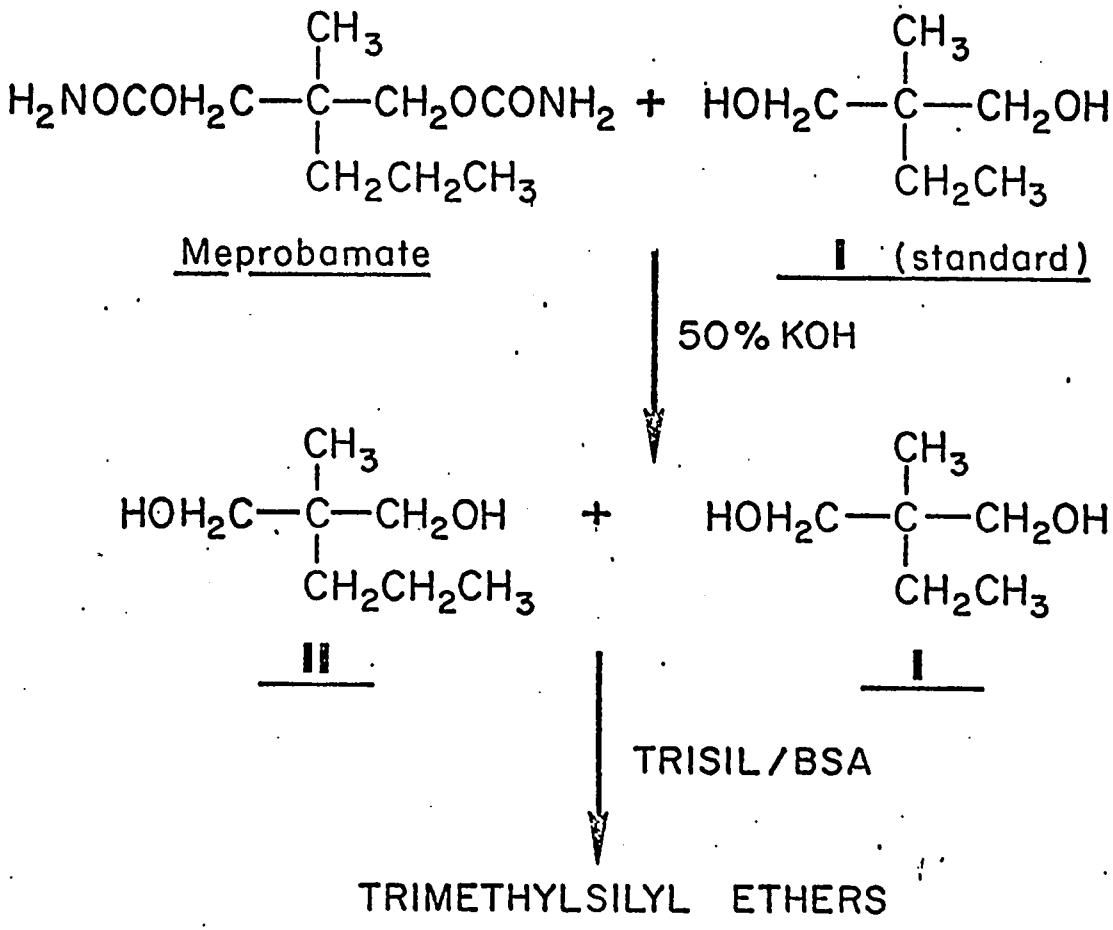

Scheme 2 Hydrolysis and silylation of Meprobamate

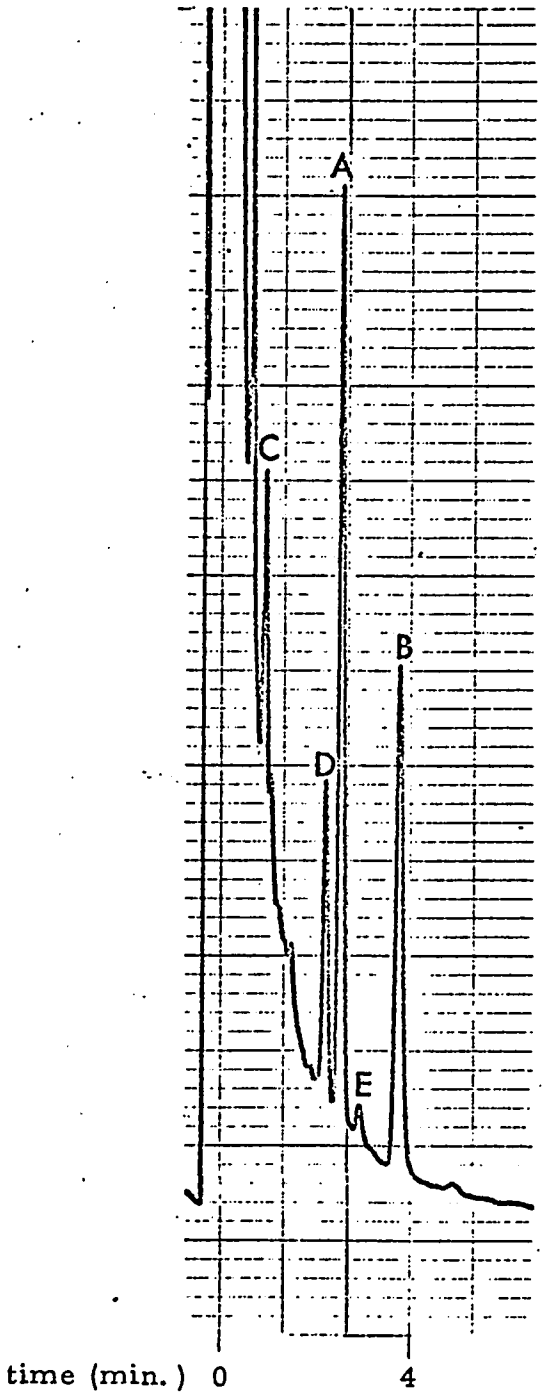

Figure 2. Chromatogram of a plasma sample (containing 6.5 μg. of meprobamate) obtained after I. V. administration of 30 mg./kg. of meprobamate to a dog. Key: Peak A, due to internal standard; Peak B, due to meprobamate; C, D and E are foreign peaks.

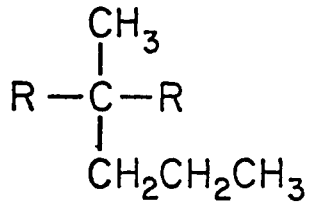

Meprobamate (R, D, H)

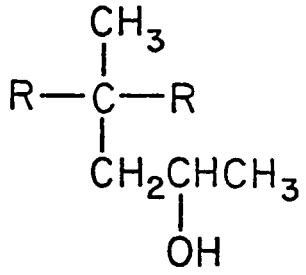

Hydroxy-meprobamate (R, D, H)

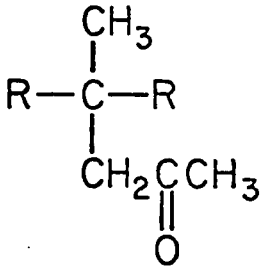

Keto-meprobamate (R)

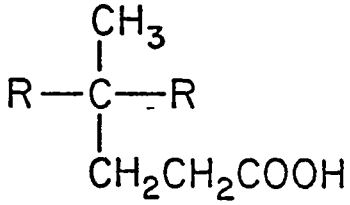

Carboxy-meprobamate (R)

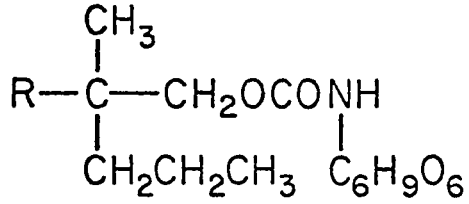

N-glucuronide of meprobamate (R, D, H)

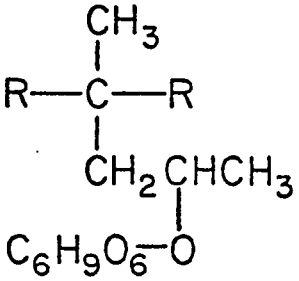

Ether-type o-glucuronide (R, D)

R = rabbit
D = dog
H = human

$R = -CH_2OCONH_2$

Figure 3. STRUCTURE OF MEPROBAMATE AND ITS KNOWN METABOLITES

necessary to test for the specificity of the method. In the present method, any metabolite of meprobamate which undergoes a change in the carbamate moiety without any change in the rest of the molecule can interfere with the assay. Figure 3 lists the known metabolites of meprobamate in dog, rabbit (13, 48) and man (8, 18). Out of these, only the N-glucuronide of meprobamate can yield II upon alkaline hydrolysis and thus interfere with the determination of unchanged drug in biological samples. It is necessary therefore, to introduce an ether extraction step before alkaline hydrolysis in order to remove meprobamate, leaving the N-glucuronide of meprobamate in the aqueous phase.

To test the specificity of the ether-extraction step, the following experiment was performed: an oral dose of 800 mg. of meprobamate dissolved in water was administered to a male volunteer and eight venous blood samples were collected at predetermined intervals which extended for 8 hr. The plasma fraction was harvested from each sample. Each of the eight plasma samples was divided into three one-milliliter portions, thus yielding three identical lots of samples A, B and C. In order to test whether II was present as a metabolite in drug-treated man, the plasma samples of lot A were extracted with ether and the residue obtained after evaporation of ether was allowed to react with silylating reagent. It was found that neither II nor I were present in vivo. The plasma samples of lot B were assayed as described under Plasma Standards, except for the addition of meprobamate stock solution and the initial ether extraction step. The plasma samples of lot C were analyzed as described under

Biological Samples from Drug-treated Dogs, where the initial ether extraction step is included. It was found that plasma samples collected later than 60 min. after drug administration yielded generally higher values from the samples of lot B than from those of lot C, Table III.

TABLE III

Plasma Levels of Meprobamate in a Human Subject Following an Oral Dose of 800 mg. (Solution)

Time (hr.)	Concentration of meprobamate in plasma (μg./ml.)	
	Hydrolysis before ether extraction	Hydrolysis after ether extraction
0.5	12.487	12.480
1.0	15.297	15.369
1.5	13.462	12.705
2.0	13.971	12.666
3.0	13.294	11.086
4.0	10.158	9.836
6.0	10.792	8.197
8.0	9.085	6.497

These results suggest that the N-glucuronide of meprobamate at least in part is not extracted by ether and that it could interfere with the determination of unchanged drug if selective separation were not achieved.

In order to test whether any N-glucuronide at all was extracted into ether, the following experiment was performed: an oral dose of 800 mg. of meprobamate was administered to a male subject and urine was collected over a 48 hr. period. The hydrolysis of the N-glucuronide of meprobamate in urine sample was carried out with β-glucuronidase as follows (49): 1 ml. of urine whose pH had been adjusted to 5 by the addition of H_2SO_4 was transferred to a 15 ml. pyrex test tube fitted

with a teflon-lined screw cap. To this 0.1 ml. of sodium acetate buffer (pH 5) and 300 Fishman Units of β-glucuronidase were added. The mixture was incubated at 37° for 11 days. Control urine samples which did not contain β-glucuronidase were also run. It can be seen in Table IV that maximum hydrolysis occurred between the third and the fifth day. A

TABLE IV

Enzymatic Hydrolysis of N-glucuronide of Meprobamate

Days	Mean PHR's of Samples containing β-glucuronidase (2 determinations)	Mean PHR's of Control Samples (2 determinations)
0	--	0.763
1	1.114	0.780
3	1.295	0.788
5	1.551	0.822
7	1.568	1.136
9	1.560	1.027
11	1.535	1.317

slight increase in PHR's of control samples was probably due to slow hydrolysis of N-glucuronide of meprobamate at the incubation temperature. β-glucuronidase was allowed to react for 5 days on 4 samples of evaporated ether extracts of urine which were then carried through the assay. Controls which did not contain β-glucunonidase were also run through this procedure. PHR's obtained for samples and controls were compared using a paired t-test and found to be not significantly different at $P = 0.05$. The same experiment was repeated using $CHCl_3 + CCl_4$. It was found that this mixture did not extract any N-glucuronide of meprobamate. However, as seen in Table V,

ether extracted about 30% more meprobamate than a mixture of $CHCl_3 + CCl_4$.

TABLE V

Specificity of Separation Procedure

Extraction solvent	Amount of β-glucuronidase	Mean PHR $\frac{IV}{III}$ (4 determinations)
Ether	300 units	0.749
Ether	--	0.746
$CHCl_3 + CCl_4$	300 units	0.580
$CHCl_3 + CCl_4$	--	0.576

(ii) Mass Spectra of Trimethylsilyl Derivative of II: Although the above experiments demonstrated that the N-glucuronide of meprobamate does not interfere with the assay, it is still possible that an unknown metabolite could yield a peak having identical retention characteristics as those of IV. In order to test for this possibility, the trimethylsilyl derivative of II prepared from an aliquot of the 48 hour-urine sample obtained from a human subject (after oral administration of 800 mg. of meprobamate) and the one prepared from pure meprobamate were analyzed by a combination of GLC-Mass spectroscopy. It was found that the mass spectra of IV obtained from the urine sample and the one resulting from reacting pure meprobamate were identical. Thus, it could be concluded that peak B corresponds only to meprobamate and that there was no interference from any other metabolite.

(iii) Formation of Trimethylsilyl Derivatives of I and II: In order to eliminate errors due to possible losses in preparation of the sample or to inaccurate injection, a known amount of an internal standard was added to the sample. Physico-chemical properties of compounds to be used for this purpose should closely resemble the drug to be measured. Also, the compound chosen to be the internal standard should not occur spontaneously in the sample. The internal standard selected in the present method was a compound which differs from II by a methylene group. The internal standard was added to the sample before hydrolysis of the drug and it was carried through the steps of ether extraction and silylation. The peak due to the trimethylsilyl derivative of this internal standard III, was symmetrical, well resolved, and had a retention time close to that of IV. Formation of trimethylsilyl derivatives of I and II was required to overcome adsorption of these compounds on the column. Table VI gives PHR's of IV to III as a function of time following the addition of

TABLE VI

Formation of Trimethylsilyl Derivatives of I and II at 25° and 60°

Minutes after addition of Silylating Reagent	IV/III Peak Height Ratio Amount of Meprobamate		
	10 mcg. (25°)	10 mcg. (60°)	20 mcg. (60°)
5	0.791	1.00	1.810
10	0.894	1.038	1.997
20	0.993	1.040	2.031
45	1.001	1.040	2.030
120	1.003	1.037	2.020

silylating reagent at two temperatures and at two different meprobamate concentrations. The PHR reached the maximum value within 10 min. at 60° and remained constant for at least 15 hr. when the samples were kept in the refrigerator. Under the operating conditions of the present method, III and IV were found to be stable.

(iv) Accuracy and Presicion: PHR's were calculated by dividing the height of the peak due to meprobamate (IV) by the height of the peak due to the internal standard (III). Calibration curves were constructed from "spiked" plasma and urine samples by plotting the concentration of meprobamate against the PHR. A typical calibration curve obtained from "spiked" plasma samples is shown in Figure 4. Table VII gives PHR's of IV to III for various amounts of meprobamate in urine. In

TABLE VII

Determination of Meprobamate: Peak Height Ratios of IV to III at Five Different Amounts of Meprobamate in Urine

Amount of Meprobamate, mcg.	Number of Determinations	IV/III Peak Height Ratio Mean ± Standard Deviation
5	6	0.872 ± 0.0133 (1.5)[a]
10	2	1.836
15	6	2.535 ± 0.0237 (0.9)[a]
20	2	3.337
25	6	4.243 ± 0.0986 (2.3)[a]

[a]Corresponding coefficient of variation in percent.

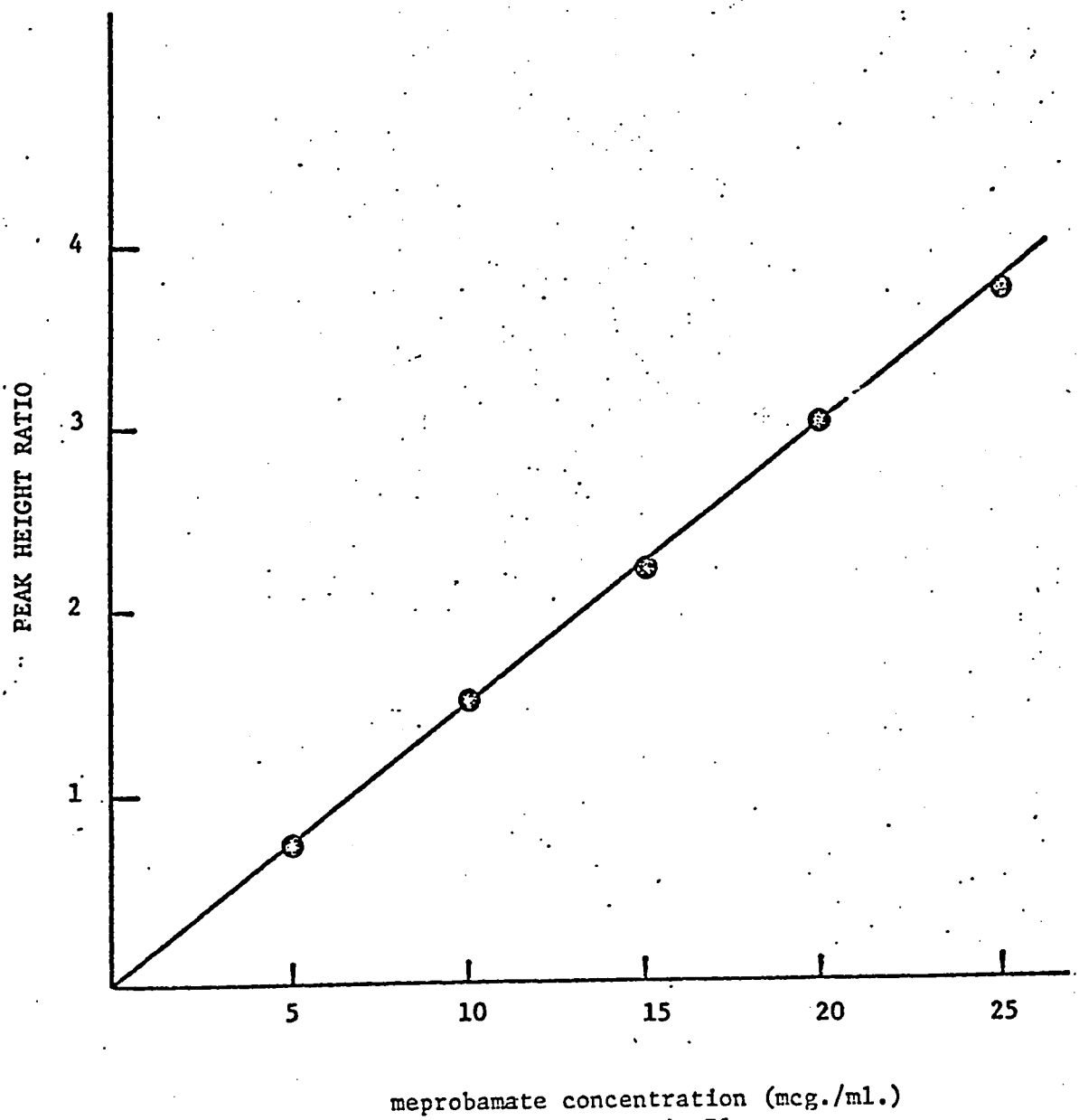

Figure 4 Calibration curve for meprobamate in Plasma.

both the instances, a plot of the data (PHR versus amount of meprobamate) yielded a straight line passing through the origin with correlation coefficients of 0.999 and 0.998 for plasma and urine respectively. The small coefficients of variation indicated that the reproducibility of the method was adequate. The amount of drug in the biological samples from a drug-treated animal could be read from the calibration curve constructed simultaneously (which took care of slight day to day variations of the slope of the calibration curve) with the sample to be assayed.

III - 2 PHARMACOKINETIC STUDY OF MEPROBAMATE IN DOGS

2-a I. V. Bolus Administration

(i) Plasma Concentration—Time Data: A significant amount of information regarding the distribution and elimination of a drug can be gained from a plasma concentration—time (PCT) curve obtained after I. V. bolus administration. Single dose I. V. studies are essential for an accurate estimation of the volume of distribution obtained by extrapolating the linear portion of the semilogarithmic plot of PCT data to zero time and the elimination half-life of a drug. However, for establishing the validity of distribution and elimination parameters at more than one dose level, the single dose I. V. studies should be performed at several dose levels.

Figures 5 through 8 show the semilogarithmic plots of PCT data obtained after I. V. bolus administration of 7, 10, 30 and 50 mg./kg.

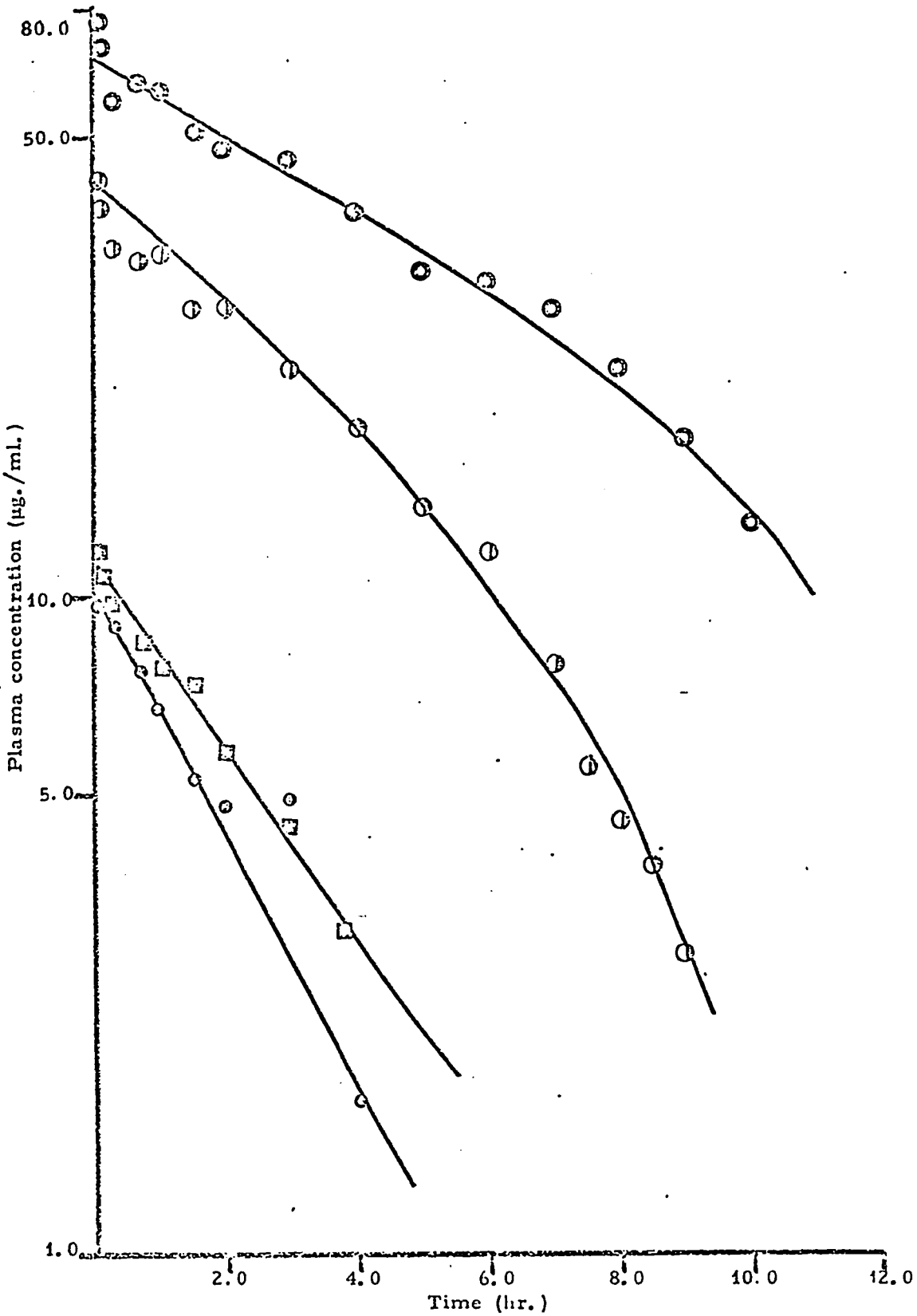

Figure 5. Semilogarithmic plots of PCT data obtained after I. V. administration of 7 (○), 10 (□), 30 (◑) and 50 (◎) mg./kg. of meprobamate to dog # 510.

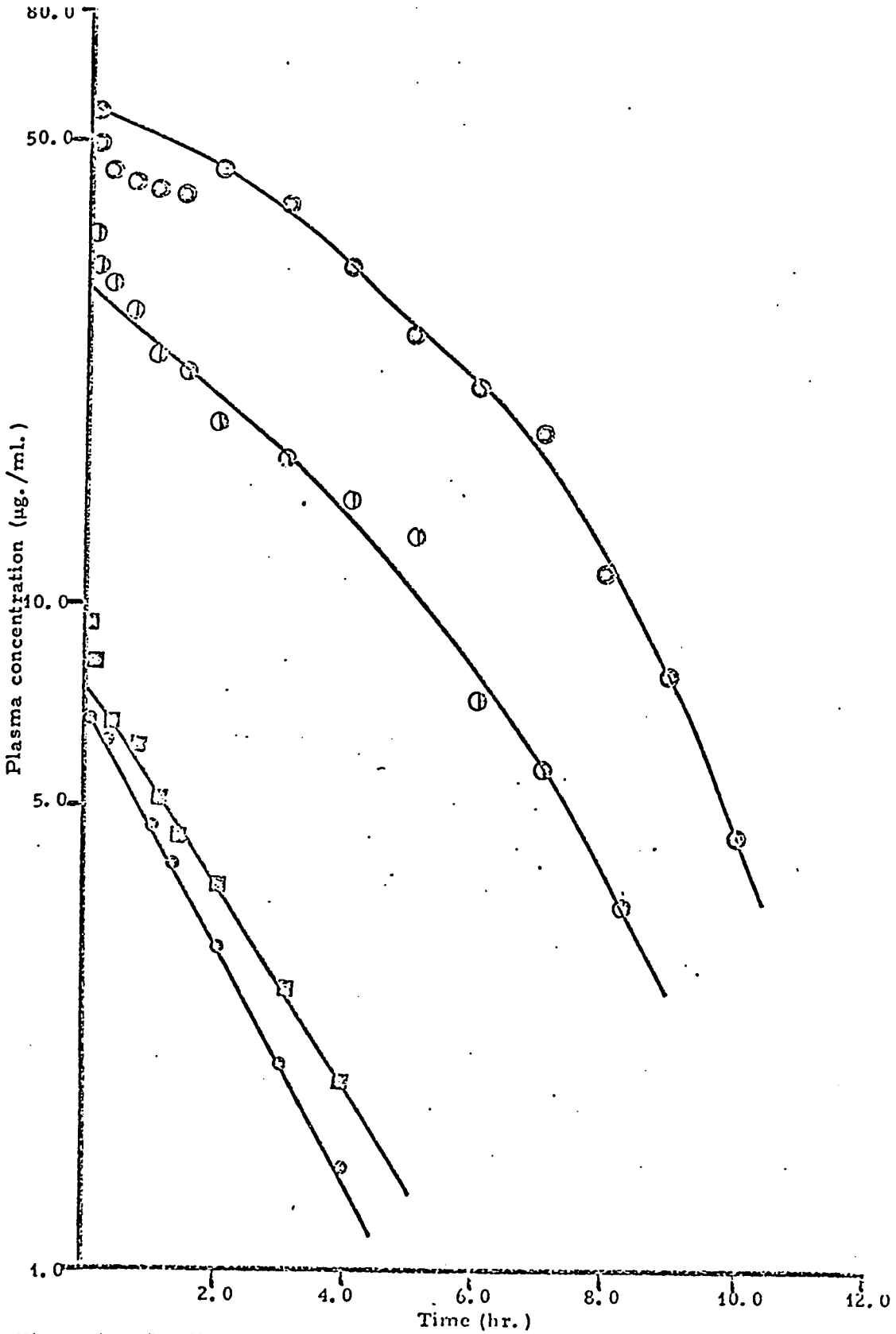

Figure 6. Semilogarithmic plots of PCT data obtained after I. V. administration of 7 (O), 10 (□), 30 (◑) and 50 (◉) mg./kg. of meprobamate to dog #970.

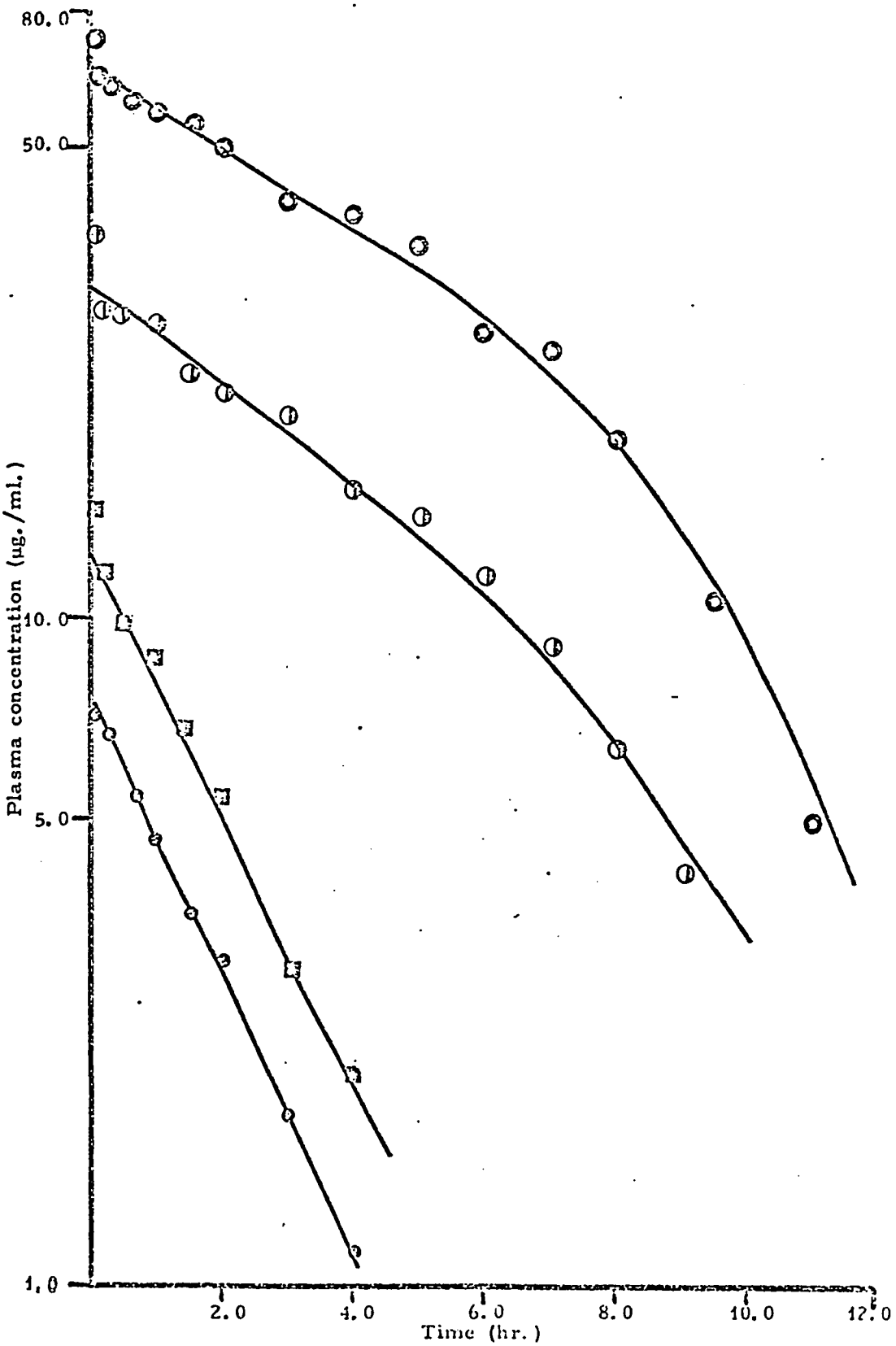

Figure 7. Semilogarithmic plots of PCT data obtained after I. V. administration of 7 (●), 10 (□), 30 (◑) and 50 (◉) mg./kg. of meprobamate to dog #1065.

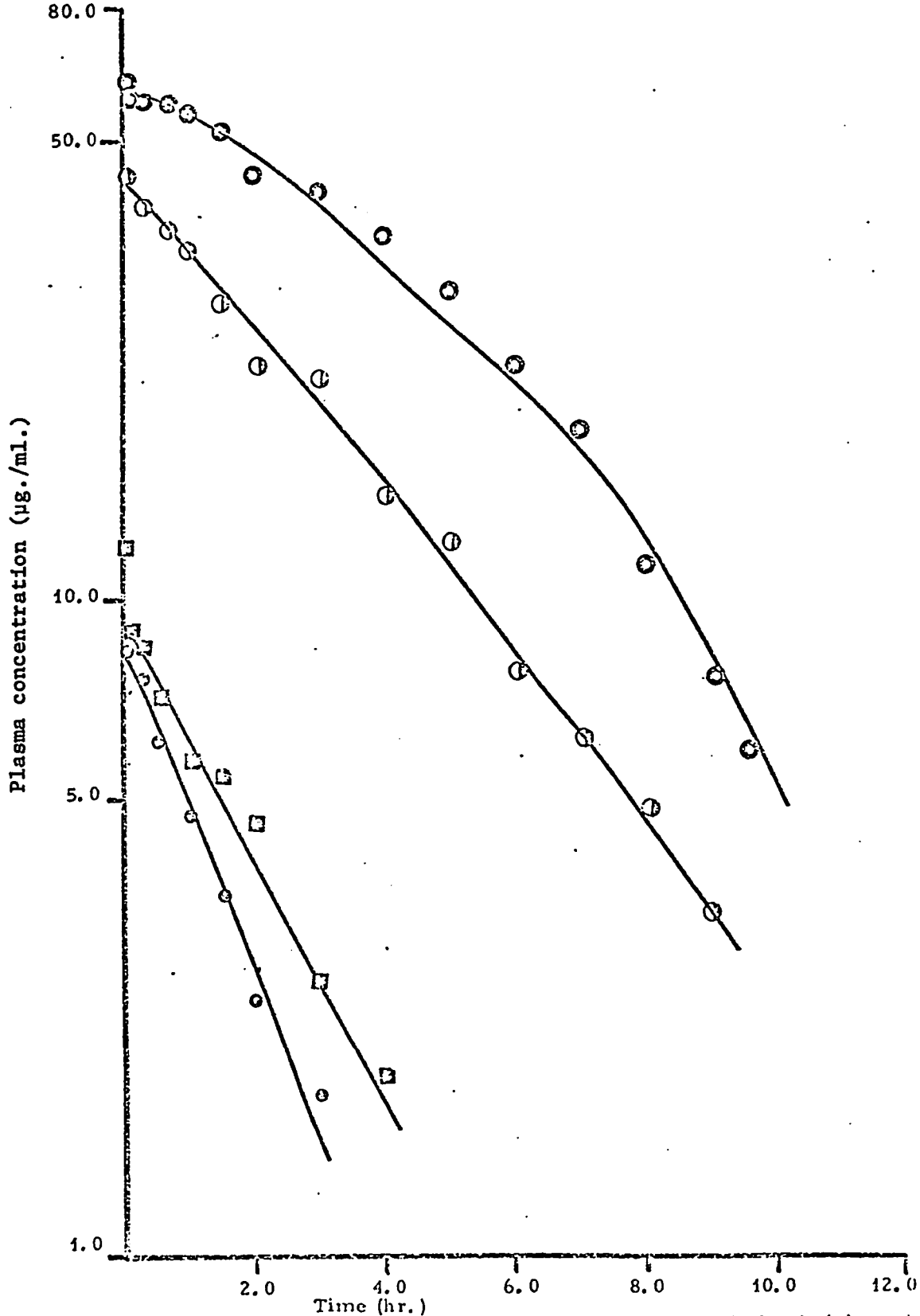

Figure 8. Semilogarithmic plots of PCT data obtained after I. V. administration of 7 (O), 10 (□), 30 (◐) and 50 (●) mg./kg. of meprobamate to dog #1122.

doses of meprobamate to each of the four dogs. From inspection of these PCT curves the following generalizations can be made:

(a) The kinetics of meprobamate can be described by a one compartment (50) body model since the semilogarithmic plots show a negligible distribution phase. Few PCT curves do show an early rapid decline of drug concentration. However this distribution phase seems to be over within 30 min.

(b) The overall elimination of the drug cannot be assumed to occur according to exponential processes only, since the time needed for the drug concentration to decrease by 50 percent increases with dose (Figures 5 through 8 and Table VIII). When elimination of a drug occus from a

TABLE VIII

Dependence of Elimination Half-life on the Plasma Concentration of Meprobamate in Dogs (Data Taken from Figures 5 Through 8)

Meprobamate Concentration (μg./ml.)		Half-life (hr.)
From	To	Mean ± S. D.
55. 0	27. 5	4. 58 ± 0. 59
25. 0	12. 5	2. 95 ± 0. 60
7. 0	3. 5	1. 46 ± 0. 24

one compartment body model by first-order processes only, semilogarithmic plots of PCT data obtained at several doses yield parallel straight lines indicating the constancy of the half-life. Hence, the

elimination of meprobamate cannot be represented by simple first-order linear differential equations.

(c) A more than proportional increase in area under the PCT curve (AUC) with dose shows that the elimination of meprobamate cannot be explained by linear kinetics. Table IX lists the AUC of Figures 5 through 8 computed using the trapezoidal rule. A plot of these results shows a parabolic relationship between AUC and dose (Figure 9). When the pharmacokinetics of a drug are describable by first-order linear differential equations, the dose to AUC ratio (or clearance) is constant.

TABLE IX

AUC After I. V. Bolus Administration of Meprobamate to Dogs

Dog No.	Dose (mg./kg.)	AUC ($\frac{\mu g \cdot hr.}{ml.}$)	$\frac{Dose}{AUC}$ ($\frac{liter}{kg \cdot hr.}$)
510	7	22.18	0.316
510	10	31.12	0.321
510	30	163.47	0.184
510	50	402.91	0.124
970	7	14.964	0.468
970	10	18.987	0.527
970	30	120.217	0.250
970	50	280.229	0.178
1065	7	14.50	0.483
1065	10	27.37	0.365
1065	30	159.59	0.188
1065	50	366.93	0.136
1122	7	13.89	0.504
1122	10	20.81	0.481
1122	30	155.559	0.193
1122	50	310.57	0.161

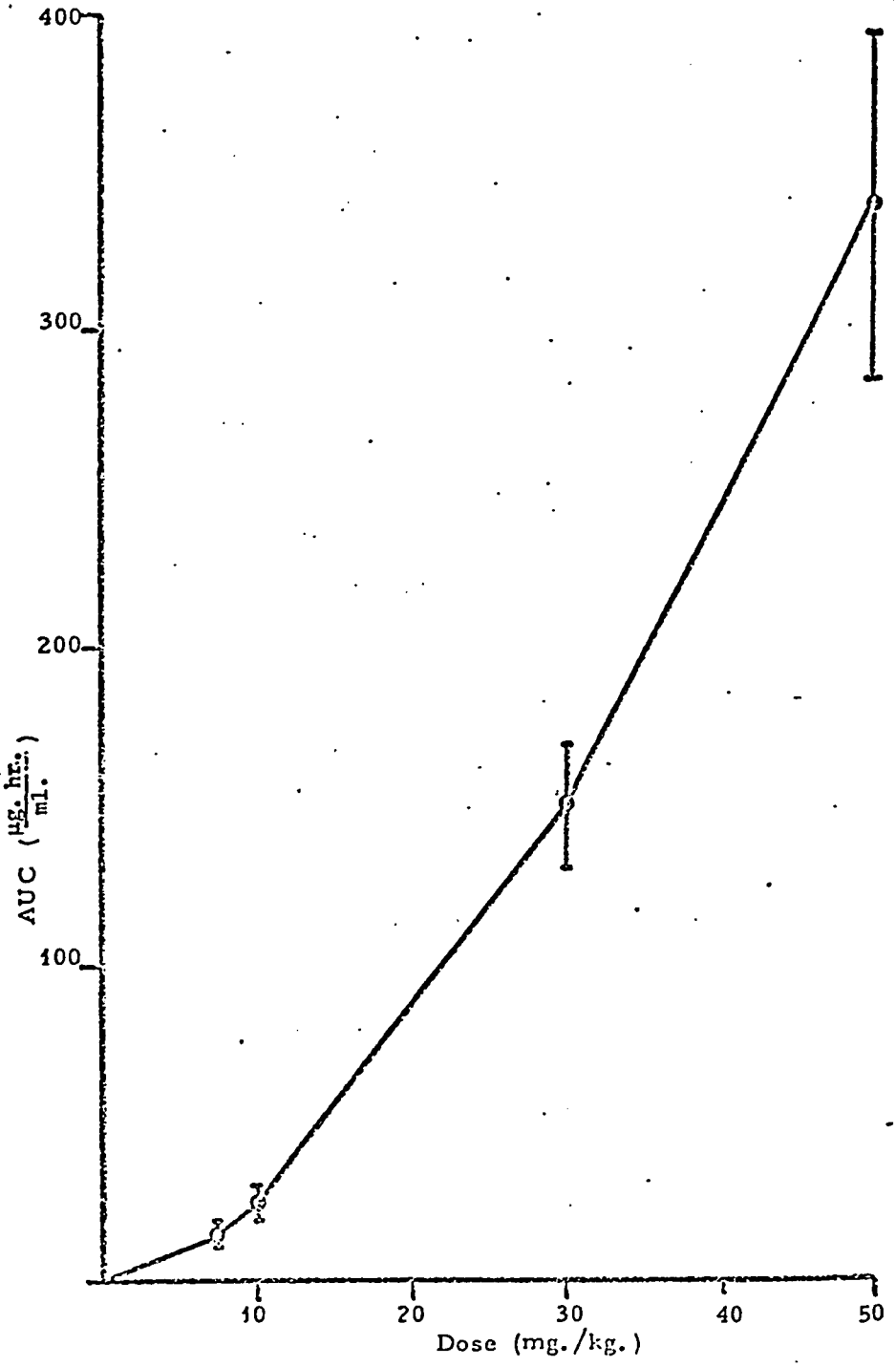

Figure 9. A plot of mean AUC versus Dose (Data taken from Figures 5 through 8).

The above findings clearly indicate that a simple linear pharmacokinetic model cannot adequately describe the kinetic behavior of the drug and that a non-linear model would be more appropriate.

(ii) Reasons for Non-linearity in Meprobamate Kinetics: Deviations from linearity in pharmacokinetic relationships may be due to a non-linear step involving absorption, distribution and/or elimination processes. Non-linearity in absorption may result from low intrinsic solubility of a drug, a formulation induced limited dissolution rate, and/or saturble active absorption processes. However, absorption processes cannot be implicated to explain the kinetic behavior described above since the I. V. bolus administration of the drug bypassed the absorption step.

With respect to drug distribution, deviations from the usual linear dose-concentration relationships can sometimes be caused by protein binding, tissue binding and/or changes in volumes of distribution. Since free, unbound, drug molecules are presumed to be available for transport to the tissues, protein binding can control the diffusion rate and hence, elimination rate of drugs (51). Recently, Wagner and Disanto (52, 53) described non-linear pharmacokinetic models which take into account the non-linear tissue binding of drug to one or more tissues. Protein binding and/or tissue binding are unlikely causes of non-linearity in meprobamate kinetics for the following reasons:

(a) The binding capacity of meprobamate to plasma proteins of the dog is quite small (54). In the concentration range shown in Figures

5 through 8, the fraction bound is less than 10 percent.

(b) When non-linearity in drug kinetics is caused by protein binding and/or tissue binding, a semilogarithmic plot of PCT data shows an early rapid decline of plasma concentration followed by an exponential decay of drug concentration. Such a pattern can be seen at low doses (7 and 10 mg./kg.) but is not consistent with the convex PCT curves (Figures 5 through 8) obtained for meprobamate at doses of 30 and 50 mg./kg.

Dose-dependency of clearance (dose/AUC) can occur as a result of changes in volumes of distribution with dose. However, in such cases the elimination half-life is expected to remain constant which is not the case for meprobamate. Furthermore, the dose/C_o ratio (where C_o is the concentration of the drug at zero-time obtained by extrapolation of the least-square line through the PCT data as described in the theoretical section) does not show any consistent trend with increases in dose. These results indicate that distribution processes are not likely causes for non-linearity in meprobamate kinetics.

Capacity-limited biliary excretion of drugs may be another cause of non-linearity in pharmacokinetics. In order to test for this possibility, feces were collected for 48 hours after I. V. and oral administration of the drug to three dogs. Table X shows that meprobamate is present in the feces but the amount found after I. V. administration is very small. The presence of the drug in the feces can be attributed to biliary and/or salivary excretion. The amount found in the feces need not necessarily be equal to

TABLE X

Forty-eight Hour Fecal Excretion of Meprobamate After I. V. and Oral Administration of the Drug to Dogs

Dog No.	Dose (mg.)	Route of Administration	Amount of Meprobamate in feces (mg.)
510	550	I. V.	0.3
510	550	Oral	2.86
970	115	I. V.	0.091*
1065	475	I. V.	0.486*

*Analysis was done on an aliquot of the feces.

amount excreted through the bile and/or salivary glands since the excreted drug might be reabsorbed in the gastro-intestinal tract. This phenomenon could in fact be the cause for the "bumps" (or absorption noses) seen in Figures 5 through 8. However, it would not explain a systematic increase in half-life and a more-than-proportional increase in AUC with dose.

Non-linearity in pharmacokinetics may be caused by non-linear process in elimination. Elimination processes are comprised of excretion of unchanged drug and/or biotransformation. Drug excretion occurs by passive diffusion and/or active secretory processes. Examples of passive diffusion processes are glomerular filteration and tubular reabsorption, both of which are dose-independent. Tubular secretion is generally assumed to be an active process which is saturable by large drug concentrations. Drug metabolism may be described by first-order kinetics only if the concentration of the enzyme involved is high relative to the drug concentration. Higher drug concentrations which might result in saturation of the reaction sites of the enzyme will cause dose-dependent kinetics (53). A pharmacokinetic model depicting the elimination process according to

a saturable pathway can account for the increase in half-life with dose, convex shapes of semilogarithmic plots of PCT data obtained after I. V. bolus administration of the drug and a parabolic increase in AUC with dose. It would appear therefore, that in the case of meprobamate, deviations from linear kinetics are caused by saturable elimination processes.

(iii) Urinary Excretion Data: The amount of drug excreted unchanged in the urine up to 36 hr. (when elimination of meprobamate is practically complete) after I. V. administration of meprobamate was measured (Table XI). The urinary excretion of unchanged drug appeared

TABLE XI

Urinary Excretion of Meprobamate After I. V. Bolus Administration of the Drug to Dogs

Dog No.	Dose ($\frac{mg.}{kg.}$)	Percent of dose Excreted in the Urine in 36 hr.
510	7	4.5
510	10	5.3
510	30	8.9
510	50	16.3
970	7	4.6
970	10	4.0
970	30	8.5
970	50	12.2
1065	7	3.8
1065	10	4.9
1065	30	9.5
1065	50	15.19
1122	7	4.8
1122	10	4.99
1122	30	10.49
1122	50	16.4

to be a minor pathway in the elimination of meprobamate (less than 5 percent at 7 mg./kg.). The fraction of the dose excreted unchanged increased with dose in all four animals from less than 5 percent to approximately 15 percent at 50 mg./kg. These results are consistent with the hypothesis that non-linearity in meprobamate kinetics is due to elimination processes, for if deviations in pharmacokinetics were caused only by distribution and/or enterohepatic cycling of a drug, the fraction of the dose excreted as unchanged drug should remain constant. As discussed in the theoretical section, (pp.82-83) when the elimination of a drug occurs from simultaneous first-order and capacity-limited processes, the fraction of the dose lost through saturable pathways decreases with increase in dose whereas the fraction of the dose eliminated through the first-order processes increases with increase in dose.

2-b Oral Administration

(i) Plasma Concentration-Time Data: Figures 10 through 12 show the semilogarithmic plots of PCT data obtained after oral administration of 7, 10, 30 and 50 mg./kg. doses of meprobamate in solution to each of the three dogs. In dog #970 oral studies could not be performed because the drug produced emesis soon after the administration. From these PCT curves of Figures 10 through 12 the following observations can be made:

(a) Absorption of meprobamate in aqueous solution from the gastrointestinal tract occurs rapidly, peak drug concentrations appearing in 10-60 min.

(b) The time needed for 50 percent of the drug to be eliminated, calculated from the post-absorptive phase of the PCT curves, increases with the dose, thus indicating the deviations from linearity in meprobamate kinetics. This observation is consistent with the results obtained from the PCT curves depicting data from I. V. administration (Figures 5 through 8 and Table VIII).

(c) The AUC increases more than proportionately with dose. Table XII lists AUC of Figures 10 through 12 computed using the trapezoidal rule. This parabolic increase in AUC (Figure 13 and Table XII) with dose is consistent with the results obtained after I. V. administration of meprobamate.

TABLE XII

AUC After Oral Administration of Meprobamate to Dogs

Dog No.	Dose (mg./kg.)	AUC ($\frac{\text{mg. hr.}}{\text{ml.}}$)	$\frac{\text{Dose}}{\text{AUC}}$ ($\frac{\text{liter}}{\text{kg. hr.}}$)
510	7	21.46	0.326
510	10	25.08	0.399
510	30	174.58	0.172
510	50	374.69	0.133
1065	7	10.41	0.672
1065	10	18.00	0.556
1065	30	155.54	0.193
1065	50	329.64	0.152
1122	7	10.59	0.661
1122	10	17.04	0.587
1122	30	153.50	0.195
1122	50	291.40	0.172

(ii) Urinary Excretion Data: The amount of the drug excreted unchanged over a period of 36 hr. after oral administration of meprobamate was measured (Table XIII). The fraction of the dose excreted unchanged

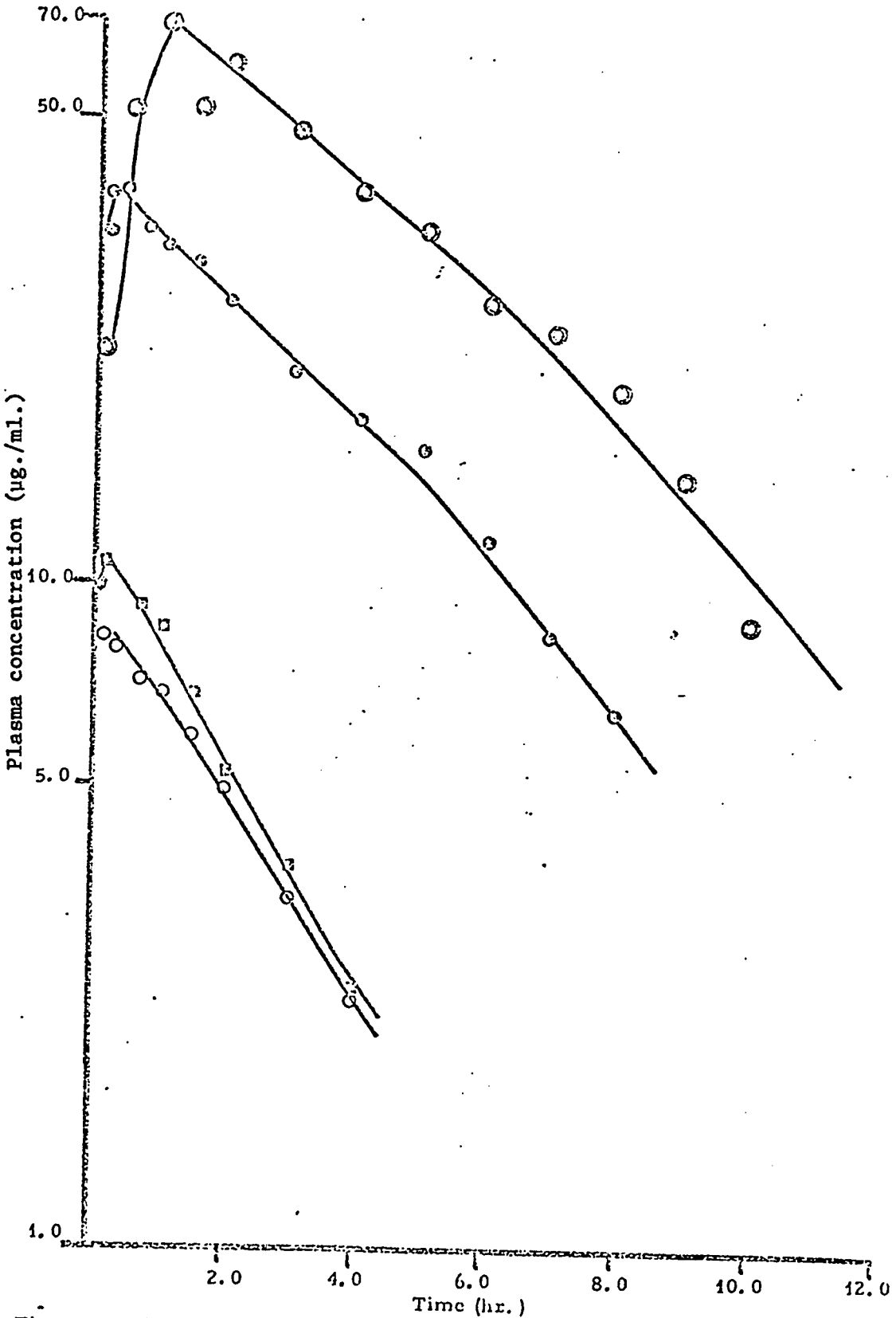

Figure 10. Semilogarithmic Plots of PCT Data obtained after oral administration of 7 (O), 10 (□), 30 (Q) and 50 (Q) mg/kg. of meprobamate to dog #510.

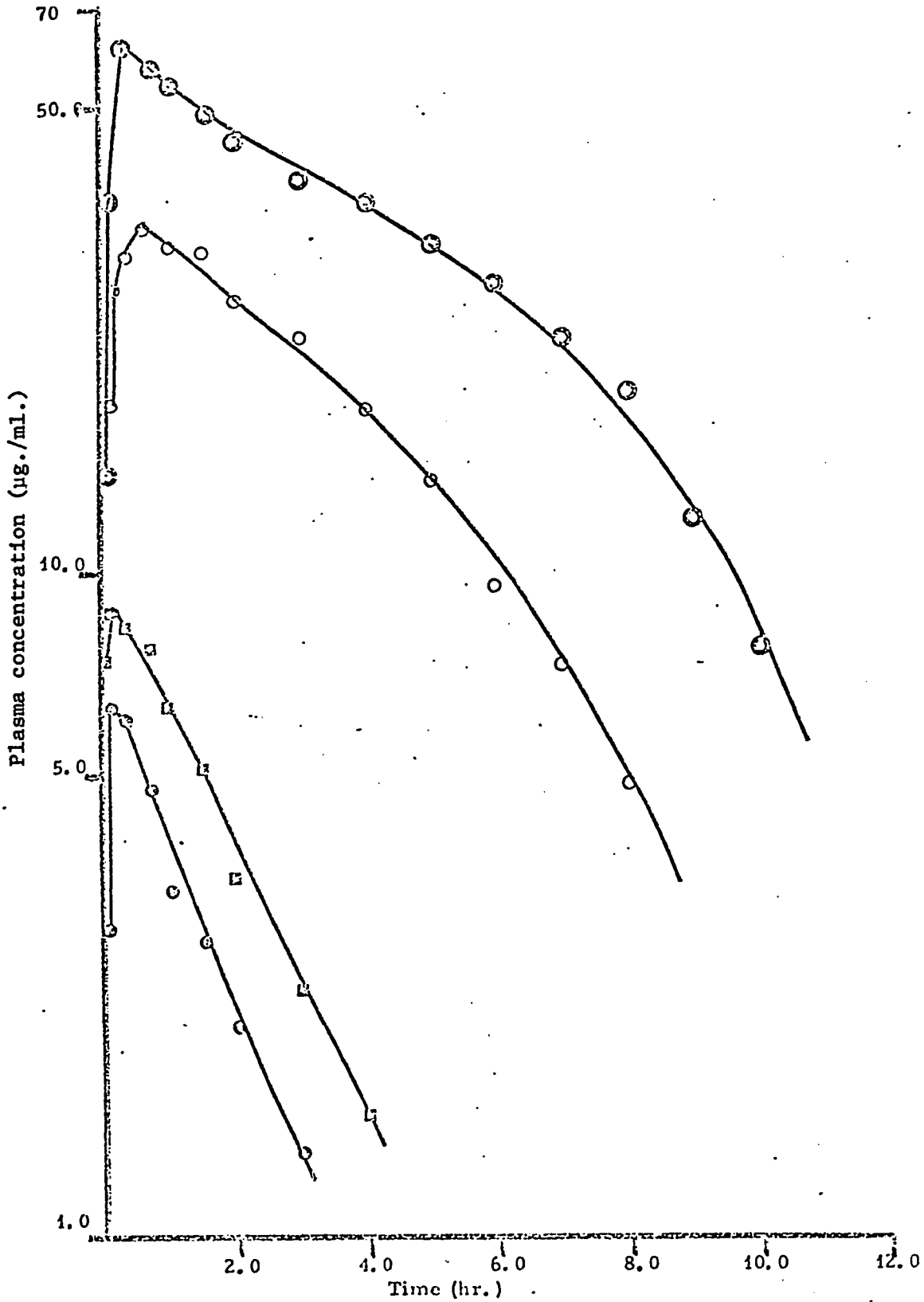

Figure 11. Semilogarithmic Plots of PCT data obtained after oral administration of 7 (○), 10 (□), 30 (○) and 50 (●) mg./kg. of meprobamate to dog #1065.

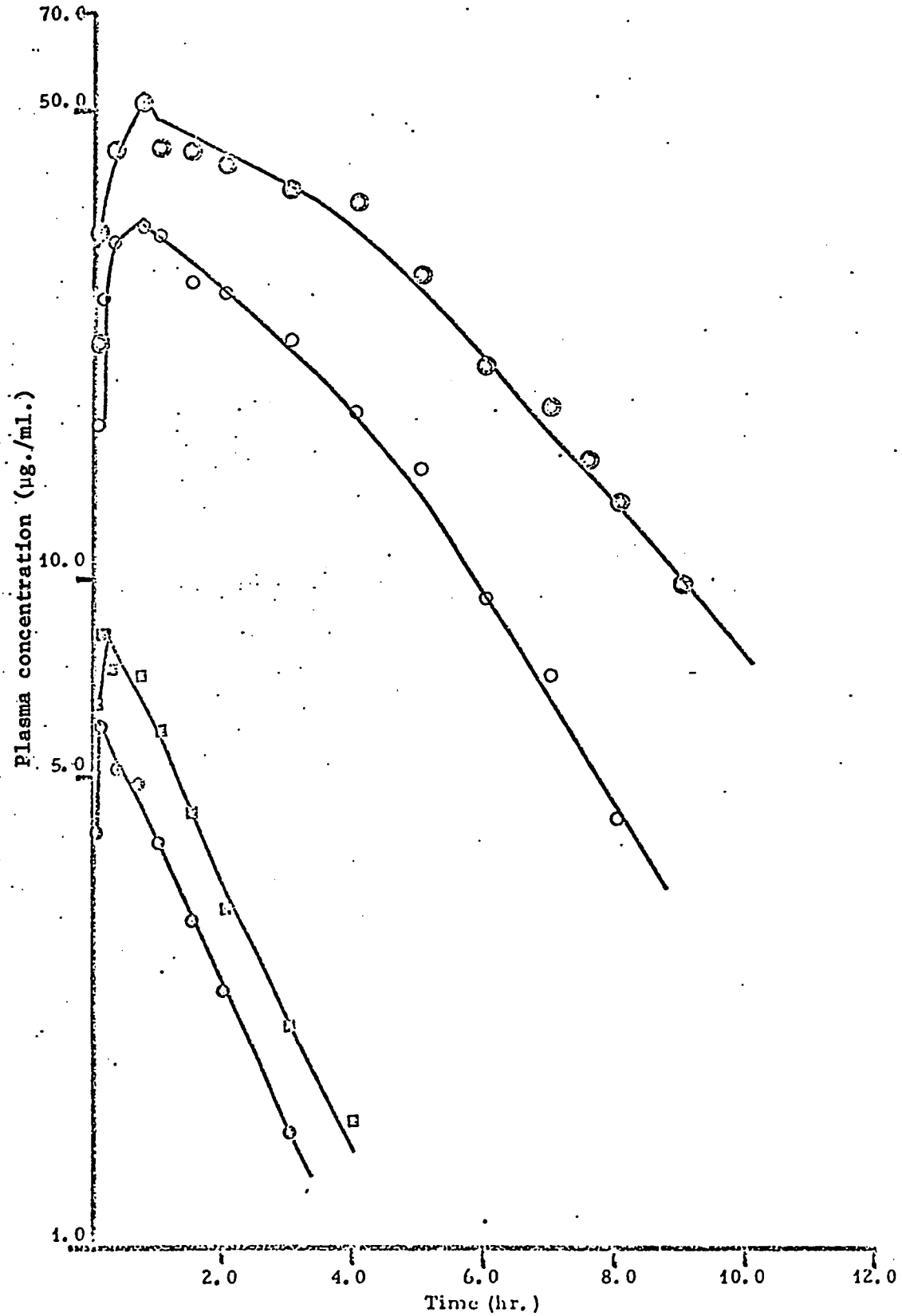

Figure 12. Semilogarithmic Plots of PCT data obtained after oral administration of 7 (O), 10 (□), 30 (O) and 50 (Ⓞ) mg./kg. of meprobamate to dog #1122.

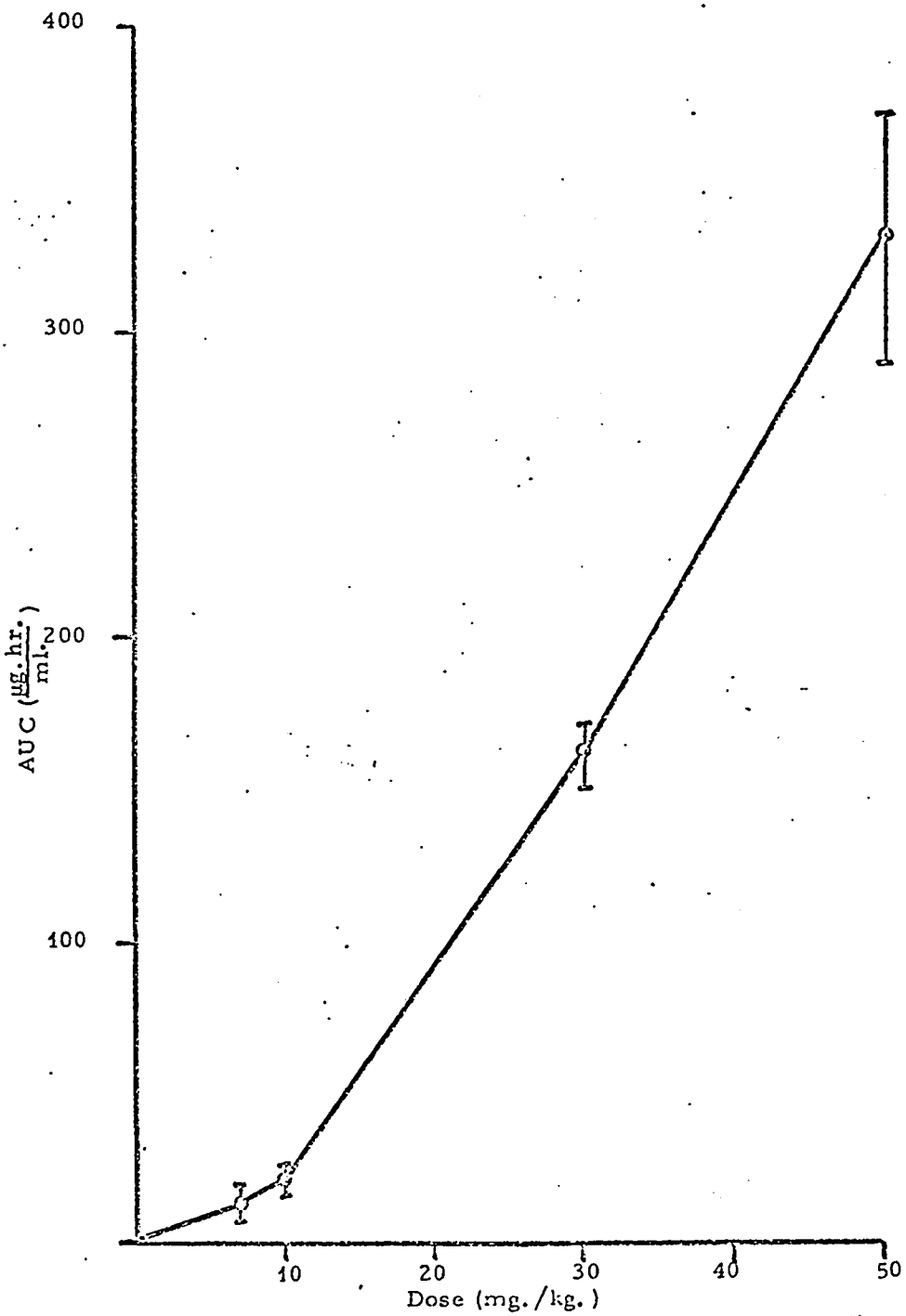

Figure 13. A plot of mean AUC versus dose (data taken from Figures (10 through 12).

TABLE XIII

Urinary Excretion of Meprobamate After Oral Administration of the Drug to Dogs

Dog No.	Dose (mg./kg.)	Percent of the Dose Excreted in Urine in 36 hr.
510	7	3.7
510	10	4.2
510	30	8.7
510	50	8.7
1065	7	4.1
1065	10	4.5
1065	30	7.8
1065	50	13.98
1122	7	3.7
1122	10	4.28
1122	30	10.32
1122	50	14.25

increases with dose in all three dogs, indicating the exponential nature of the excretion process operating in parallel with a capacity-limited process. This observation is again consistent with the hypothesis that elimination of meprobamate occurs by simultaneous first-order and capacity-limited processes.

III - 3 THEORETICAL

3-a Pharmacokinetic Model for Meprobamate in Dogs

(i) Introduction: Pharmacokinetic modeling is a method for rationalization and generalization of experimental data. Pharmacokinetic modeling basically consists of describing the body as a compartment or a series of discrete compartments interconnected by rate processes. The

description of a pharmacokinetic model is useful to develop general mathematical relationships describing the kinetics of a drug. The mathematical relationships are useful in dosage regimen and bioavailability calculations which enhance the safe and effective use of therapeutic agents. The strategy in pharmacokinetic modeling is to develop the model based on physiological and biochemical studies and to test experimentally the predictions of the model. Several reports on the problems associated with compartmental analysis of experimental drug kinetic data can be found in the literature (55-57)

A review of the literature shows that several drugs such as alcohol (58-59), salicylamide (60), slicylate (61-64), diphenylhydantion (65-72), sulfanilamide (73), probenecid (65, 74), etc. exhibit dose-dependency in elimination kinetics. In spite of this large amount of experimental data, theoretical approaches to the kinetic analysis of PCT data for drugs showing non-linearity in elimination kinetics are in their infancy. Lundquist and Wolthers (58) derived an equation to predict the concentration of a drug whose elimination occurs from a one compartment model by a single capacity-limited process. They applied this model to describe the kinetics of alcohol elimination in man. The largest contribution to the understanding of the phenomenon of dose-dependency in elimination is probably that of Levy et al. (60, 62, 75-78). Through urinary excretion measurements of unchanged drug and various metabolites it was shown that salicylate elimination involves two capacity-limited pathways namely, salicyluric acid and salicyl phenolic glucuronide formation. This approach

of characterization of dose-dependency in elimination is a direct one, but it cannot be generalized since it involves the measurement of each metabolite in urine. In addition, it involves the assumptions that the metabolites formed are excreted in urine without undergoing any further change and the excretion rate is much faster than the formation rate. Wagner (79) recently described relationships between dose and several pharmacokinetic parameters namely, AUC, urinary excretion rate of the metabolite etc., using the case of a one compartment model with drug elimination occurring by a single capacity-limited process. Wagner also described two methods for obtaining the initial estimates of model parameters which were then refined by fitting PCT data to the integrated form of the differential equation representing the drug concentration in the plasma. However, Wagner's model is limited in scope since the elimination of the majority of drugs involves more than one pathway. Krüger-Thiemer (51) extended Wagner's model to involve a first-order pathway for the excretion of unchanged drug and derived the equation to represent the concentration of a drug at any time in the blood. However, he did not develop any relationships between dose and pharmacokinetic quantities such as AUC, half-life, amount of drug excreted unchanged and as various metabolites.

From the PCT and urinary excretion data obtained after I. V. and oral administration of meprobamate to dogs, it was established that this drug exhibits non-linear pharmacokinetics which appear to be due to dose-dependent elimination of the drug. The pharmacokinetic model

proposed here for meprobamate is a one compartment body model from which drug elimination occurs by simultaneous first-order and capacity-limited processes. This model involves the following assumptions:

(a) The distribution of meprobamate is assumed to be describable by a one compartment body model. This assumption is based on the fact that the plots of PCT data obtained after I. V. administration of the drug show a negligible distribution phase.

(b) The elimination of the drug involves a capacity-limited process which accounts for the non-linearity in meprobamate kinetics at higher plasma concentration. In the proposed model the capacity-limited process can be represented by the Michaelis-Menten equation (80). Several investigators (51, 58, 62, 70, 81-84) have used the Michaelis-Menten equation to depict a capacity-limited process because it accounts for the saturability of a metabolic reaction. The non-linearity in elimination could also be due to product-inhibition of a metabolic reaction. Recently, Levy et al. (69, 71, 72) demonstrated that dose-dependency in elimination can occur due to the inhibition of enzyme-substrate reaction by one or more metabolites of a drug. This type of dose-dependency has been demonstrated for diphenylhydantoin in rats. When non-linearity in drug kinetics is due to product-inhibition of the enzyme-substrate reaction, semilogarithmic plots of PCT data at various doses become linear at low concentrations of the drug in the body and slopes of these lines decrease with increase in dose.

In the case of meprobamate this possibility is eliminated on the basis of the data presented in Table XIV. The elimination half-life calculated at concentrations less than 18 mcg./ml. (I. V. data) does not increase uniformly with the original dose.

TABLE XIV

Half-lives* in hr. Calculated from the Terminal Portions of PCT Curves and Figures 5 Through 8

Dose (mg./kg.)	Plasma Half-life Dog No.				Mean hrs.
	510 hrs.	970 hrs.	1065 hrs.	1122 hrs.	
7	1.394	1.678	1.471	1.242	1.524
10	1.414	1.991	1.487	1.805	1.734
30	2.081	1.69	1.768	2.359	1.961
50	2.038	1.533	1.593	1.525	1.740

*Half-lives were calculated by fitting the PCT data to a mono-exponential equation using a non-linear least-squares program (90)

(c) The elimination of meprobamate includes a first-order process which operates in parallel with the capacity-limited process. The urinary excretion data already presented in Tables XI and XIII showed that excretion of unchanged drug occurs through an exponential process. In addition to excretion of unchanged drug, some other metabolic processes may exhibit first-order kinetics. In the proposed model the individual rate constants for each first-order process are grouped to yield one apparent overall first-order rate constant.

(d) Biliary and/or salivary excretion of meprobamate is neglected because of the apparently minor nature of this phenomenon. Meprobamate in solution is absorbed rapidly from the gastrointestinal tract. Consequently, if the fraction of the dose cycled in bile was extensive, a relatively large scatter in PCT curves at early times after administration (absorption noses) with only a small amount of unchanged drug being eliminated in the feces should be observed. However, the data represented in Figures 5 through 8 and in Table X show that biliary and/or salivary excretion of meprobamate is probably not a major cause of nonlinearity in meprobamate kinetics. For this reason no attempt was made to take biliary and/or salivary excretion into account in the proposed model for meprobamate. Also, because bile production, gall bladder emptying and salivary secretion depend on psychic influences and other factors such as ingestion of certain foods, it is difficult to describe these processes by mathematical equations.

In the following sections of this chapter several pharmacokinetic properties of the proposed model such as nature of PCT curves, relationships between dose and AUC, half-life and urinary excretion of unchanged drug will be described and compared with the experimental results presented earlier. Equations needed for bioavailability calculations involving this model are derived and applied to meprobamate data. Also, several relationships describing the accumulation characteristics of a drug which

follows this model and methods of performing dosage regimen calculations are presented.

(ii) Nature of I. V. and Oral PCT Curves: Scheme 3 represents a one compartment body model where elimination of a drug after I. V. bolus administration of a dose D_o, occurs by one or more apparent first-order processes in parallel with a capacity-limited process.

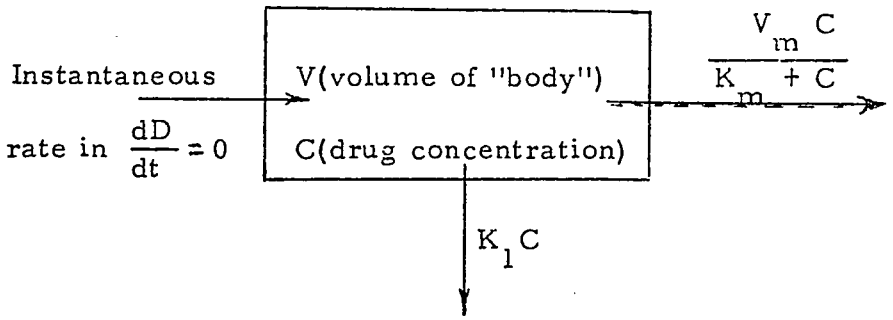

Scheme 3: Model Ia

The differential equation describing concentration of drug C at any time in the body is:

$$\frac{dC}{dt} = -K_1 C - \frac{V_m C}{K_m + C} \qquad \text{Eq. (III-1)}$$

where V_m is the theoretical maximum velocity of the capacity-limited process in concentration per time, and K_m represents the Michaelis constant in concentration units. The integrated form of Eq. (III-1) is given by (58) (Appendix 1):

$$t = \frac{1}{K_1 K_m + V_m} \left[K_m \ln \frac{C_o}{C} + \frac{V_m}{K_1} \ln \frac{(C_o + K_m) K_1 + V_m}{(C + K_m) K_1 + V_m} \right] \qquad \text{Eq. (III-2)}$$

where C_o $(= \frac{D_o}{V})$ is the concentration of drug in the body at zero time.

It is not possible to write an explicit solution of C and hence it is somewhat impractical to use Eq. (III-2) for calculations of C at any given time t. It is however, possible to numerically integrate Eq. (III-2) to obtain C at any given time t. Several methods are available for computing numerical solution of differential equations and are described by Southworth and Deleeuw (85), among others. These methods are quite popular because a large number of differential equations representing the physical and biological systems cannot be integrated to obtain analytical expressions for the dependent variables.

Scheme 4 represents a one compartment model whose elimination characteristics are similar to Model Ia. In Scheme 4, a dose D_o is administered orally and a fraction F of the dose is absorbed. If we

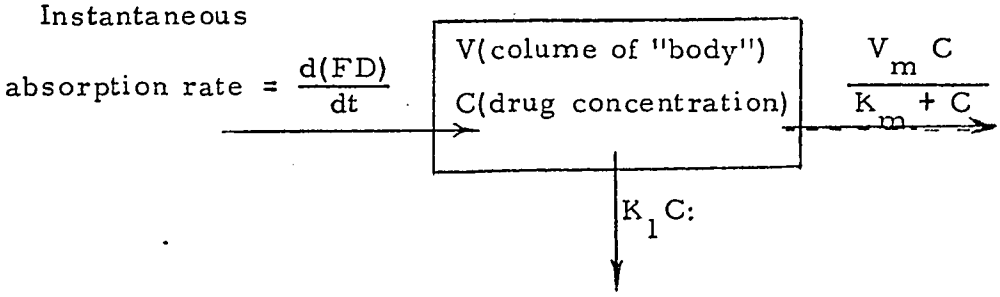

Scheme 4: Model Ib

assume that absorption of the drug occurs by first-order process, the following differential equations can be written for Model Ib:

$$\frac{d(FD)}{dt} = -K_a FD \qquad \text{Eq. (III-3)}$$

and

$$\frac{dC}{dt} = K_a \frac{FD}{V} - K_1 C - \frac{V_m C}{K_m + C} \qquad \text{Eq. (III-4)}$$

In Eqs. (III-3) and (III-4) D represent the amount of drug in the gastrointestinal tract at any time t and K_a is an assumed first-order rate constant for the purpose of the following derivations. Eq. (III-4) involves two dependent variables (D and C) which make it difficult to separate independent and dependent variables and hence, it is impossible to obtain an analytical solution of this equation. However, Eq. (III-4) is amenable to numerical integration after integration of Eq. (III-3) and substitution into Eq. (III-4) as follows:

Integration of Eq. (III-3) (initial conditions are at $t = 0$, $D = D_o$) gives the following expression for FD:

$$FD = FD_o e^{-K_a t} \qquad \text{Eq. (III-5)}$$

Substituting Eq. (III-5) for FD in Eq. (III-4) and noting that $D_o/V = C_o$ we have:

$$\frac{dC}{dt} = K_a F C_o e^{-K_a t} - K_1 C - \frac{V_m C}{K_m + C} \qquad \text{Eq. (III-6)}$$

Eqs. (III-1) and (III-6) exhibit interesting limiting characteristics (for detailed derivations see Appendix 3). When $C << K_m$, Eq. (III-1) reduces to:

$$\frac{dC}{dt} = -(K_1 + \frac{V_m}{K_m}) C \qquad \text{Eq. (III-7)}$$

Integration of Eq. (III-7) gives:

$$C = C_o e^{-(K_1 + \frac{V_m}{K_m})t} \qquad \text{Eq. (III-8)}$$

Eq. (III-8) shows a linear dose-concentration relationship* with overall first-order elimination rate constant equal to $(K_1 + \frac{V_m}{K_m})$. When $C >> K_m$, Eq. (III-1) becomes:

$$\frac{dC}{dt} = -K_1 C - V_m \qquad \text{Eq. (III-9)}$$

Integrated expression of the above equation can be written as

$$C = (C_o + \frac{V_m}{K_m}) e^{-K_1 t} - \frac{V_m}{K_1} \qquad \text{Eq. (III-10)}$$

Eq. (III-10) gives a non-linear dose-plasma concentration relationship: an expression for half-life shows dose-dependency. Eqs. (III-8) and (III-10) can be used to calculate C at a given time t if the assumptions made in deriving these equations are valid in the concentration range under investigation. When $C << K_m$, Eq. (III-6) reduces to:

$$\frac{dC}{dt} = K_a F C_o e^{-K_a t} - (K_1 + \frac{V_m}{K_m}) C \qquad \text{Eq. (III-11)}$$

---

*A linear dose-concentration relationship is represented by the equation:

$$C = D_o f(t, \theta_1, \theta_2, \ldots\ldots)$$

where $\theta_1, \theta_2, \ldots$ describe the pharmacokinetic properties of the drug with respect to absorption, distribution and elimination (51). In the above equation $f(t, \theta_1, \theta_2, \ldots\ldots)$ is independent of dose.

Eq. (III-11) can be solved using Laplace transforms to give the following expression for C:

$$C = \frac{K_a F C_o}{(K_l + \frac{V_m}{K_m} - K_a)} [e^{-K_a t} - e^{-(K_l + \frac{V_m}{K_m}) t}] \qquad \text{Eq. (III-12)}$$

According to Eq. (III-12), in the post-absorptive phase, a semilogarithmic plot of C versus t is linear indicating the apparent first-order elimination of the drug. When $C >> K_m$, Eq. (III-6) reduces to:

$$\frac{dC}{dt} = K_a F C_o e^{-K_a t} - K_l C - V_m \qquad \text{Eq. (III-13)}$$

Solution of Eq. (III-14) using Laplace transforms leads to:

$$C = \frac{K_a F C_o}{K_l - K_a} [e^{-K_a t} - e^{-K_l t}] - \frac{V_m}{K_l} [1 - e^{-K_l t}] \qquad \text{Eq. (III-14)}$$

The above equation shows that a non-linear dose-concentration relationship exists even in the post-absorptive phase.

(iii) Computer Simulations: As mentioned above, Eqs. (III-1) and (III-6) can be solved by numerical integration. Standard computer programs capable of performing numerical integrations of differential equations are available (86) and these programs are simple to use. The choice of the numerical method depends on the accuracy sought and the computer time needed in obtaining the solution. Eqs. (III-1) and (III-6) can be solved with excellent accuracy by using the fourth-order

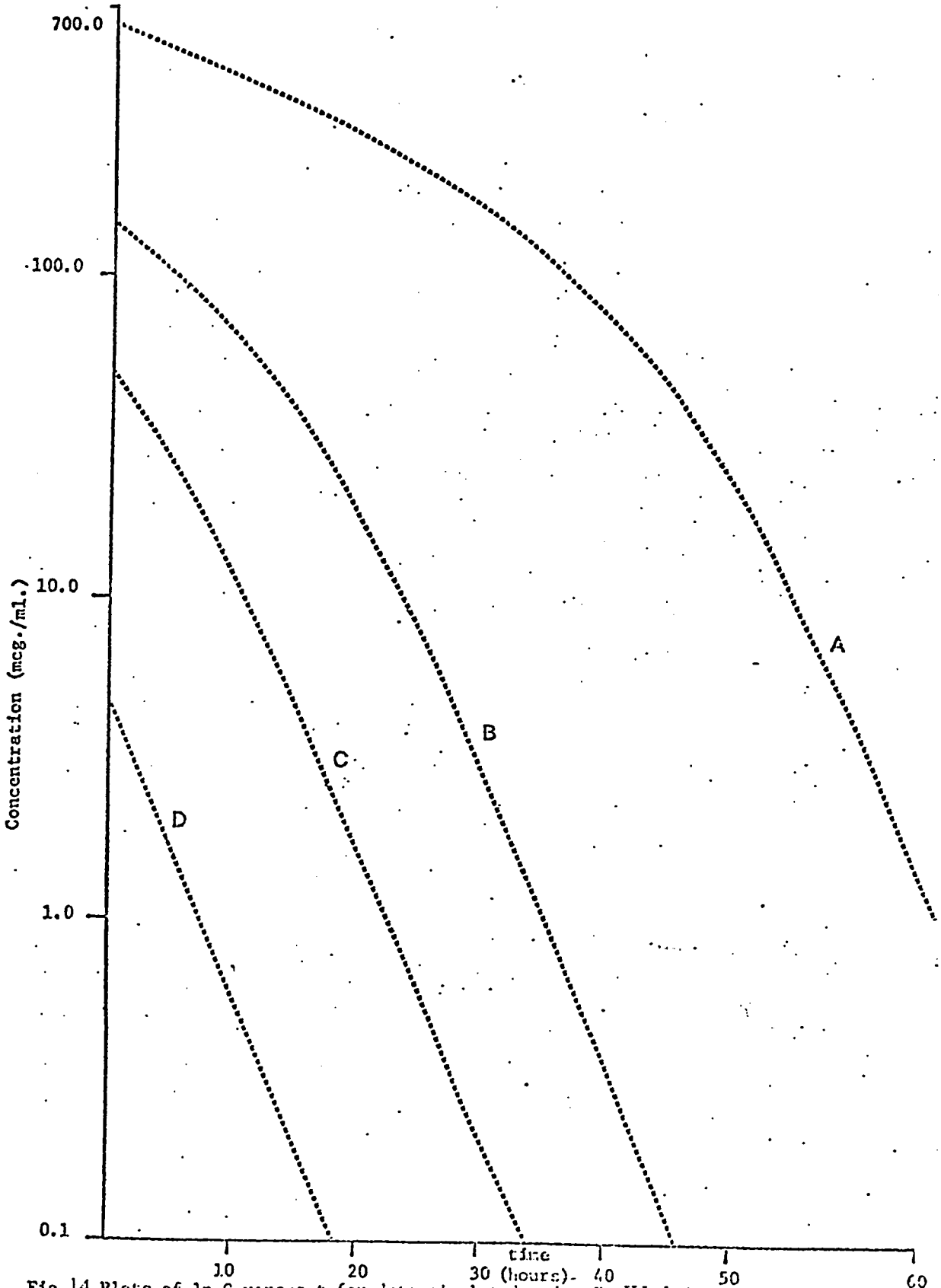

Fig.14 Plots of ln C versus t for data simulated using Eq.III-1 The following values were used in the simulation: C_0 (mcg./ml.)=615.38 (A), 153.84 (B), 50.22 (C) and 4.8 (D), K_1=0.0155 hr^{-1}: V_m=10.46 mcg./ml. hr; and K_m=52.31 mcg./ml.

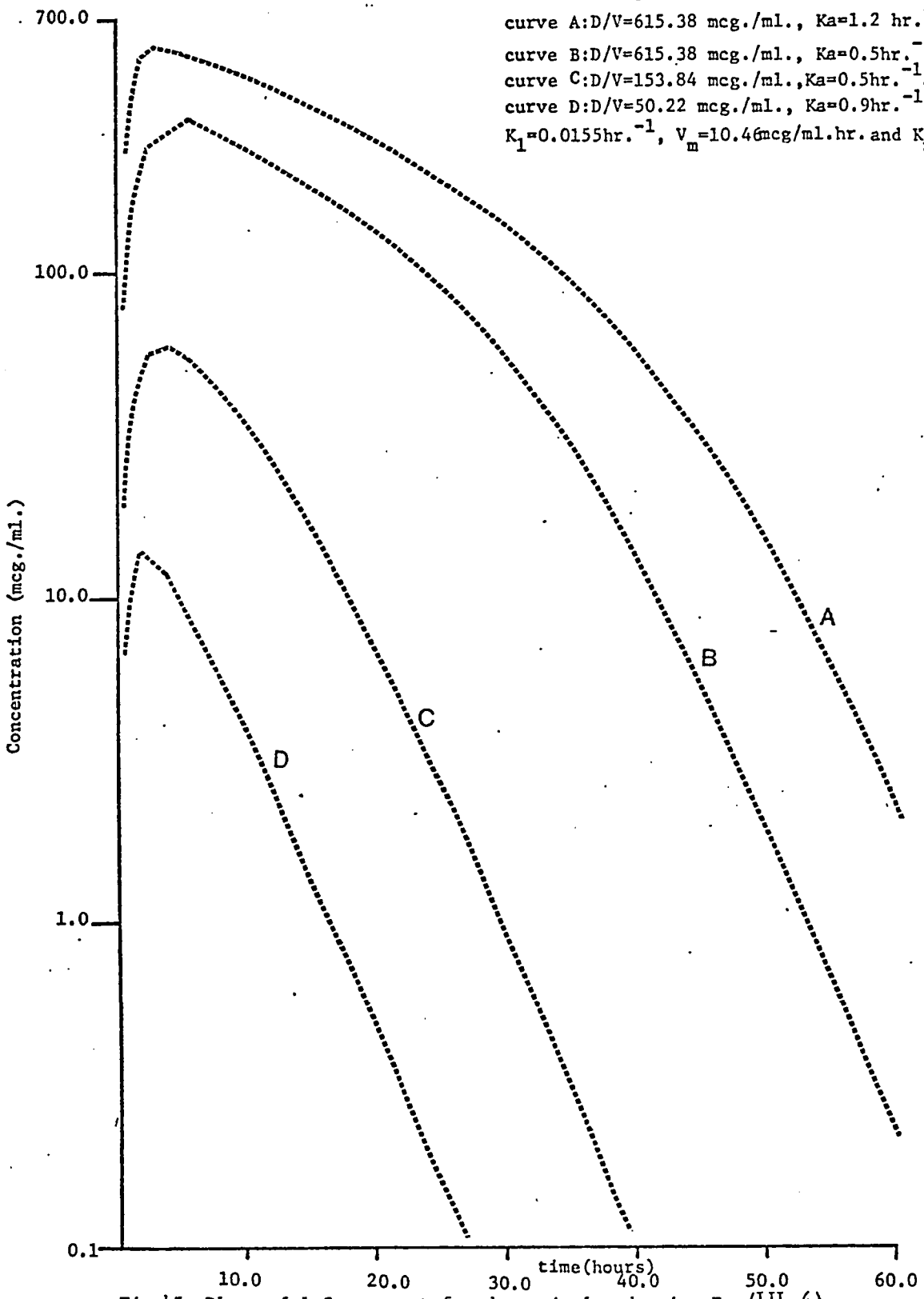

Fig.15 Plots of lnC versus t for data simulated using Eq. (III-6)

Runga-Kutta method (85) (Appendix 2). Sets of C, t data were generated for different C_o values by numerical integration of Eq. (III-1). The values of K_l, V_m and K_m used for generating the data were those reported for salicylate in man, namely $K_l = 0.0155$, $V_m = 10.46$ and $K_m = 52.31$ (78) (ignoring the salicyl phenolic glucuronide formation pathway which is a second saturable but relatively minor pathway in salicylate elimination). Figure 14 shows semilogarithmic plots of C, t data. All curves in Figure 14 have the same shape in a given concentration region and they become apparently linear when $C << K_m$ as defined by Eq. (III-8). Figure 15 shows semilogarithmic plots of C, t data generated from numerical integration of Eq. (III-6) with various values of K_a and F. When $C << K_m$, the plots become apparently linear in the post-absorptive phase which is consistent with Eq. (III-12). The nature of the plots shown in Figures 5 through 8 is similar to the pattern of those in Figure 14. Similarly the plots of PCT data obtained after oral administration of meprobamate (Figures 10 through 12) resemble those shown in Figure 15. This indicates the appropriateness of models Ia and Ib to describe the pharmacokinetics of meprobamate in the dog after I. V. bolus and oral administration, respectively.

3-b Estimation of Model Parameters

Estimation of model parameters is one of the most challenging areas in the analysis of pharmacokinetic data . Model parameters are necessary in order to calculate drug concentrations in each compartment of a model,

thus allowing a more precise understanding of pharmacokinetic phenomena. They are of general applicability when their values are independent of dose and concentration, i.e., the parameters estimated at one dose properly describe drug behavior at any other dose level.

As described in the previous section, Models Ia and Ib give non-linear dose-concentration relationships. In this section, methods presently available to calculate the parameters of these models are discussed and new, more versatile methods are presented.

(i) Available Methods: Kruger-Thiemer and Levine (87) reported a method for estimating the parameters of Model Ia, when K_e is a first-order rate constant for excretion of unchanged drug. To obtain initial estimates of the parameters their procedure requires the following experimentally measured values: initial concentration of drug in plasma C_o, total amount of drug excreted unchanged in the urine A_u^∞, $AUC = \int_o^\infty C\,dt$, and several values of dC/dt with the corresponding values of C. The parameter values are calculated from the following equations:

$$V = \frac{D_o}{C_o} \qquad \text{Eq. (III-15)}$$

$$K_e = \frac{A_u^\infty}{V \cdot \int_o^\infty C\,dt} \qquad \text{Eq. (III-16)}$$

and

$$-\frac{1}{\frac{dC}{dt} + K_e C} = \frac{K_m}{V_m} \cdot \frac{1}{C} + \frac{1}{V_m} \qquad \text{Eq. (III-17)}$$

Eq. (III-17) which is obtained from rearrangement of Eq. (III-1) states that a Lineweaver-Burke type (88) plot of $1/-(dC/dt + K_e C)$ versus $1/C$ is linear with a slope of K_m/V_m and an intercept of $1/V_m$. K_m and V_m can then be calculated from such a plot. However, Krüger-Thiemer and Levine did not give a method of refining these graphical estimates by fitting the PCT data to model equations. The main limitation of their method is the assumption that excretion of unchanged drug is the only first-order pathway of elimination and therefore it is not applicable to the general scheme represented in Model Ia.

An alternative method of calculating the model parameters has been reported by Nelson et al. (62) and Levy and Amsel (84). The theory behind their method is as follows: If m_1 is the amount of metabolite formed by the capacity-limited process in plasma at any time t, and m_2 is the corresponding amount of metabolite excreted in urine by a first-order process, the differential equation for m_2 can be written as:

$$\frac{dm_2}{dt} = V\left[\frac{V_m C}{K_m + C}\right] - \frac{dm_1}{dt} \qquad \text{Eq. (III-18)}$$

Assuming that excretion rate is much larger than formation rate, dm_1/dt can be neglected and Eq. (III-18) can be rearranged to give:

$$\frac{V}{\frac{dm_2}{dt}} = \frac{K_m}{V_m} \cdot \frac{1}{C} + \frac{1}{V_m} \qquad \text{Eq. (III-19)}$$

According to Eq. (III-19) a plot of $1/dm_2/dt$ versus $1/C$ is linear with a slope of K_m/V_m and an intercept equal to $1/V_m$.

The applicability of Eq. (III-19) is seriously limited. This equation is valid only if dm_1/dt is small enough that it can be neglected without any appreciable error. Furthermore, it is necessary to measure the excretion rate of the metabolite formed by the capacity-limited process. Identification of the capacity-limited process from urinary excretion measurements of metabolites requires considerable amount of experimental work and is not always practically possible.

(ii) Proposed Methods: The methods for estimation model parameters presented in this section can be divided into two groups. In the first, an approach which uses approximations of the differential equation (III-1) is discussed. In the second group, two methods which use a non-linear least-squares estimation procedures are presented.

(a) Estimation of Parameters Using Approximations of Eq. (III-1)- Method I:

Dividing both sides of Eq. (III-9) by C yields:

$$-\frac{d\ell n\, C}{dt} = K_1 + \frac{V_m}{C} \qquad \text{Eq. (III-20)}$$

According to Eq. (III-20) a plot of $-d\,\ell nC/dt$ versus $1/C$ will be linear with a slope equal to V_m and an intercept equal to K_1. Rearrangement of Eq. (III-7) gives:

$$-\frac{d\ell n\, C}{dt} = K_1 + \frac{V_m}{K_m} \qquad \text{Eq. (III-21)}$$

Therefore, a plot of $-d\,\ell nC/dt$ versus $1/C$ will reach an asymptotic value given by Eq. (III-21) from which K_m can be calculated.

The main drawback of the above method is that it is necessary to obtain I. V. C, t data at high plasma concentrations. This is not always possible.

(b) Estimation of Model Parameters Using Least-squares Procedures:

The second approach to estimating the model parameters involves fitting C, t data to one of the equations describing the model. The criterion of best fit most widely used is that the sum of squares of the deviations should be minimum. An excellent discussion of non-linear least-squares fitting procedures is given by Draper and Smith (89).

(b-i) Principle of Non-linear Least-squares Estimation of the Parameters:

Suppose the postulated model is of the form:

$$Y = f(t, \theta) \qquad \text{Eq. (III-22)}$$

where Y is the dependent variable, t is the independent variable and θ's are the model parameters. When there are n observations, one can write Eq. (III-22) in the alternate form:

$$Y_u = f(t_u, \theta) \qquad \text{Eq. (III-23)}$$

where $u = 1, 2, \cdots\cdots n$. The error sum of squares can be written as:

$$S(\theta) = \sum_{u=1}^{n} [Y_u - f(t_u, \theta)]^2 \qquad \text{Eq. (III-24)}$$

Since Y_u and t_u are fixed observations, the sum of squares is a function of θ's. Let us denote a least-square estimate of θ by $\bar{\theta}$, that is a

value of θ which minimizes $S(\theta)$. To find the least-squares estimate $\bar{\theta}$, Eq. (III-24) is to be differentiated with respect to θ and equated to zero. This provides p normal equations (where p represents the number of parameters) which must be solved for θ_r, where $r = 1,2,\cdots p$. The normal equations take the form:

$$-2\sum_{u=1}^{n} [\, Y_u - f(t_u, \bar{\theta}] \left\{ \frac{\partial f(t_u, \theta)}{\partial \theta_r} \right\}_{\theta = \bar{\theta}} = 0 \qquad \text{Eq. (III-25)}$$

where the quantity denoted by brackets is the partial derivative of $f(t_u, \theta)$ with respect to θ_r. Therefore, the parameter estimation procedure using non-linear least-squares technique consists of two stages. The first stage involves finding an initial set of parameter estimates θ, to compute $f(t_u, \theta)$. The procedures used to find these estimates need not be efficient, although good initial estimates will reduce the calculation involved in the second stage namely, the solution of the normal equations. The normal equations are usually solved by using iterative techniques and a detailed description of the available methods can be found in the literature (89). There are computer programs available which solve the normal equations to give least-squares parameters. In this work, the BMDX85 (90) has been used for this purpose.

(b-ii) Initial Estimates of the Parameters:

Rearrangement of the differential equation (III-1) and the Taylor expansion of the resulting expression gives (Appendix 4):

$$-\frac{C}{dC/dt} = \frac{K_m}{K_2} + \left[\frac{1}{K_2} - \frac{K_m K_1}{K_2^2}\right] C + \left[\frac{K_m K_1^2}{K_2^2} - \frac{K_1}{K_2^2}\right] C^2 \quad \text{Eq. (III-26)}$$

where

$$K_2 = V_m + K_1 K_m \quad \text{Eq. (III-27)}$$

Eq. (III-26) can be written as:

$$-C/dC/dt = a_o + a_1 C + a_2 C^2 \quad \text{Eq. (III-28)}$$

The above equation is a second degree polynomial in C, the coefficients (a_o, a_1 and a_2) of which can be solved for the model parameters. Initial estimates of K_1, V_m, and K_m can be obtained from the following series of equations (Appendix 4):

$$K_2 = a_1/(a_1^2 - a_o a_2) \quad \text{Eq. (III-29)}$$

$$K_m = K_2 a_o \quad \text{Eq. (III-30)}$$

$$K_1 = -a_2 K_2/a_1 \quad \text{Eq. (III-31)}$$

and

$$V_m = K_2 - K_1 K_m \quad \text{Eq. (III-32)}$$

An approximate value of the fourth parameter C_o of Model Ia is obtained by extrapolating PCT curve obtained after I. V. bolus administration of the drug to zero time.

In addition to K_1, V_m and K_m, Model Ib involves two additional parameters namely, the fraction of the dose absrobed F, and the

absorption rate constant K_a. An initial estimate of F can be obtained from the following expression:

$$F = \frac{[\int_0^\infty C\,dt]_{oral}}{[\int_0^\infty C\,dt]\ I.V.} \qquad \text{Eq. (III-33)}$$

Integrals in the numerator and the denominator of Eq. (III-33) are to be evaluated after administration of equal doses of the drug. To obtain initial estimate of K_a, it is necessary first to evaluate dC/dt at $t \rightarrow 0$ from C,t data exhibiting the characteristics of Model Ib. At $t = 0$ Eq. (III-6) reduces to:

$$dC/dt = K_a F C_o \qquad \text{Eq. (III-34)}$$

From Eqs. (III-33) and (III-34) an approximate value of K_a can be obtained.

(b-iii) Estimation of Parameters Using Numerical Partial Derivatives of C,t Data—Method II:

As seen in the previous section it is not possible to write an expression for an explicit solution of C for Models Ia and Ib, and hence determination of the model parameters by direct application of Eq. (III-25) presents some difficulties. However, it is possible to obtain solutions of Eq. (III-1) by numerical integration and hence to calculate the value of $f(t_u, \theta)$ which is needed for setting up the normal equations. The partial derivatives of $f(t_u, \theta)$ with respect to each parameter can be computed numerically using the following approximation (91):

$$\frac{\partial f(t_u, \theta)}{\partial \theta_r} = \frac{[f(t, (\theta_1 \cdots \theta_r + \Delta_r \cdots, \theta_p) \quad f(t, \theta)]}{\Delta_r} \qquad \text{Eq. (III-35)}$$

for $r = 1, 2, \cdots p$. The right side of Eq. (III-35) is the finite difference analog of the partial derivative of C with respect to θ_r and approaches the derivative as Δ_r approaches zero. A subroutine which computes numerical solutions of differential Eq. (III-1), and numerical partial derivatives of C with respect to each parameter (at t values corresponding to the experimental C values) has been writen (Appendix 5). This subroutine is capable of computing the value of the function and the partial derivatives n times (n is the number of data points) for each iteration performed by the BMDX85 program to refine the parameters.

Method II presents a significant advantage over Method I in that it can also be used to estimate the parameters of Model Ib.

(b-iv) Estimation of the Parameters Using Eq. (III-2) - Method III:

In this approach Y_u of Eq. (III-25) is replaced by t_u and the partial derivatives of t with respect to each parameter are computed for the purpose of setting up the normal equations. The value of the function is calculated using Eq. (III-2) and the partial derivatives are computed using the following equations: (Appendix 6):

$$\frac{\partial t}{\partial K_1} = \frac{2V_m K_1 K_m + V_m^2}{(K_1^2 K_m + K_1 V_m)^2} \ln\left(\frac{CK_1 + K_1 K_m + V_m}{C_o K_1 + K_1 K_m + V_m}\right) - \frac{K_m^2}{(K_1 K_m + V_m)^2} \ln \frac{C_o}{C}$$

$$+ \frac{V_m^2 (C_o - C)}{(K_1^2 K_m + K_1 V_m)(CK_1 + K_1 K_m + V_m)(C_o K_1 + K_1 K_m + V_m)} \qquad \text{Eq. (III-36)}$$

$$\frac{\partial t}{\partial K_m} = -\frac{K_1^2 V_m}{(K_1^2 K_m + K_1 V_m)^2} \ln \left(\frac{CK_1 + K_1K_m + V_m}{C_o K_1 + K_1 K_m + V_m}\right) + \frac{V_m}{(K_1 K_m + V_m)^2} \ln \frac{C_o}{C}$$

$$+ \frac{K_1^2 V_m (C_o - C)}{(K_1^2 K_m + K_1 V_m)(CK_1 + K_1 K_m + V_m)(C_o K_1 + K_1 K_m + V_m)} \qquad \text{Eq. (III-37)}$$

$$\frac{\partial t}{\partial V_m} = -\frac{K_m}{(K_1 K_m + V_m)^2} \ln \frac{C_o}{C} + \frac{K_1 V_m (C - C_o)}{(K_1^2 K_m + K_1 V_m)(CK_1 + K_1 K_m + V_m)(C_o K_1 + K_1 K_m + V_m)}$$

$$+ \frac{K_1^2 K_m}{(K_1^2 K_m + K_1 V_m)^2} \ln \left(\frac{C_o K_1 + K_1 K_m + V_m}{C K_1 + K_1 K_m + V_m}\right) \qquad \text{Eq. (III-38)}$$

and

$$\frac{\partial t}{\partial C_o} = \frac{K_m}{C_o (K_1 K_m + V_m)} + \frac{K_1 V_m}{(K_1^2 V_m + K_1 V_m)(C_o K_1 + K_1 K_m + V_m)} \qquad \text{Eq. (III-39)}$$

It should be pointed out that Method III is limited to estimation of parameters from I. V. PCT data.

(iii) Test of the Proposed Methods: In order to test the applicability of the proposed methods, the parameters from the generated C, t data shown in Figure 14 are calculated.

(a) Estimation of Model Parameters Using Method I: Calculation of model parameters using Method I requires first the computation of - dC/dt values at various t values by numerical differentiation of C, t

data (Appendix 8). $-dC/dt$ values are then divided by the corresponding C values to obtain $-d\ell n\, C/dt$. The latter is plotted against $1/C$ to yield a plot as shown in Figure 16. Using Eqs. (III-20) and (III-21) together with the values of the intercept and the asymptote of the plot of $-d\ell n\, C/dt$ versus $1/C$, K_1, V_m and K_m are calculated. When C,t data represented by curve A of Figure 15 are used to obtain the parameters using this method, the following values are obtained: K_1 = 0.016, V_m = 10.35 and K_m = 52.01. These values are in close agreement with those used as the input in generating C,t data by numerical integration of Eq. (III-1) (Figure 14).

(b) Estimation of Parameters Using Least-squares Procedures

(b-i) Initial Estimates of the Parameters: The first step in obtaining the initial estimates of the parameters is to differentiate numerically C,t data at various t values. $-C/dC/dt$ at various C values are then computed by dividing C by the corresponding $-dC/dt$ values. Table XV shows C,t data represented by curve C of Figure 14

TABLE XV

Calculations of $-C/dC/dt$ Values for Obtaining the Initial Estimates of the Model Parameters, C,t Data is Taken from Curve C of Figure 14

t(hr.)	C(μg./ml.)	$-\frac{dC}{dt}$ ($\frac{\mu g.}{ml/hr.}$)	$-\frac{C}{dC/dt}$ (hr.)
8.0	29.852	4.265	7.004
10.0	22.157	3.465	6.412
12.0	16.013	2.7	5.932

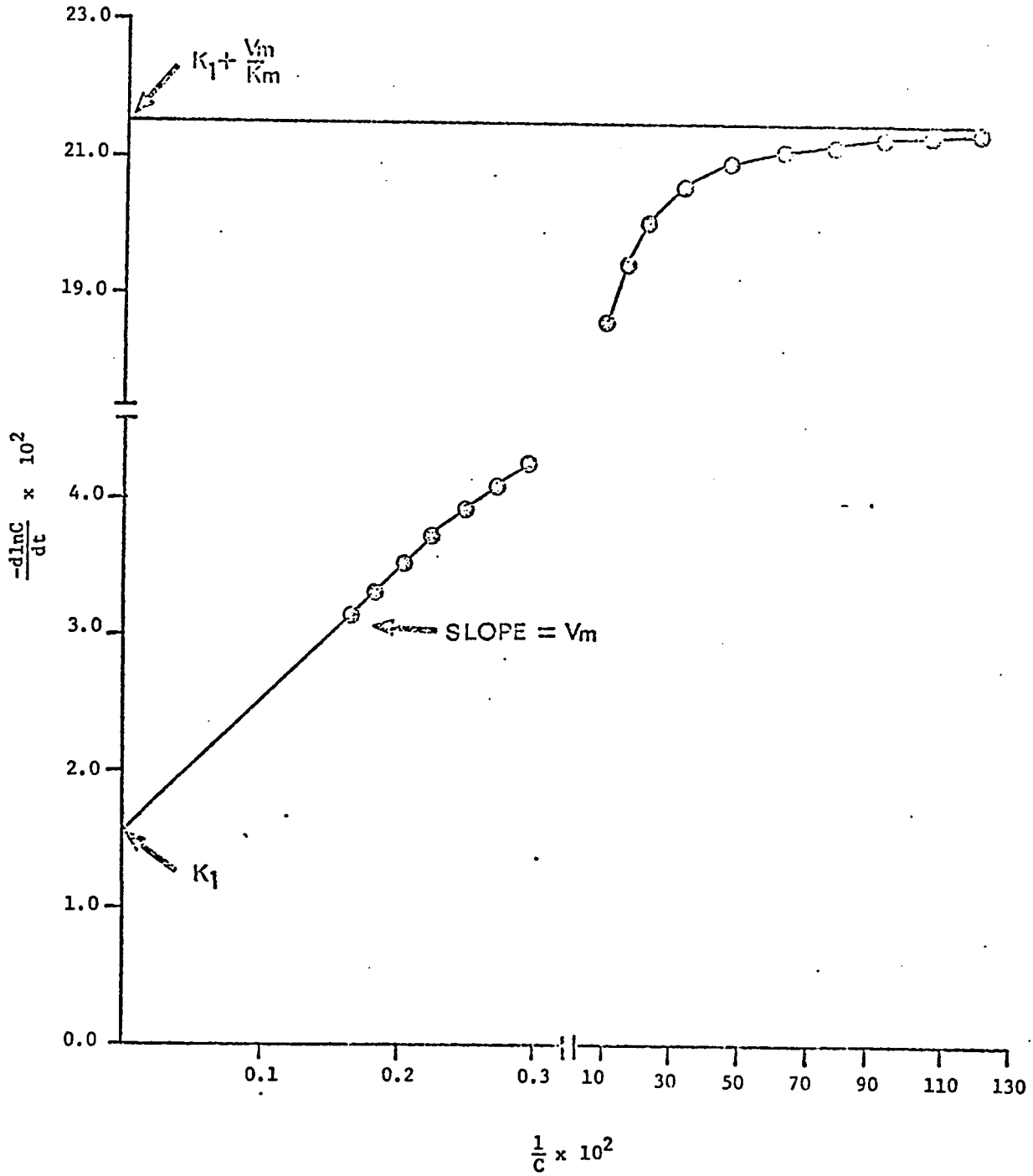

Fig. 16 Plot of $\frac{-dlnC}{dt}$ versus $\frac{1}{C}$ for the data represented by curve A in Fig. 14.

together with -dC/dt and the respective -C/dC/dt values. The latter are fitted to a second degree polynomial in C by means of Boeing computer program FLSQFY (92) (Appendix 9). The equation of the polynomial thus obtained is:

$$-C/dC/dt = 4.642 + 8.223 \times 10^{-2} C - 1.053 \times 10^{-4} C^2 \qquad \text{Eq. (III-40)}$$

Solutions of the coefficients of the above polynomial for model parameters using Eqs. (III-29) through (III-32) leads to the following estimates of the parameters: $K_1 = 0.015$, $V_m = 10.57$ and $K_m = 52.64$. These initial estimates of the parameters are in close agreement with the actual values of the parameters (Figure 14). It should be pointed out that at least three C, t data points are necessary to obtain the estimates of the parameters by this approach. It is found that C values in the neighborhood of K_m result in good initial estimates (for example in Figure 14 data in curve C provides with best estimates of the parameter).

(b-ii) Estimation of Parameters Using Methods II and III: C, t data represented by curve C of Figure 14 are used to calculate the model parameters. Estimation of parameters using Methods II and III is performed by using the computer programs shown in Appendix 5 and 7 respectively on a CDC 6400 computer. Table XVI gives the least-squares estimates of the parameters obtained. It can be seen that both methods give excellent estimates of the parameters.

TABLE XVI

Least-squares Estimates of the Parameters Using the Data Generated with the Following Values: $K_1 = 0.0155$, $V_m = 10.46$, $K_m = 52.3$ and $C_o = 76.92$

	Least-squares Estimates				
	K_1	V_m	K_m	C_o	$S \cdot S \times 10^7$
Method II	0.0154	10.461	52.283	76.911	4.895
Method III	0.0155	10.414	52.237	76.92	1.25

Method I gave the following values of the parameters: $K_1 = 0.016$, $V_m = 10.35$ and $K_m = 52.01$.

3-c Relationships Between Dose and Various Pharmacokinetic Parameters

(i) Dose-AUC Relationship: If absorption, distribution and elimination of a drug can be represented by a system of linear differential equations, the AUC is directly proportional to dose and the constant of proportionality is equal to the clearance of the drug. This linear relationship between dose and AUC provides the basis for bioavailability calculations performed by comparing AUC corresponding to different formulations and/or modes of administration of a drug. Thus the AUC is a useful pharmacokinetic quantity and it becomes important to define the relationship between dose and AUC for a drug exhibiting the characteristics of Model Ia, page 25.

Since it is not possible to write an explicit solution for concentration using the differential equation (III-1), Eq. (III-2) can be used to

derive an expression for $\int_0^\infty Cdt$ by making use of the following relationship:

$$\text{Area } O \rightarrow \infty = \int_0^\infty C\ dt = \int_0^{C_o} t\ dC \qquad \text{Eq. (III-41)}$$

Substituting for t in Eq (III-41) using Eq. (III-2) and integrating the resulting expression yields (Appendix 10):

$$\int_0^\infty C\ dt = \frac{C_o}{K_1} - \frac{V_m}{K_1^2}\ \ell n\ \left[\frac{K_1}{K_2} C_o + 1\right] \qquad \text{Eq. (III-42)}$$

Eq. (III-42) shows that there is no linear relationship between AUC and C_o. Further, Eq. (III-42) predicts a more than porportional increase in AUC with increase in C_o and hence with dose since $C_o = \frac{D_o}{V}$. The simulated C,t data for Model Ia (Figure 14) shows that this is in fact the case. The AUC calculated using the trapezoidal rule for curves A, B, C and D are respectively 13020, 1570, 359 and 25 $\frac{\mu g.\ hr.}{ml.}$ and the corresponding C_o values are 615.38, 153.84, 50.22 and 4.8. Referring to Tables VIII and X, it can be seen that the dose-AUC relationships obtained for meprobamate in several dogs are consistent with the predictions of Eq. (III-42) and the simulated C,t data for Model Ia. Eq. (III-42) with model parameters can be used to compute AUC.

(ii) Dose-elimination Half-life Relationship: The elimination half-life ($T_{\frac{1}{2}}$) of a drug is a useful pharmacokinetic parameter since it represents an index of how rapidly the drug is eliminated from the body.

For drugs showing first-order elimination kinetics, the half-life of elimination is independent of dose.

An expression for $T_{\frac{1}{2}}$ can be derived for a drug exhibiting the elimination characteristics of Model Ia, where half-life is defined as the time needed to reduce a particular amount of drug in the body by one-half. Substituting $C_o/2$ for C in Eq. (III-2) yields the following equation for $T_{\frac{1}{2}}$:

$$T_{\frac{1}{2}} = \frac{1}{K_2}\left[K_m \ell n \frac{C_o}{C_o/2} + \frac{V_m}{K_1} \ell n \frac{(C_o + K_m)K_1 + V_m}{(C_o/2 + K_m)K_1 + V_m}\right] \qquad \text{Eq. (III-43)}$$

or

$$T_{\frac{1}{2}} = \frac{0.693\, K_m}{K_2} + \frac{V_m}{K_1} \ell n \frac{(C_o + K_m)K_1 + V_m}{(C_o/2 + K_m)K_1 + V_m} \qquad \text{Eq. (III-44)}$$

The second term in Eq. (III-44) contains C_o and hence $T_{\frac{1}{2}}$ is a function of C_o. Eq. (III-44) also predicts an increase in $T_{\frac{1}{2}}$ with C_o. This behavior is apparent from the plots of simulated date (Figure 14) and of meprobamate data (Figures (5-8, 10-12) and Table (VIII)).

When $C << K_m$, an equation for $T_{\frac{1}{2}}$ is derived as follows: Substituting $C_o/2$ for C in Eq. (III-8) results in:

$$\frac{C_o}{2} = C_o\, e^{-\left(K_1 + \frac{V_m}{K_m}\right) T_{\frac{1}{2}}} \qquad \text{Eq. (III-45)}$$

Cancelling the like terms in Eq. (III-45) and rearranging the resulting expression gives:

$$T_{\frac{1}{2}} = \frac{0.693}{K_1 + \frac{V_m}{K_m}} \qquad \text{Eq. (III-46)}$$

Eq. (III-46) shows that when $C << K_m$, $T_{\frac{1}{2}}$ is independent of the concentration of the drug in the body and that drug elimination occurs by an apparent first-order process. An illustration is seen in the plots of $\ell n\ C$ versus t when $C << K_m$ (curve D, Figure 14). Also, the meprobamate half-lives calculated from the terminal portions of the plots in Figures 5-8 (Table XIV) are consistent with the prediction of Eq. (III-46).

When $C >> K_m$, $T_{\frac{1}{2}}$ can be calculated by substituting $C_o/2$ for C in Eq. (III-10):

$$\frac{C_o}{2} = (C_o + \frac{V_m}{K_m})\, e^{-K_1 T_{\frac{1}{2}}} - \frac{V_m}{K_1} \qquad \text{Eq. (III-47)}$$

Rearranging the above equation and solving the resulting expression for $T_{\frac{1}{2}}$ gives:

$$T_{\frac{1}{2}} = \frac{1}{K_1}\ \ell n\ \left(\frac{C_o + V_m/K_m}{C_o/2 + V_m/K_1}\right) \qquad \text{Eq. (III-48)}$$

According to Eq. (III-48), that when $C >> K_m$, $T_{\frac{1}{2}}$ increases with C_o. The C, t data represented in Figure 14 and the plots in Figures 5-8 are consistent with this result.

(iii) Fraction of a Dose Excreted Unchanged in Urine: When the elimination of a drug occurs by exponential processes, the fraction of the

dose excreted unchanged in urine is a constant. The differential equation representing the excretion of unchanged drug for Models Ia and Ib can be written as:

$$\frac{1}{V}\frac{dA_u}{dt} = K_e C \qquad \text{Eq. (III-49)}$$

where K_e is the first-order rate constant for urinary excretion of unchanged drug and A_u is the cumulative amount of unchanged drug eliminated in urine at any time t. Integration of Eq. (III-49) from $t = 0$ to ∞ results in the following expression for the total amount of unchanged drug found in urine $(A_u)^{\infty}$:

$$A_u^{\infty} = K_e V \int_o^{\infty} C\, dt \qquad \text{Eq. (III-50)}$$

The integral in Eq. (III-50) represents AUC. As shown by Eq. (III-42) an increase in dose produces a more than proportional increase in AUC for drugs exhibiting the characteristics of Model Ia. Hence with an increase in dose, a more than proportional increase in $(A_u)^{\infty}$ is expected since $K_e V$ is a constant in Eq. (III-50). As a result, the fraction of a dose excreted unchanged in urine should increase with an increase in dose. Tables XI and XIII show that in case of I. V. and oral administration of meprobamate the fraction of the dose excreted unchanged increases with dose.

(iv) Fraction of a Dose Excreted as a Metabolite in Urine: The fraction of a dose ultimately found in urine as a particular metabolite

remains constant with dose if a) the overall elimination of a drug occurs according to a first-order process, b) the excretion rate of the metabolite is much greater than its formation rate and c) the metabolite does not undergo any further chemical changes before it is excreted in urine.

The following differential equation can be written to represent the excretion rate of a metabolite for Models Ia and Ib:

$$\frac{1}{V}\frac{dA_m}{dt} = K_m C \qquad \text{Eq. (III-51)}$$

where K_m is the first-order rate constant for the formation of the metabolite and A_m is the amount found in the urine at any time t. In writing Eq. (III-51) it is assumed that formation rate of the metabolite is much larger than the excretion rate and the metabolite does not undergo any further chemical changes before excretion in urine. Integration of Eq. (III-51) from 0 to ∞ results in the following expression for the total amount of drug excreted as a particular metabolite in urine $(A_m)^{\infty}$:

$$(A_m)^{\infty} = K_m V \int_0^{\infty} C \, dt \qquad \text{Eq. (III-52)}$$

In Eq. (III-52) $K_m V$ is a constant and according to Eq. (III-42) $\int_0^{\infty} C \, dt$ increases more than proportionately with dose. Therefore, an increase in dose produces a more than proportional increase in $(A_m)^{\infty}$ and hence in the fraction of the dose excreted as a particular metabolite. This observation is similarly true for all metabolites which are formed according to a first-order process. As shown above in section (iii),

this relationship is also true for the fraction excreted unchanged in urine through an exponential process. Therefore, it can be deduced that the fraction of the dose eliminated by a capacity-limited process decreases with increase in dose.

In sections 3-a and 3-c of this chapter, four characteristics of Models Ia and Ib, namely the nature of I. V. and oral curves and the relationships between dose and AUC, $T_{\frac{1}{2}}$, and $(A_u)^{\infty}$ have been considered and compared with the corresponding experimental results for meprobamate. From the agreement between theoretical expectations and experimental findings it may be concluded that Models Ia and Ib are appropriate to describe the pharmacokinetics of meprobamate in dog.

3-d Bioavailability Calculations for Drugs Showing Simultaneous First-order and Capacity-limited Elimination Kinetics

(i) Introduction: Bioavailability is a term used to indicate the rate and relative amount of an administered drug which reaches the general circulation intact (93). The determination of bioavailability is becoming a recognized method for evaluating the equivalence of drug products containing the same pharmacological agents. There exist several methods for estimating bioavailability. These methods have been classified into two major groups, namely pharmacokinetic and clinical methods (94). In general the former are more discriminating than the latter and have, therefore, received wide acceptance. Most pharmacokinetic methods assume kinetic linearity and, hence are applicable only to drugs whose

pharmacokinetic behavior can be represented by a set of linear differential equations. Common methods of estimating bioavailability from plasma level measurements are based on the Dost's principle of corresponding areas (95) from which one can derive the following expression for F:

$$F = \frac{[\int_0^\infty C\,dt]_{oral}}{[\int_0^\infty C\,dt]_{I.V.}} \qquad \text{Eq. (III-53)}$$

where F is the fraction of the dose absorbed.

Eq. (III-53) assumes that dose/AUC or clearance of a drug is dose-independent, which is not the case for a drug exhibiting the characteristics of Models Ia and Ib and consequently its use in these models will yield erroneous values of F. Large errors can be involved in calculating the extent of absorption from non-linear data by assuming linear kinetics as will shown using the C, t data of Figures 14 and 15. Since several drugs including meprobamate exhibit simultaneous first-order and capacity-limited elimination kinetics, it should be useful to develop generalized method for bioavailability calculations and demonstrate its application for Models Ia and Ib.

(ii) Principle of the Proposed Method: The principle of the proposed method of bioavailability calculations make use of the fact that the area under the curve of a plot of $-\frac{dC}{dt}$ versus t obtained after I. V. bolus administration of a drug is directly proportional to dose, the

constant of proportionality being $\frac{1}{V}$. This proportionality can be seen from the following relationships:

$$\int_o^\infty -\frac{dC}{dt}\,dt = -\int_o^\infty dC = -[0 - C_o] = \frac{D_o}{V} \qquad \text{Eq. (III-54)}$$

Hence one can determine C_o by numerical differentiation of C, t data to yield $-\frac{dC}{dt}$ at various t values and by measurement of the area under the curve of a plot of $-\frac{dC}{dt}$ versus t. A plot of this area versus C_o will be linear with a slope of one and will pass through the origin.

The rate of elimination of a drug from the body after oral administration of a dose D_o for a drug exhibiting the characteristics of Model Ib is given by

$$\frac{1}{V}\frac{dA_e}{dt} = K_1 C + \frac{V_m C}{K_m + C} \qquad \text{Eq. (III-55)}$$

where A_e is the amount of drug eliminated at any time t. If the amount eliminated is equal to the amount absorbed, then:

$$\frac{1}{V}\int_o^\infty \frac{dA_e}{dt}\,dt = \int_o^\infty \left(K_1 C + \frac{V_m C}{K_m + C}\right) \qquad \text{Eq. (III-56)}$$

$$= \frac{FD}{V} = FC_o$$

Hence, the area under a plot of $\frac{1}{V}\frac{dA_e}{dt}$ versus t provides an estimate of FC_o. The values of $\frac{dA_e}{dt}$ at various times are calculated by use of the equation parameters namely K_1, V_m and K_m in conjunction with oral C, t data.

When equal doses of a drug are administered, the fraction of the dose absorbed after oral administration is obtained from Eqs. (III-54) and (III-56):

$$F = \frac{FC_o}{C_o} = \frac{\left[\frac{1}{V}\int_o^\infty \frac{dA_e}{dt}\,dt\right]_{oral}}{\left[\int_o^\infty -\frac{dC}{dt}\,dt\right]_{I.V.}} \qquad \text{Eq. (III-57)}$$

(iii) Construction of Percent Absorbed vs Time Plots and Calculation of Absorption Rate: In many instances it is desirable to calculate not only the extent of absorption but also the rate at which the drug is absorbed from the gastrointestinal tract. It can be shown that for a drug exhibiting the characteristics of Model Ib, the percent absorbed up to any time t, $\frac{At}{FD_o} \times 100$, is given by (Appendix 11):

$$\frac{A_t}{FD} \times 100 = \frac{C + \int_o^t \left(K_1 C + \frac{V_m C}{K_m + C}\right) dt}{\int_o^\infty \left(K_1 C + \frac{V_m C}{K_m + C}\right)\,dt} \qquad \text{Eq. (III-58)}$$

where A_t is the amount absorbed up to time t. The percent remaining to be absorbed, $F_t \times 100$, can be written as (Appendix 11):

$$F_t \times 100 = \left(1 - \frac{A_t}{FD}\right) \times 100 \qquad \text{Eq. (III-59)}$$

Hence, if the absorption of a drug occurs by a first-order process, the plot of $\ell n\ (F_t \times 100)$ versus time will be linear with a slope equal to

the apparent first-order absorption rate constant.

(iv) Application of the Proposed Bioavailability Calculations Method for Simulated (C, t) Data of Models Ia and Ib: C, t data, examples of which are shown in Figures 14 and 15 are used to calculate the extent of absorption by Eq. (III-57). The integral in Eq. (III-54) which is the denominator of Eq. (III-57) is calculated for each I. V. curve by numerical differentiation of C, t data and evaluating the integral by the trapezoidal rule. The results are shown in Table XVII (column IV). It can be seen that for each C_o the relationship of Eq. (III-54) is obeyed (columns IV and I yield equal values). $\frac{1}{V}\frac{dA_e}{dt}$ in Eq. (III-55) is calculated with K_l, V_m and K_m values obtained from Method I in conjunction with the oral C, t data. FC_o is then calculated using Eq. (III-56) (column VIII). The fraction of the dose absorbed F, is calculated according to Eq. (III-57) and in all instances it is found identical to the actual F values used as input in generating the oral data (column IX). The fraction of the dose absorbed is also calculated according to Eq. (III-53) which assumes linear kinetics (column X) and the percent error involved in this approach is shown in column XI. As expected, the larger the dose, the larger is the error.

Since various formulations of a drug have different release characteristics and hence varying absorption rates, computer simulations are performed to study the role of K_a. As seen in Table XVII the larger K_a, the smaller is the error when F is held constant. Additional simulations using an oral standard preparation (C_o = 615.38, F = 0.9,

TABLE XVII

Calculation of F by Using Eq. (III-57) and Effect of C_o, K_a and F on the Error Involved in Calculation of the Fraction of Dose Absorbed by Using Eq. (III-53)

I	II	III	IV	V	VI	VII	VIII	IX	X	XI
C_o	$\int_o^\infty Cdt$ I. V.	$[\frac{\int_o^\infty Cdt}{C_o}]$ I. V.	$[\int_o^\infty -\frac{dc}{dt}dt]$ I. V.	K_a	F_{Actual}	$[\int_o^\infty Cdt]$ oral	$[\frac{1}{V}\int_o^\infty \frac{dA_e}{dt}dt]$ oral	From Eq. (III-57) $F=\frac{VIII}{IV}$	From Eq. (III-53) $F=\frac{VII}{II}$	% Error in F (Calculated in Column X)
615.38	13020.0	21.158	615.28	0.3	0.4	2834.0	245.8	0.4	0.218	45.5
615.38	13020.0	21.158	615.28	0.3	0.6	5403.0	368.5	0.6	0.415	30.83
615.38	13020.0	21.158	615.28	0.9	0.4	3064.0	245.4	0.4	0.253	36.75
153.84	1570.0	10.205	153.78	0.3	0.4	385.1	61.48	0.4	0.245	38.75
153.84	1570.0	10.205	153.78	0.3	0.6	659.0	92.18	0 6	0.420	30.00
153.84	1570.0	10.205	153.78	0.9	0.4	413.5	61.4	0.4	0.263	34.25
50.22	359.0	7.149	50.10	0.3	0.4	103.15	20.06	0.4	0.287	28.25
50.22	359.0	7.149	50.10	0.3	0.6	162.65	30.09	0.6	0.453	24.5
50.22	359.0	7.149	50.10	0.9	0.4	106.48	20.04	0.4	0.296	26.0
4.8	25.0	5.208	4.79	0.3	0.4	8.987	1.917	0.4	0.36	10.0
4.8	25.0	5.208	4.79	0.3	0.6	13.548	2.876	0.6	0.542	9.67
4.8	25.0	5.208	4.79	0.9	0.4	8.998	1.914	0.4	0.36	10.0

$K_l = 0.0155$, $K_m = 52.31$, $V_m = 10.46$ and $K_a = 1.2$) show that when K_a for the test preparation is increased from 0.1 to 0.3 and 0.9 the % error (calculated as in column XI of Table XVII) decreases from 19.4 to 5.2 and 0.6 respectively. Some important practical considerations can be derived from these predictions. The error involved in using Eq. (III-53) to perform bioavailability calculations for a drug exhibiting the elimination characteristics of Models Ia and Ib can be minimized if the standard and test preparation are used at the same dose and if they exhibit similar plasma level versus time curves (i.e., similar to K_a and F values).

In order to test the practical applicability of the proposed method of bioavailability calculation random errors of 1%, 5%, and 10% are introduced into the C values (14 sampling times, 2 hr. apart) of curve C of Figure 14 and in the corresponding oral data with $K_a = 0.9$ and $F = 0.4$ (Table XVIII). The error in

$$-\int_0^{28\ \text{hr.}} \frac{dC}{dt}\, dt$$

increases as the error introduced in the C values increases. Such a trend is not apparent in the calculation of

$$\frac{1}{V}\int_0^{28\ \text{hr.}} \frac{dA_e}{dt}\, dt \ .$$

The resulting error in F (calculated using Eq. (III-57) is also found to increase as the error in the C values increases, but more important,

TABLE XVIII

Calculation of F Using Simulated C,t Data with Random Error

Random Error in C (%)	$[-\int_0^{28\text{ hr.}} \frac{dC}{dt}\,dt]$ [a]	$\frac{1}{V}[\int_0^{28\text{ hr.}} \frac{dA_e}{dt}\,dt]$ [b]	Error in F (%) (F Calculated Using Eq. (III-57)	Error in F (%) (F Calculated Using Eq. (III-53)
1.0	49.296	18.99	3.7	24.12
5.0	48.282	19.264	3.99	38.23
10.0	47.016	19.617	4.3	44.0

[a] $[-\int_0^{\infty} \frac{dC}{dt}\,dt] = C_o = 50.22$

[b] $\frac{1}{V}[\int_0^{\infty} \frac{dA_e}{dt}\,dt] = FC_o = 20.09$

random error as large as 10% cause less than 5% error in F. The fraction of the dose absorbed is also calculated according to Eq. (III-53) and the resulting error (Table XVIII, column 5) is much larger than the corresponding error involved in the proposed method.

Figure 17 shows two plots of percent of drug remaining to be absorbed versus time for two K_a values, constructed according to Eq. (III-59). The plots are found to be linear and the apparent absorption rate constants calculated from the slope of the plots are exactly equal to those used to generate oral C,t data by using Eq. (III-4), thus indicating the validity of Eq. (III-59).

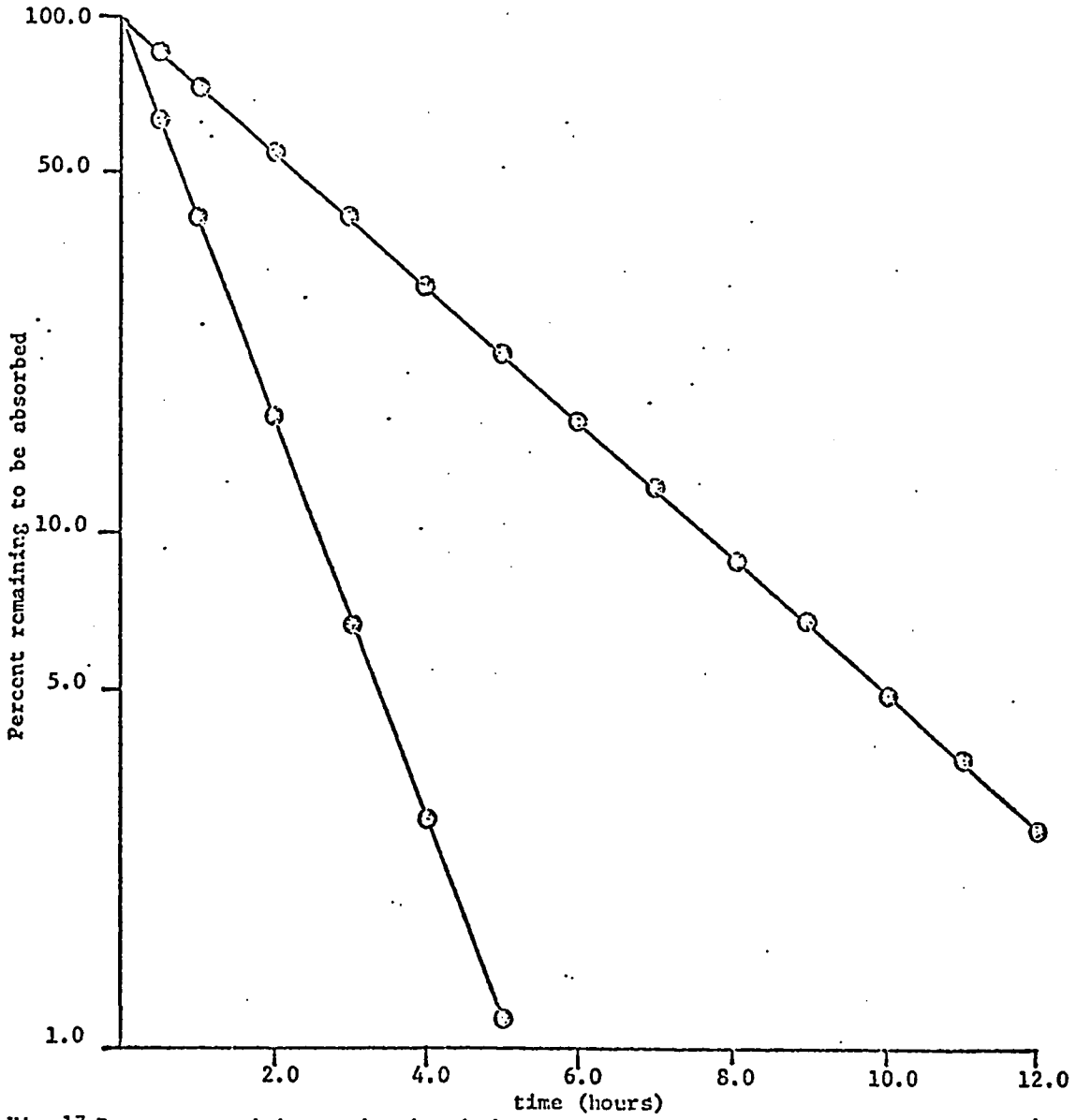

Fig. 17 Percent remaining to be absorbed - Time plots constructed according to Eq. (III-59) for two sets of C,t data generated using Eq. (III-6. Ka calculated from the slopes of the plots are 0.9 and 0.3 which are exactly equal to those used to generate the C.t data.

3-e Drug Accumulation Characteristics of Model Ia

(i) Continuous I. V. Zero-order Infusion: Generally, the simplest case to consider in analyzing the accumulation characteristics of a drug in the body is the situation where the input rate is zero-order. When a drug is infused into a system at a constant rate and is eliminated at an exponential rate, the drug will accumulate until a steady state is achieved. At steady state the input rate to the system is equal to the output rate from the system. This principle, also called the plateau principle, is the basis of several dosage regimen calculations when drug elimination occurs by exponential processes. In this section, drug accumulation characteristics will be examined in the case of elimination by simultaneous first-order and capacity-limited elimination kinetics.

(a) Infusion Curve Equations: Scheme 5, Model II represents a one compartment body model where drug elimination after constant

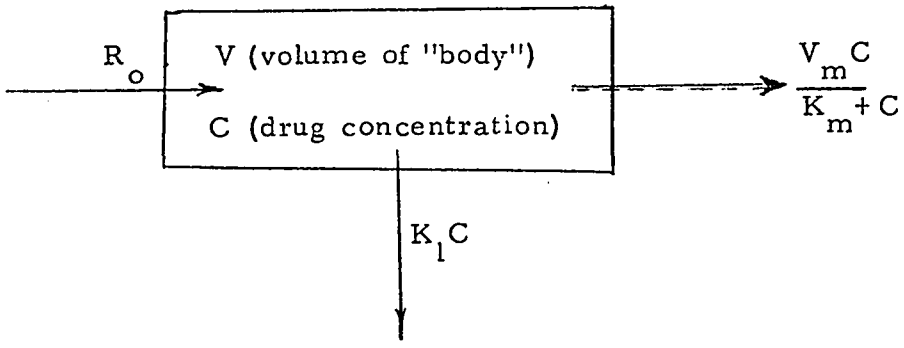

Scheme 5: Model II

intravenous infusion (R_o in mg./hr.) occurs by simultaneous first-order and capacity-limited elimination kinetics. The differential equation

representing the concentration of the drug in the body at any time t is written as:

$$\frac{dC}{dt} = \frac{R_o}{V} - K_1 C - \frac{V_m C}{K_m + C} \qquad \text{Eq. (III-60)}$$

The integrated form of Eq. (III-60) gives rise to (Appendix 12):

$$t = \left[\frac{X + 2K_1 K_m}{2K_1}\right] \frac{K_m}{(\epsilon + X^2)^{1/2}} \log\left[\frac{-2K_1 C(X+\sqrt{X^2+\epsilon})+\epsilon}{-2K_1 C(X-\sqrt{X^2+\epsilon})+\epsilon}\right]$$

$$+ \frac{1}{2K_1} \log\left[\frac{\frac{R_o K_m}{V}}{\frac{R_o K_m}{V} + VC - K_1 C^2}\right] \qquad \text{Eq. (III-61)}$$

where $X = \frac{R_o}{V} - K_1 K_m - V_m$ Eq. (III-62)

and $\epsilon = \frac{4R_o K_1 K_m}{V}$ Eq. (III-63)

It is not possible to write an explicit solution for C and hence, to calculate C at a given t, one has to resort to numerical integration of Eq. (III-60).

(b) Steady-State Concentration: When a drug is infused into the body at a constant rate and is eliminated only by a capacity-limited process, a steady state is not achieved when $\frac{R_o}{V} > V_m$ and drug accumulation will occur without an upper limit. However, for the scheme represented in Model II, a plateau is always reached because of the first-order process which operates in parallel with the capacity-limited

process. At steady-state $\frac{dC}{dt} = 0$, and Eq. (III-60) becomes

$$\frac{R_o}{V} = K_1 C^* + \frac{V_m C^*}{K_m C^*} \qquad \text{Eq. (III-63)}$$

where C^* represents steady-state concentration of the drug. Rearranging Eq. (III-63) and substituting K_2 for $K_1 K_m + V_m$ results in a quadratic expression for C^*.

$$K_1 C^{*2} + (K_2 - \frac{R_o}{V}) C^* - K_m \frac{R_o}{V} \quad 0 \qquad \text{Eq. (III-64)}$$

whose roots are:

$$C^* = \frac{-K_2 + \frac{R_o}{V} \pm \sqrt{(K_2 - \frac{R_o}{V})^2 + \frac{4K_m K_1 R_o}{V}}}{2K_1} \qquad \text{Eq. (III-65)}$$

Eq. (III-65) can be used to predict the steady-state levels at various infusion rates of a drug, if one root of C^* can be eliminated. A careful look at Eq. (III-65) reveals that the only realistic root of C^* is:

$$C^* = \frac{-K_2 + \frac{R_o}{V} + \sqrt{(K_2 - \frac{R_o}{V})^2 + \frac{4K_m K_1 R_o}{V}}}{2K_1} \qquad \text{Eq. (III-66)}$$

The other root of C^* always gives a negative value for C^* since the quantity under the square root sign is always greater than $|-K_2 + \frac{R_o}{V}|$. When $\frac{R_o}{V} = K_2$ Eq. (III-66) simplifies to:

$$C^* = [\frac{K_m R_o}{K_1 V}]^{\frac{1}{2}} \qquad \text{Eq. (III-67)}$$

Eq. (III-66) and (III-68) show that C^* is a function of the infusion rate and the elimination parameters.

(c) Time to Reach Steady-State: An expression for the time (t') to reach steady state can be obtained by substituting for C in Eq. (III-61) by C^* from Eq. (III-66). Such a substitution reveals that steady state is achieved at infinite time (Appendix 12). However, one can obtain an expression for the time to reach a certain fraction (F) of the steady-state concentration by substituting C^* from Eq. (III-66) for C in Eq. (III-61). The following equation for t'_f is obtained (Appendix 12):

$$t'_f = \left[\frac{X+2K_1K_m}{2K_1}\right] \frac{K_m}{(\epsilon+X^2)^{\frac{1}{2}}} \log\left[\frac{-F(X+(X^2+\epsilon)^{\frac{1}{2}})^2+\epsilon}{\epsilon(F+1)}\right]$$

$$+ \frac{1}{2K_1} \log \frac{R_o K_m}{\frac{R_o K_m}{V} + \frac{F}{2K_1}\left[X+(X^2+\epsilon)^{\frac{1}{2}}\right]\left[X-\frac{F}{2}(X+(X^2+\epsilon)^{\frac{1}{2}}\right]} \qquad \text{Eq. (III-68)}$$

Eq. (III-68) shows that t'_f is a complex function of infusion rate and the elimination parameters. When the elimination of a drug occurs by exponential processes, the time needed to reach a certain percent of steady-state is independent of infusion rate and solely dependent on the elimination rate constant(s).

(d) Computer Simulations: Figure 18 shows the concentration-tim curves generated at various infusion rates using numerical integration of Eq. (III-60) using the same salicylate parametes as previously (78). At all infusion rates an apparent steady-state is achieved but the time

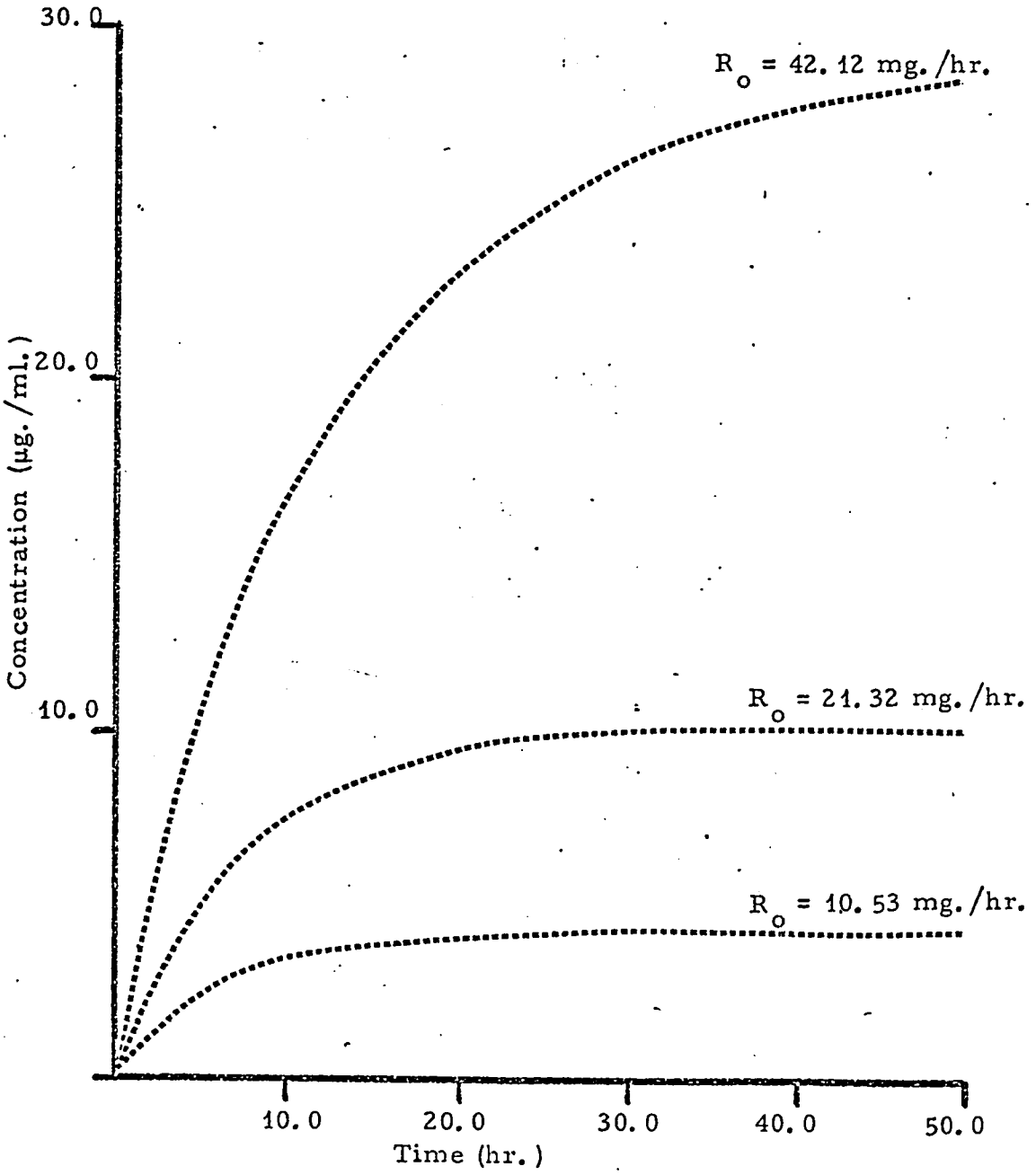

Figure 18. Computer simulated infusion curves for Model II.

needed to reach a certain percent of the steady-state concentration increases with the infusion rate. Further, doubling the infusion rates results in more than twice the original steady-state level. This can be clearly seen in Table XIX which gives the percent change in apparent

TABLE XIX

Effect of Infusion Rates on Steady-State Levels

$\frac{R_o}{V}$ Changed From	To	% Increase in Apparent C*
1.0	2.0	219.2
2.0	4.0	245.2
5.0	10.0	382.4
10.0	20.0	444.7
15.0	30.0	340.6
30.0	60.0	248.9
35.0	70.0	239.7

The value of K_2 in the above simulations is 11.27.

steady-state levels resulting from doubling the infusion rates. An interesting observation which has some important clinical implications can be made from these simulations. Doubling the infusion rate (or dose) when its value is in the neighborhood of K_2V results in the largest increase in the steady-state level. At small and large infusion rates (in comparison to K_2V) the increase in steady-state level by doubling the infusion rate is more than proportional but relatively less drastic.

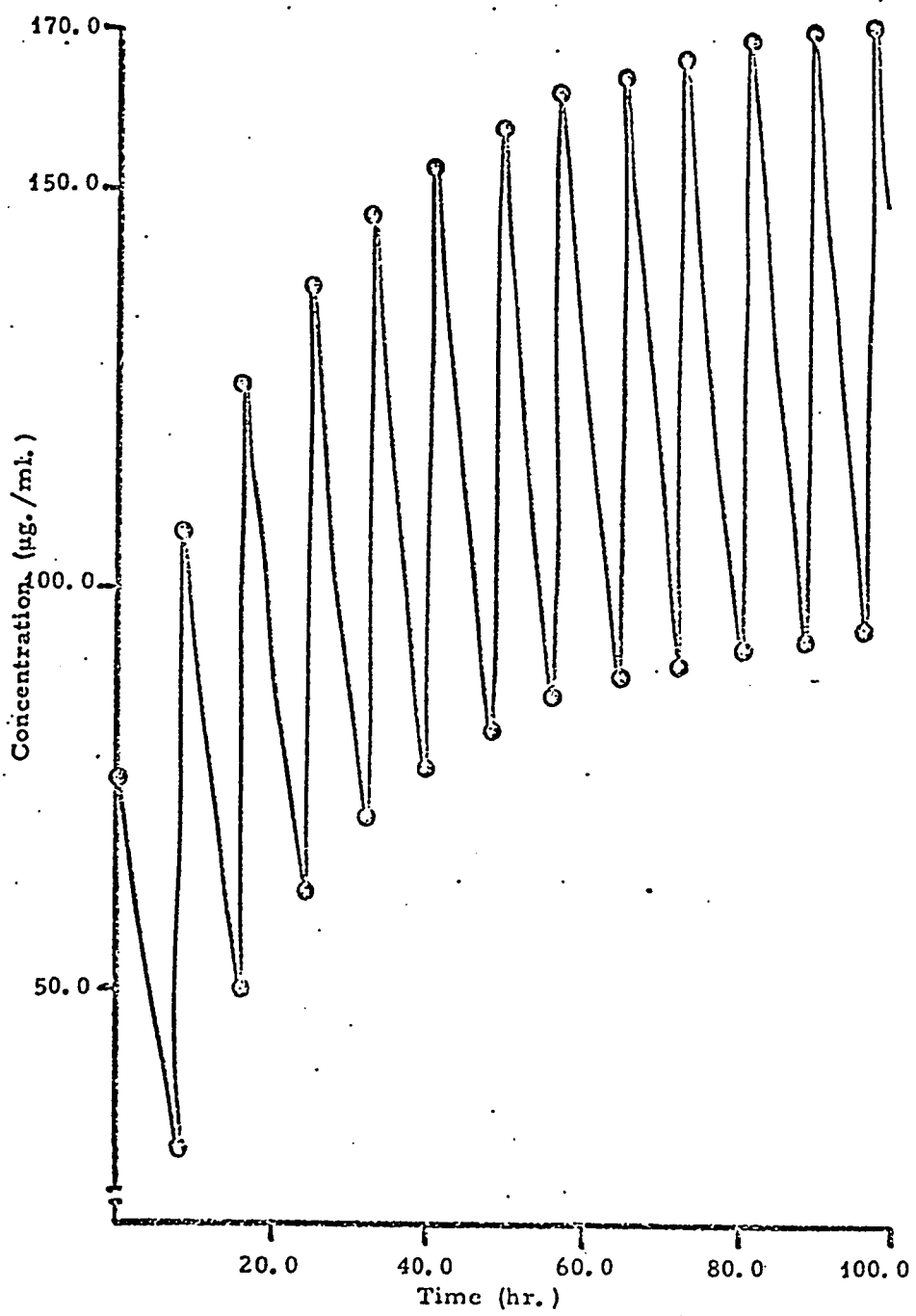

Figure 19. Computer simulated curve showing PCT data during fixed dose-fixed time schedule.

(ii) Discontinuous I. V. Modes of Administrations

(a) Fixed Dose—Fixed Time Schedules: Under a fixed dose (D_o)—fixed time (T) schedule, the accumulation characteristics of a drug exhibiting simultaneous first-order and capacity-limited elimination kinetics are similar to these described under constant infusion except that in this case, the concentration-time curve exhibit a maxima and minima. Figure 19 shows a typical concentration-time curve expected after administration of equal I. V. doses of 500 mg. of aspirin at constant time intervals of 8 hr. (Appendix 13). An apparent steady-state is eventually achieved and at steady state

$$(C_{max.} - C_{min.})\, V = D_o \qquad \text{Eq. (III-69)}$$

The average concentration at steady state ($\bar{C}$) can be estimated by substitution of D_o/T for R_o in Eq. (III-66):

$$\bar{C} = \frac{-K_2 + \frac{D_o}{TV} + \sqrt{(K_2 - \frac{D_o}{TV})^2 + \frac{4K_m K_1 D_o}{TV}}}{2K_1} \qquad \text{Eq. (III-70)}$$

The above equation allows calculation of $\bar{C}$ in Figure 19 where $\bar{C} = 147.367 \frac{mcg.}{ml.}$. This value is consistent with $C_{max.}$ and $C_{min.}$ values of 170.41 and 93.44 respectively.

(b) Priming Dose—Maintenance Dose Schedules: In those cases where an effective drug concentration must be rapidly achieved, the administration of a priming dose becomes necessary. If C_o is the concentration obtained after administration of a priming dose D_o and if

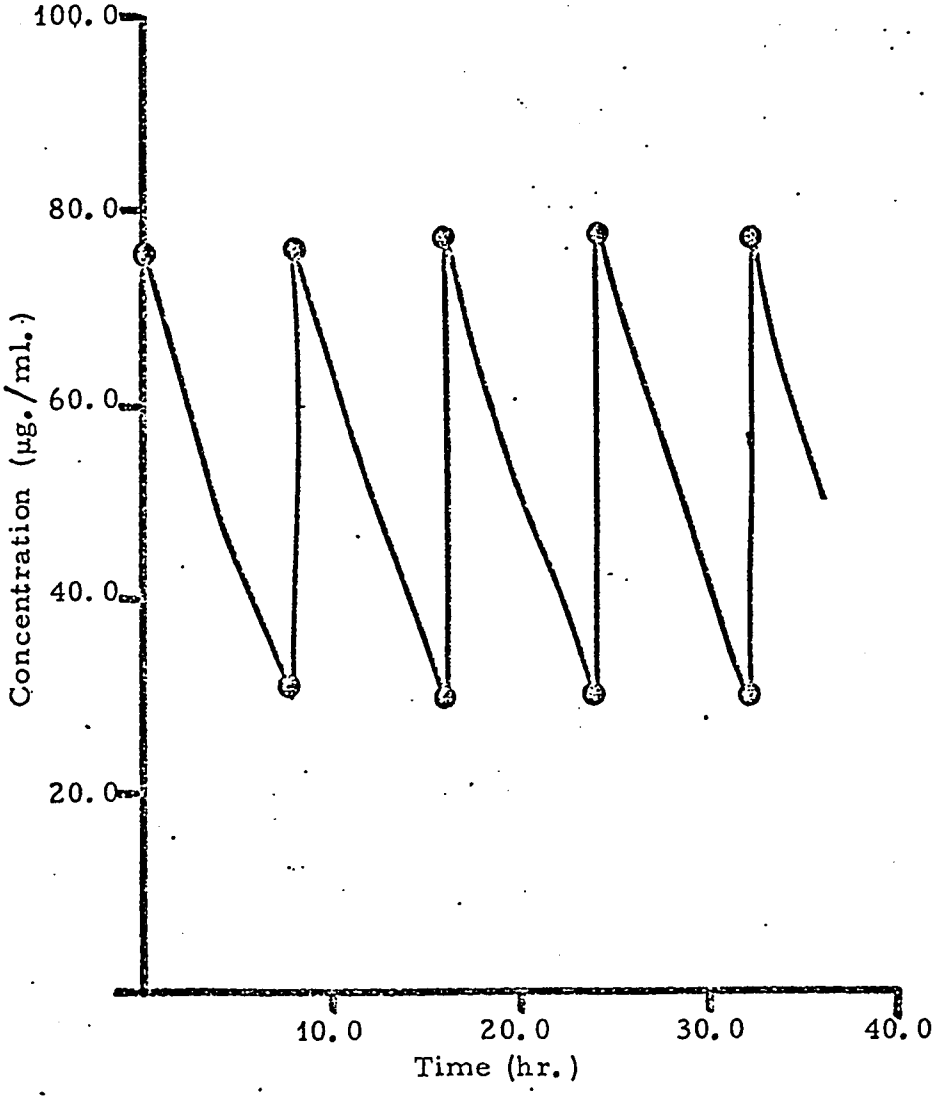

Figure 20. Computer simulated curve showing PCT data during priming dose-maintenance dose schedule.

$C_{eff.}$ represents the minimum effective concentration, the time needed for the body to eliminate an amount equal to $V(C_o - C_{eff.})$ can be calculated by using Eq. (III-2) or by numerical methods which compute the time needed for C_o to decrease to $C_{eff.}$ (Appendix 14). Figure 20 shows a typical concentration-time curve obtained after I. V. administration of a priming dose of 500 mg. of aspirin followed by a maintenance dose of 305.8 mgm. every 8 hr. These simulations demonstrate a way of performing dosage regimen calculations for a drug exhibiting simultaneous first-order and capacity-limited elimination kinetics.

III - 4 ESTIMATION OF PHARMACOKINETIC PARAMETERS FROM I. V. PCT DATA IN DOGS

In section 3-b of this chapter three methods are presented for the estimation of the parameters of Model Ia. In the case of meprobamate, Method I cannot be used since Eq. (III-9) is found to be invalid even at the large concentrations achieved with a 50 mg./kg. dose. Hence Methods II and III are used for the estimation of parameters.

Table XX lists the pharmacokinetic parameters obtained using Method III from the (C, t) data shown in Figures 5 through 8. The continuous curves of Figures 5 through 8 are the theoretical PCT curves generated using the parameters listed in Table XX. It can be seen from these figures that the fit is adequate and that the data points are distributed on either side of the theoretical curves with no systematic trend. It becomes apparent therefore that the differential equation (III-1) of

TABLE XX

Equation Parameters for PCT Data Obtained After I. V. Bolus Administration of the Drug

Dog No.	Dose ($\frac{mg.}{kg.}$)	K_1 (hr^{-1})	K_m ($\frac{\mu g}{ml.}$)	V_m ($\frac{\mu g}{ml.hr.}$)	C_o ($\frac{\mu g}{ml.}$)
510	7	0.265	8.289	2.34	10.10
510	10	0.164	10.94	2.15	10.31
510	30	0.146	2.282	2.12	42.6
510	50	0.099	11.47	2.15	65.07
970	7	0.321	16.22	1.89	7.25
970	10	0.242	16.30	2.12	7.348
970	30	0.085	5.91	3.00	29.64
970	50	0.128	0.899	1.88	57.59
1065	7	0.329	10.36	1.89	7.5
1065	10	0.319	9.44	2.33	13.58
1065	30	0.08	1.68	1.89	30.45
1065	50	0.064	0.01	3.41	65.49
1122	7	0.424	14.835	2.95	8.66
1122	10	0.212	11.76	2.95	8.96
1122	30	0.224	12.25	1.49	43.05
1122	50	0.122	0.045	2.58	67.15

Model Ia adequately represents the change in concentration of meprobamate with respect to time.

The parameters K_1, V_m and K_m shown in Table XX seem to vary in no orderly fashion as the dose changes. Thus these parameters are no longer unique parameters of the model but are merely empirical parameters of Eq. (III-1). Greater variations in parameters with dose

was found when Method II was used to estimate the parameters. In order to determine the cause for this variation in parameters, several computer simulations were performed on generated C, t data with random errors. When C, t data have error, the parameters vary considerably. Large errors (> 10%) cause wide variations in parameters and eventual disappearance of one parameter, which one depending upon the concentration region used. The variation in parameters with error is a function of number of data points. Large number of data points distributed over a wide concentration range could tolerate more error than a small number of data points distributed in a narrow concentration range. The relative values of the parameters can be another cause of large variations in the parameters in the presence of random errors. When there is a high correlation between the parameters, compensation of one with another occurs during the solution of the normal equations (III-25). The degree of correlation can be determined from the correlation coefficients of the parameters which appear in the output from the main computer program.

The variations in parameters with dose in the case of meprobamate is due to the following reasons: a) There is approximately 1 - 5% error in plasma concentration values which occur during the quantitative determination of the drug, b) Due to the "bumps" in the initial portions of the PCT curves obtained at 30 and 50 mg./kg. doses, only those data points obtained after 2 hr. can be used, and c) The parameters show a high correlation coefficient and the BMDX 85 computer program used for solving the normal equations cannot prevent the compensation of

the parameters of Eq. (III-1). In a few instances, one of the parameters tended towards zero, in which case it was fixed to its initial estimate. Fixing of the parameter to the initial estimate value was necessary because disappearance of a parameter will lead to a different differential equation and hence to a different model which is not consistent with the experimental results.

The major problem presented by the variation of parameters with dose is that they become inappropriate as model parameters and therefore have no physiological meaning. Hence, instead of being unique model parameters, they become equation parameters. However, these parameters can still be used for the purpose of bioavailability calculations and predictions of multiple dose levels as illustrated in the following sections.

III - 5 USE OF EQUATION PARAMETERS IN BIOAVAILABILITY CALCULATIONS AND IN PREDICTIONS OF DRUG LEVELS DURING MULTIPLE DOSING

5-a Bioavailability Calculations

The extent of absorption of meprobamate after oral administration of an aqueous solution to dogs is calculated using Eq. (III-57) which assumes simultaneous first-order and capacity-limited elimination kinetics and also using Eq. (III-53) which assumes linear kinetics. Table (XXI) lists the values of the fraction of the dose absorbed calculated using both methods. The parameters K_1, V_m and K_m used for the calculation of F using Eq. (III-57) are those obtained from the

TABLE XXI

Fraction of Dose Absorbed Calculated Using Eqs. (III-57) and (III-53)

Dog No.	Dose (mg./kg.)	F from Eq. (III-57)	F from Eq. (III-53)
510	7.0	0.957	0.857
510	10.0	0.817	0.792
510	30.0	1.008	1.066
510	50.0	0.960	0.919
1065	7.0	0.749	0.717
1065	10.0	0.696	0.659
1065	30.0	0.981	0.975
1065	50.0	0.938	0.898
1122	7.0	0.813	0.762
1122	10.0	0.856	0.819
1122	30.0	1.09	1.04
1122	50.0	0.912	0.893

single dose I. V. studies (Table XX). Calculation of the numerator in Eq. (III-57)

$$\left(\int_0^\infty \frac{1}{V}\,\frac{dA_e}{dt}\right)$$

requires low concentration values and in some instances these are obtained by extrapolation of the least-square lines of oral data (solid lines in Figures 10 through 12). It is interesting to note that the F values calculated using Eqs. (III-57) and (III-53) are in close agreement with each other even though the assumption of constant clearance implicit in Eq. (III-53) does not apply for meprobamate data. However, as shown in section 3-d, Eq. (III-53) does give nearly correct values of F in

cases of large absorption rate constant and F value close to one. An inspection of Figures 5-8 and 10-12 reveals that this in fact is the case for meprobamate in dog. The results of Figures 10 through 12 and Table XXI indicate that meprobamate is rapidly and completely absorbed from an oral solution.

5-b Multiple Dose Studies

Another use of equation parameters is demonstrated in predicting the plasma levels of meprobamate during a multiple dosing schedule. Using the equation parameters obtained from single dose I. V. studies and the theory outlined in pp. for loading dose-maintenance dose schedule, the appropriate multiple dosage regimen may be calculated. In order to maintain the plasma levels of meprobamate between 42.6 and 10.3 mcg./ml. in dog no. 510, and between 30.45 and 10.63 mcg./ml. in dog no. 1065, it is necessary to administer meprobamate under the following conditions: dosing interval = 6 hr., loading dose = 30 mg./kg. maintenance dose = 22.74 mg./kg. for dog no. 510 and 19.58 mg./kg. for dog no. 1065.

Figures 21 and 22 show the predicted curves (continuous lines) with the observed plasma levels (solid circles) for dogs nos. 510 and 1065 respectively. Although a good agreement is obtained between predicted and observed maximum and minimum drug concentrations, there appears to be a systematic trend in the lack of fit (the data points obtained after the administration of the third dose are below the predicted

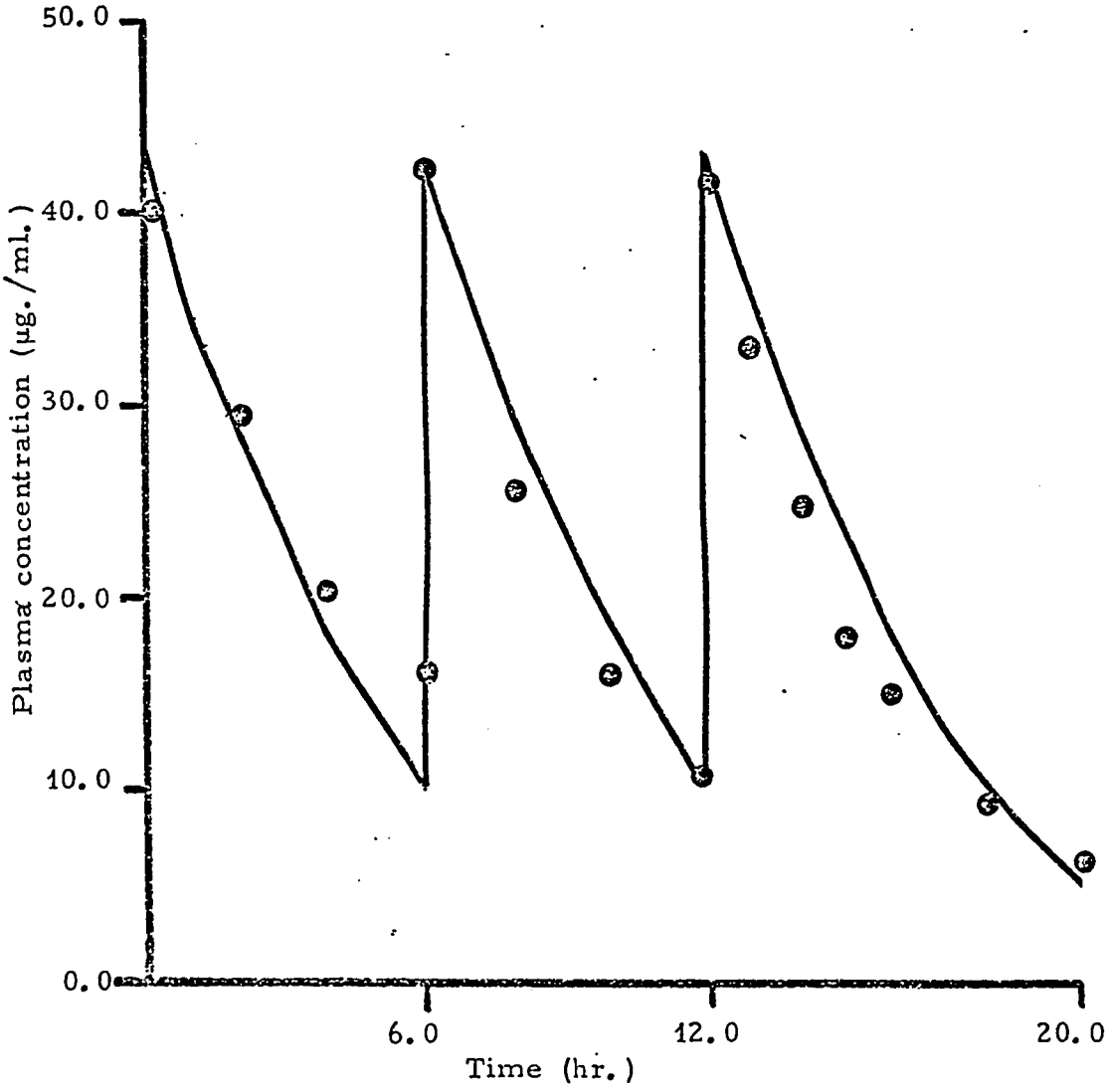

Figure 21. Multiple dose study in Dog #510: Priming dose-maintenance dose schedule. (—)-theoretical curve; (●) observed plasma levels of meprobamate.

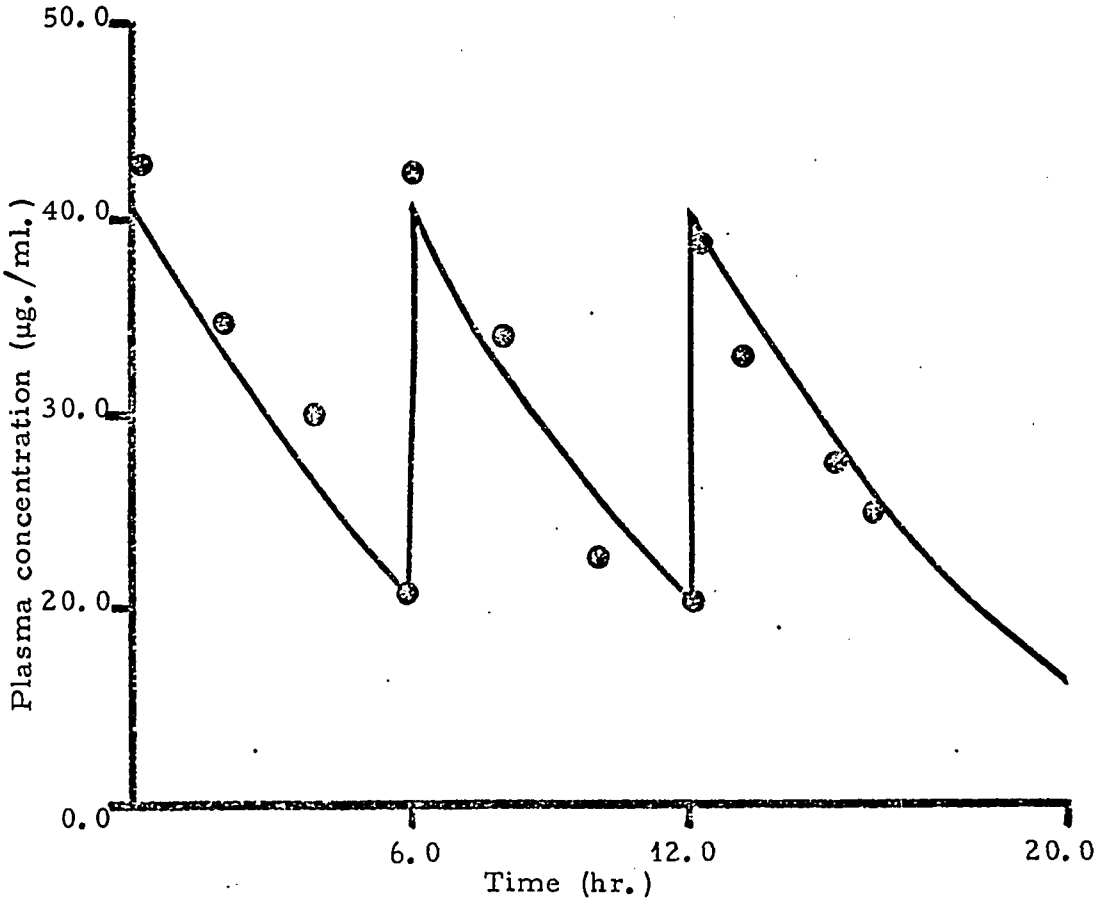

Figure 22. Multiple dose study in Dog #1065: Priming dose-maintenance dose schedule. (—)-theoretical curve; (●) observed plasma levels of meprobamate.

curve). The value for the area $\int_{o}^{\infty} Cdt$ is decreasing with the number of doses ($\int_{o}^{6} Cdt > \int_{6}^{12} Cdt > \int_{12}^{18} Cdt$). Such a phenomenon is usually observed in the presence of enzyme induction and meprobamate is known to induce its own metabolism (96). The effective predictions of maintenance dose plasma levels from single dose data requires that all pharmacokinetic parameters remain constant between the single dose and multiple dose studies as well as during the multiple dosing sequence itself. With all known biological variables, such requirements are often not attained.

CHAPTER IV

CONCLUSIONS

The results presented in this thesis can be divided into two major groups, namely, those pertaining specifically to meprobamate and those more generally related to dose-dependent elimination kinetics.

IV - 1 STUDIES ON MEPROBAMATE

An analytical method for the quantitation of meprobamate in biological fluids using GLC is developed. This method is found to be specific, sensitive and reproducible and should prove to be useful for the routine analysis of biological samples from meprobamate-treated subjects.

With regard to the kinetics of meprobamate in the dog, the following conclusions can be made:

(a) The pharmacokinetics of meprobamate in dog can be satisfactorily described using a one compartment body model.

(b) Meprobamate is rapidly and completely absorbed in the gastrointestinal tract from an aqueous solution.

(c) The drug is extensively metabolized and the urinary excretion of unchanged drug is a minor pathway in the overall elimination.

(d) The elimination of meprobamate occurs by simultaneous first-order and capacity-limited processes.

IV - 2 DOSE-DEPENDENT ELIMINATION KINETICS

A pharmacokinetic model involving simultaneous first-order and capacity-limited elimination processes is proposed and experimentally tested for meprobamate. New mathematical relationships are developed

to describe the nature of PCT curves (I. V. and oral) and the relationships between dose and several critical and useful pharmacokinetic parameters, namely, AUC, half-life and fraction of the dose excreted unchanged. These relationships as general guidelines are useful in establishing the phenomenon of dose-dependency in elimination. A new method is developed to calculate bioavailability of drugs exhibiting simultaneous first-order and capacity-limited elimination kinetics. In such cases, the use of most common method of bioavailability calculations (which compares AUC of PCT data and are applicable for linear pharmacokinetic systems) produces large error.

New methods are proposed for obtaining model parameters from PCT data of drugs exhibiting simultaneous first-order and capacity-limited elimination. The problems associated with the use of least-squares procedures for estimating pharmacokinetic parameters are pointed out and the usefulness of the parameters thus obtained is discussed.

Equations are developed to describe the accumulation characteristics of drugs showing first-order elimination in parallel with a capacity-limited elimination process. Methods for performing dosage regimen calculations are presented and the predictions of levels resulting from a priming dose-maintenance dose schedule are tested experimentally for meprobamate in the dog.

The one compartment model with first-order and capacity-limited elimination processes which is proposed for meprobamate undoubtedly has

wider applicability than any model previously used to describe dose-dependent elimination from PCT data.

REFERENCES

1. B. J. Ludwig and E. C. Piech, J. Amer. Chem. Soc., 73, 5779 (1951).

2. F. M. Berger, in "Psychopharmacology (A Review of Progress 1957-1967)," D. H. Efron, Ed., U. S. Govt. Printing Office, Washington, D. C., 1968, pp. 139-152.

3. T. A. Ban, "Psychopharmacology," Williams and Wilkens, Baltimore, Maryland, 1969, pp. 313-325.

4. F. J. Ayd, Psychosomatics, 5, 82 (1964).

5. F. M. Berger, J. Pharmacol. Exp. Therap.; 112, 413 (1954).

6. B. W. Agranoff, R. M. Bradley and J. Axelrod, Proc. Soc. Exptl. Biol. Med.; 96, 261 (1957).

7. S. S. Walkenstein, C. M. Knebel, J. A. MacMullen and J. Seifter, J. Pharmacol. Exptl. Therap.; 123, 254 (1958).

8. B. J. Ludwig, J. F. Douglas, L. S. Powell, M. Meyer and F. M. Berger, J. Med. Pharm. Chem.; 3, 53 (1961).

9. H. Tsukamoto, H. Yoshimura and K. Tatsumi, Chem. Pharm. Bull. 11, 421 (1963).

10. H. Tsukamoto, H. Yoshimura and K. Tatsumi, Life Sciences, 6, 382 (1963).

11. R. Wiser and J. Seifter, Federation Proc. 19, 390 (1960).

12. A. Yamamoto, H. Yoshimura and H. Tsukamoto, Chem. Pharm. Bull.; 10, 522 (1962).

13. A. Yamamoto, H. Yoshimura and H. Tsukamoto, ibid., 10, 540 (1962).

14. A. H. Conney and J. J. Burns, Ann. N. Y. Acad. Sci.; 86, 167 (1960).

15. R. Kato, Experientia, 16, 427 (1960).

16. E. Rubin, H. Gang, P. S. Misra and C. S. Lieber, Am. J. Med., 49, 801 (1970).

17. B. M. Phillips, T. A. Miya and G. K. W. Yim, J. Pharmacol. Exptl. Therap.; 135, 223 (1962).

18. J. F. Douglas, B. J. Ludwig and N. Smith, Proc. Soc. Exptl. Biol. Med., 112, 436 (1963).

19. J. J. Heyman, W. Krumholz and S. Merlis, Terap. Res., 4, 416 (1962).

20. E. Van der Kleijn, Arch. Int. Pharmacodyn; 178, 457 (1969).

21. A. J. Hoffman and B. J. Ludwig, J. Am. Pharm. Assoc. Sci., Ed., 48, 740 (1959).

22. L. E. Hollister and G. Levy, Chemotherapia, 9, 20 (1964).

23. D. J. Greenblatt and R. I. Shader, Am. J. Psychiat., 127, 1297 (1971).

24. D. J. Greenblatt and R. I. Shader, in "Psychotropic Drug Side Effects: Clinical and Theoretical Perspectives," R. I. Shader and A. DiMasso, Eds.; Williams and Wilkens, Baltimore, 1970, pp. 214-234.

25. J. M. Davies, E. Bartlett and B. A. Termini, Dis. Nerv. Syst., 29, 157 (1968).

26. R. K. Maddock and H. A. Bloomer, JAMA, 201, 999 (1967).

27. E. S. Harris and J. J. Reick, Clin. Chem., 4, 241 (1958).

28. H. S. Bedson, Lancet, 1, 288 (1959).

29. A. E. Bagnarelli, Rev. Sanid. Milit. Argent. 66, 146 (1967).

30. G. H. Ellis and C. A. Hetzel, Anal. Chem., 31, 1090 (1959).

31. S. L. Kanter, Clin. Chim. Acta, 8, 2 (1963).

32. J. W. Poole, G. M. Irwin and S. Young, J. Pharm. Sci., 60, 1850 (1971).

33. L. Kazyak and E. C. Knoblock, Anal. Chem., 35, 1448 (1963).

34. L. R. Goldbaum and T. J. Domanski, J. Forensic Sci., 11, 233 (1966).

35. B. S. Finkle, ibid., 12, 509 (1967).

36. R. K. Maddock and H. A. Bloomer, Clin. Chem., 13, 333 (1967).

37. J. F. Douglas, T. F. Kelly, N. B. Smith and J. A. Stockage, Anal. Chem. 39, 957 (1967).

38. R. Maes, N. Hodnett, H. Landisman, G. Kananen, B. Finkle and T. Sunshine, J. Forensic Sci., 14, 235 (1969).

39. K. Holch and J. C. Gjaldbaek, Dansk Tidsskr, Farm., 45, 32 (1971).

40. R. F. Skinner, J. Forensic Sci., 12, 230 (1967).

41. O. Cerri, Boll. Chim. Farm. 108, 217 (1969).

42. K. Holch, Dansk Tidsskr, Farm., 45, 107 (1971).

43. L. Martis and R. H. Levy, J. Pharm. Sci., 61, 1341 (1972).

44. M. P. Rabinowitz, P. Reisberg and J. I. Bodin, ibid., 61, 1974 (1972).

45. C. Cardini, V. Quercia and A. Caló, Boll. Chim. Farm., 107, 300 (1968).

46. "The United States Pharmacopeia," 18th rev., Mack Publishing Co., Easton, Pa., 1970, p. 402.

47. "First Supplement to the Pharmacopeia of the United States," 18th rev., October 1, 1971, p. 19.

48. H. Tsukamoto, H. Yoshimura and K. Tatsumi, Chim. Pharm. Bull. 11, 421 (1963).

49. C. T. Beer and T. F. Gallagher, J. Biol. Chem., 214, 335 (1955).

50. T. Teorell, Arch. Intern. Pharmacodyn., 57, 205 (1937).

51. E. Kriiger-Thiemer, Il. Farmaco, Sci. Ed., 23, 717 (1968).

52. A. R. DiSanto and J. G. Wagner, J. Pharm. Sci., 61, 552 (1972).

53. J. G. Wagner, "Biopharmaceutics and Relevant Pharmacokinetics," Drug Intelligence Publications, Hamilton, Ill., 1971, pp. 302-317.

54. E. Van Der Kleijn, Arch. Int. Pharmacodyn., 179, 15 (1969).

55. M. Berman and R. Shoenfeld, J. Appl. Phys., 27, 1361 (1956).

56. J. G. Wagner, Ann. Rev. Pharmacol., 8, 67 (1968).

57. J. G. Wagner, Drug Intelligence, 2, 38 (1968).

58. F. Lundquist and H. Wolthers, Acta. Pharmacol. Toxicol., 14, 265 (1958).

59. J. G. Wagner and J. A. Patel, Res. Commun. Chem. Pathol. Pharmacol., 4, 61 (1972).

60. G. Levy and T. Matsuzawa, J. Pharmacol. Exptl. Therap., 153, 159 (1966).

61. G. Levy, J. Pharm. Sci., 54, 959 (1965).

62. E. Nelson, M. Hanano and G. Levy, J. Pharmacol. Exptl. Therap., 153, 159 (1966).

63. A. J. Cummings and B. K. Martin, Biochem. Pharmacol., 13, 767 (1964).

64. A. J. Cummings, B. K. Martin and R. Renton, Brit. J. Pharmacol., 26, 461 (1966).

65. P. G. Dayton, S. A. Cucinell, M. Weiss and J. M. Perel, J. Pharmacol. Exptl. Therap., 158, 305 (1967).

66. K. Arnold and N. Gerber, Clin. Pharmacol. Therap., 11, 121 (1970).

67. L. Garrettson and O. Kim, Pediat. Res., 4, 53 (1970).

68. N. Gerber, W. L. Weller, R. Lynn, R. E. Rangano, B. J. Sweetman and M. T. Bush, J. Pharmacol. Exptl. Therap., 178, 567 (1971).

69. J. J. Ashly and G. Levy, Res. Commun. Chem. Path. Pharmacol., 4, 297 (1972).

70. A. J. Atkinson and J. M. Shaw, Clin. Pharmacol. Therap., 14, 521 (1973).

71. G. Levy and J. Arnold, J. Pharm. Sci., 62, 161 (1973).

72. J. J. Ashly and G. Levy, J. Pharmacokin. Biopharm., 1, 99 (1973).

73. R. R. Levine and C. M. Dizon, J. Pharm. Sci., 59, 1845 (1970).

74. P. G. Dayton, T. F. Yü, W. Chen, L. Berger, L. A. West and A. B. Gutman, J. Pharmacol. Exptl. Therap., 140, 278 (1963).

75. G. Levy, in, "Importance of Fundamental Principles in Drug Evaluation," D. H. Tedeschi and R. E. Tedischi, eds., Raven Press, New York, 1968, pp. 141-172.

76. G. Levy and S. J. Yaffe, Clin. Toxicol., 1, 409 (1968).

77. G. Levy, A. W. Vogel and L. P. Amsel, J. Pharm. Sci., 58, 503 (1969).

78. G. Levy, T. Tsuchiya and L. P. Amsel, Clin. Pharmacol. Therap., 13, 258 (1972).

79. J. G. Wagner, J. Pharmacokin. Biopharm., 1, 103 (1973).

80. L. Michaelis and M. L. Menten, Biochem. Z., 49, 333 (1913).

81. G. Levy, Nature, 206, 517 (1965).

82. G. Levy, J. Pharm. Sci., 55, 989 (1966).

83. G. Levy and T. Matsuzawa, ibid., 55, 222 (1966).

84. G. Levy and L. P. Amsel, Biochem. Pharm., 15, 1033 (1966).

85. R. W. Southworth and S. L. Deleeuw, "Digital Computation and Numerical Methods," McGraw-Hill, Inc., New York, 1965, pp. 420-468.

86. Boeing Library of Mathematical Routines, University of Washington Computer Center, Seattle, Washington, Vol. 4, pp. 114-126.

87. E. Krüger-Thiemer and R. R. Levine, Arzeneimittel-Forsch., 18, 1575 (1968).

88. H. Lineweaver and D. Burk, J. Amer. Chem. Soc., 56, 658 (1934).

89. N. R. Draper and H. Smith, "Applied Regression Analysis," John Wiley and Sons, Inc., New York, 1966, pp. 263-304.

90. BMDX85, University of Washington Computing Facility, Seattle, Washington.

91. I. S. Longmuir, D. C. Martin, H. J. Gold and S. Sun, Microvascular Research, 3, 125 (1961).

92. Boeing Library of Mathematical Routines, University of Washington Computer Center, Seattle, Washington, Vol. 5, pp. 192-194.

93. S. Riegelman, L. Z. Benet and M. Rowland, J. Pharmacokin. Biopharm., 1, 3 (1973).

94. J. G. Wagner, "Biopharmaceutics and Relevant Pharmacokinetics," Drug Intelligence Publications, Hamilton, Ill., 1971, p. 180.

95. F. H. Dost, "Grundlagen der Pharmakokinetik," 2nd ed., G. Thiene Verlag Stuttgart, 1968.

96. R. Kato and P. Vassanelli, Biochem. Pharmacol. 11, 779 (1962).

APPENDIX 1

Derivation of Eq. (III-2):

The differential Eq. (III-1) is:

$$-\frac{dC}{dt} = K_1 C + \frac{V_m C}{K_m + C} \qquad \text{Eq. (1-1)}$$

or

$$\frac{dC}{dt} = \frac{-K_1 K_m C - K_1 C^2 - V_m C}{K_m + C} \qquad \text{Eq. (1-2)}$$

or

$$\frac{dC}{dt} = \frac{-(K_1 K_m + V_m + K_1 C)C}{K_m + C} \qquad \text{Eq. (1-3)}$$

Separation of Variables in Eq. (1-3) results in:

$$\frac{(K_m + C)\ dC}{(K_1 K_m + V_m + K_1 C)C} = -dt \qquad \text{Eq. (1-4)}$$

Which can be written as:

$$\frac{K_m}{(K_1 K_m + V_m + K_1)}\ \frac{dC}{C} + \frac{dC}{K_1 K_m + V_m + K_1 C} = -dt \qquad \text{Eq. (1-5)}$$

Integration of Eq. (1-5) gives:

$$-\frac{K_m}{K_1 K_m + V_m}\ \ell n \frac{(K_1 K_m + V_m + K_1 C)}{C} + \frac{1}{K_1}\ \ell n\ (K_1 K_m + V_m + K_1 C) = -t + K \qquad \text{Eq. (1-6)}$$

where K is the constant of integration. Since at $t = 0$, $C = C_o$ from Eq. (1-6):

$$K = -\frac{K_m}{K_1K_m + V_m} \ln \frac{(K_1K_m + V_m + K_1C_o)}{C_o} + \frac{1}{K_1} \ln (K_1K_m + V_m + K_1C_o)$$

Eq. (1-7)

Substituting the value of K in Eq. (1-6) and rearranging the resulting expression gives:

$$t = \frac{K_m}{K_1K_m + V_m} \ln \left[\frac{C_o(K_1K_m + V_m + K_1C)}{C(K_1K_m + V_m + K_1C_o)}\right] + \frac{1}{K_1} \ln \left[\frac{K_1K_m + V_m + K_1C_o}{K_1K_m + V_m + K_1C}\right]$$

Eq. (1-8)

which can be simplified to:

$$t = \frac{1}{K_1K_m + V_m} \left[K_m \ln \frac{C_o}{C} + \frac{V_m}{K_1} \ln \frac{(C_o + K_m)K_1 + V_m}{(C + K_m)K_1 + V_m}\right].$$ Eq. (III-2)

APPENDIX 2

```
FORTRAN.
LGO.
-
      PROGRAM MAIN (INPUT,OUTPUT,TAPE5=INPUT,TAPE6=OUTPUT)
      DIMENSION DX(8),X(8),F(56)
C     N IS THE ORDER OF THE DIFFERENTIAL EQUATION
      N = 1
C     DT IS THE TIME INTERVAL OF NUMERICAL INTEGRATION
      DT = 1.0
      T=0.
C     X(1) REPRESENTS THE INITIAL CONCENTRATION
      X(1) = 76.92
   10 L=3
      M=0
   50 CALL RUNGE(T,DT,N,X,DX,F,L,M,J)
      IF(M-1) 75,10,75
   75 GO TO (100,200,999),L
C     FOLLOWING IS THE DIFFERENTIAL EQUATION
  100 DX(1) = -(0.0155*X(1)+10.46*X(1)/(52.31+X(1)))
      GO TO 50
  200 WRITE(6,800)T,X(1)
  800 FORMAT(5X,2F13.4)
C     INTEGRATION IS PERFORMED UNTIL T = 99.0
  250 IF(T-99.)260,999,999
  260 GO TO 50
  999 STOP
      END
      SUBROUTINE RUNGE(T,DT,N,Y,DY,F,L,M,J)
      DIMENSION DY(8),Y(8),F(56)
  151   GO TO (100,110,200) ,L
100     GO TO (101,110) ,IG
101     J = 1
        L = 2
        DO 106 K = 1,N
        K1 = K + 3 * N
        K2 = K1 + N
        K3 = N+K
        F(K1) = Y(K)
        F(K3) = F(K1)
106     F(K2) = DY(K)
        GO TO 406
110     DO 140 K = 1,N
        K1 = K
        K2 = K + 5 * N
        K3 = K2 + N
        K4 = K + N
        GO TO (111,112,113,114),J
111     F(K1) = DY(K) * DT
        Y(K) = F(K4) + .5 * F(K1)
        GO TO 140
112     F(K2) = DY(K) * DT
        GO TO 124
113     F(K3) = DY(K) * DT
        GO TO 134
114     Y(K) = F(K4) + (F(K1) + 2. * (F(K2) + F(K3))+ DY(K) * DT) / 6.
        GO TO 140
```

```
124     Y(K) = .5 * F(K2)
        Y(K) = Y(K) + F(K4)
        GO TO 140
134     Y(K) = F(K4) + F(K3)
140     CONTINUE
        GO TO (170,180,170,180),J
170     T = T + .5 * DT
180     J = J + 1
        IF(J -4) 404,404,299
299     M = 1
        GO TO 406
300     IG = 1
        GO TO 405
404     IG = 2
405     L = 1
406     RETURN
        END
```

APPENDIX 3

Derivation of Eq. (III-8):

Rearrangement of Eq. (I-7) results in:

$$\frac{dC}{C} = -(K_1 + \frac{V_m}{K_m}) \, dt \qquad \text{Eq. (3-1)}$$

Integration of Eq. (3-1) gives:

$$\ell nC = -(K_1 + \frac{V_m}{K_m}) \, t + K \qquad \text{Eq. (3-2)}$$

Since at $t = 0$, $C = C_o$

$$K = \ell n \, C_o \qquad \text{Eq. (3-3)}$$

Substituting K from Eq. (3-3) in Eq. (3-2) yields:

$$\ell n \frac{C}{C_o} = -(K_1 + \frac{V_m}{K_m}) \, t \qquad \text{Eq. (3-4)}$$

or

$$C = C_o \, e^{-(K_1 + \frac{V_m}{K_m}) \, t} \qquad \text{Eq. (III-8)}$$

Derivation of Eq. (III-10):

Separation of variables in Eq. (III-9) results in:

$$\frac{dC}{K_1 C + V_m} = -dt \qquad \text{Eq. (3-5)}$$

Integration of Eq. (3-5) gives:

$$\frac{1}{K_1} \, \ell n \, (K_1 C + V_m) = -t + K \qquad \text{Eq. (3-6)}$$

Sinc at $t = 0$, $C = C_o$, from Eq. (3-6)

$$K = \frac{1}{K_1} \ln (K_1 C_o + V_m) \qquad \text{Eq. (3-7)}$$

Substituting for K in Eq. (3-6) from Eq. (3-7) and the rearrangement of the resulting expression gives:

$$\frac{1}{K_1} \ln \left(\frac{K_1 C + V_m}{K_1 C_o + V_m} \right) = -t \qquad \text{Eq. (3-8)}$$

which can also be written as:

$$C = (C_o + \frac{V_m}{K_1}) e^{-K_1 t} - \frac{V_m}{K_1} \qquad \text{Eq. (III-10)}$$

Derivation of Eq. (III-12):

The differential Eq. (I-11) is:

$$\frac{dC}{dt} = K_a F C_o e^{-K_a t} - (K_1 + \frac{V_m}{K_m}) C \qquad \text{Eq. (3-9)}$$

Taking the Leplace Transforms of both sides of Eq. (3-9) we get:

$$S \bar{C} - C(0) = K_a F C_o \frac{1}{S+K_a} - (K_1 + \frac{V_m}{K_m}) \bar{C} \qquad \text{Eq. (3-10)}$$

In Eq. (3-10) $\bar{C}$ is the Leplace transform of C, $C(0)$ is the drug concentration at zero time and the symbol S represtns a real or complex number. Applying the initial condition $C(0) = 0$ and rearrangement of Eq. (3-10) results in:

$$\bar{C} = \frac{K_a F C_o}{(S+K_a)(K_1 + \frac{V_m}{K_m})} \qquad \text{Eq. (3-11)}$$

Taking the inverse transforms of the terms in Eq. (3-11) gives the following expression for C:

$$C = \frac{K_a F C_o}{(K_1 + \frac{V_m}{K_m} - K_a)} [e^{-K_a t} - e^{-(K_1 + \frac{V_m}{K_m}) t}] \qquad \text{Eq. (III-12)}$$

Derivation of Eq. (III-14):

Eq. (III-13) is:

$$\frac{dC}{dt} = K_a F C_o e^{-K_a t} - K_1 C - V_m \qquad \text{Eq. (3-12)}$$

Taking the Leplace Transforms of both sides of the above equation gives:

$$S\bar{C} - C(0) = K_a F C_o \frac{1}{S+K_a} - K_1 \bar{C} - \frac{V_m}{S} \qquad \text{Eq. (3-13)}$$

Applying the initial condition, C(0) = 0 and rearrangement of Eq. (3-13) leads to:

$$\bar{C} = \frac{K_a F C_o}{(S+K_a)(S+K_1)} - \frac{V_m}{S(S+K_1)} \qquad \text{Eq. (3-14)}$$

Taking the inverse transforms of the terms in Eq. (3-14) gives:

$$C = \frac{K_a F C_o}{(K_1-K_a)} [e^{-K_a t} - e^{-K_1 t}] - \frac{V_m}{K_1} [1 - e^{-K_1 t}] \qquad \text{Eq. (III-14)}$$

APPENDIX 4

Derivation of Eq. (III-26):

The differential Eq. (III-1) can be rearranged and written as:

$$-\frac{dC}{dt} = \frac{C(K_1K_m + V_m + K_1C)}{K_m + C} \qquad \text{Eq. (4-1)}$$

Let $$K_1K_m + V_m = K_2 \qquad \text{Eq. (4-1)}$$

Substituting for K_2 from Eq. (4-2) in Eq. (4-1) we get:

$$-\frac{dC}{dt} = \frac{C(K_2 + K_1C)}{K_m + C} \qquad \text{Eq. (4-3)}$$

or

$$-\frac{C}{dC/dt} = \frac{K_m + C}{K_2 + K_1C} \qquad \text{Eq. (4-4)}$$

Dividing the numerator and the denominator of right hand side of Eq. (4-4) by K_2 and rearrangement of the resulting expression gives:

$$-\frac{C}{dC/dt} = \left[\frac{K_m}{K_2} + \frac{C}{K_2}\right] \left(1 + \frac{K_1}{K_2} C\right)^{-1} \qquad \text{Eq. (4-5)}$$

The second term of right hand side of Eq. (4-5) can be expanded using Taylor Expansion to yield the following expression:

$$-\frac{C}{dC/dt} = \left[\frac{K_m}{K_2} + \frac{C}{K_2}\right] \left(1 - \frac{K_1}{K_2} C + \left(\frac{K_1}{K_2}\right)^2 C^2 \ldots\ldots\right) \qquad \text{Eq. (4-6)}$$

The terms containing powers greater than two of $\frac{K_1}{K_2}$ can be dropped since

in most cases $(\frac{K_1}{K_2})^2 C^2 << 1$ and the contribution of these terms to $\frac{C}{dC/dt}$ becomes insignificant. As an example, for the constants reported for salicylate, the value of $(\frac{K_1}{K_2})^2$ is equal to 1.77×10^{-6} (C/dC/dt is of the order of 5-10). Rearrangement of Eq. (4-6) leads to following polynomial in C:

$$-\frac{C}{dC/dt} = \frac{K_m}{K_2} + [\frac{1}{K_2} - \frac{K_m K_1}{K_2^2}] C + [\frac{K_m K_1^2}{K_2^3} - \frac{K_1}{K_2^2}] C^2 \qquad \text{Eq. (III-26)}$$

which can also be expressed as:

$$-\frac{C}{dC/dt} = a_o + a_1 C + a_2 C^2 \qquad \text{Eq. (4-8)}$$

Derivation of Eqs. (III-29) through (III-32):

From Eq. (4-8) and (III-26) the coefficients of the polynomial can be expressed as:

$$a_o = \frac{K_m}{K_2} \qquad \text{Eq. (4-9)}$$

$$a_1 = \frac{1}{K_2} - \frac{K_m K_2}{K_2^2} \qquad \text{Eq. (4-10)}$$

$$a_2 = \frac{K_m K_1^2}{K_2^3} - \frac{K_1}{K_2^2} \qquad \text{Eq. (4-11)}$$

Substituting for K_m in Eq. (4-10) from Eq. (4-9) we have:

$$a_1 = \frac{1}{K_2} - \frac{a_o K_2 K_1}{K_2^2} \qquad \text{Eq. (4-12)}$$

Rearrangement of Eq. (4-12) gives following expression for K_1:

$$K_1 = \frac{1}{a_o} [\, 1 - a_1 K_2] \; . \; . \qquad \text{Eq. (4-13)}$$

Substituting for K_1 from Eq. (4-13) and K_m from Eq. (4-9) in Eq. (4-11) results in:

$$a_2 = \frac{a_o K_2}{K_2^3} \frac{1}{a_o^2} (1 - a_1 K_2)^2 - \frac{1}{a_o} \frac{(1 - a_1 K_2)}{K_2^2} \qquad \text{Eq. (4-14)}$$

Expansion of the square term and rearrangent of Eq. (4-14) gives:

$$a_2 = \frac{1}{a_o K_2^2} [\, a_1^2 K_2^2 - a_1 K_2] \qquad \text{Eq. (4-15)}$$

which can also be written as:

$$a_2 = \frac{a_1}{a_o K_2} (a_1 K_2 - 1) \qquad \text{Eq. (4-16)}$$

Multiplying both sides of Eq. (4-16) by $a_o K_2$ and solving the resulting expression for K_2 gives:

$$K_2 = \frac{a_1}{a_1^2 - a_o a_2} \qquad \text{Eq. (III-29)}$$

From Eq. (4-9):

$$K_m = a_o K_2 \qquad \text{Eq. (III-30)}$$

Substituting for K_2 from Eq. (III-29) in the first term on right hand side of Eq. (4-10) gives:

$$a_1 = \frac{a_1^2 - a_o a_2}{a_1} - \frac{K_m K_1}{K_2^2} \qquad \text{Eq. (4-17)}$$

Substitution for K_m from Eq. (III-30) in Eq. (4-17) and rearrangement of the resulting expression yields:

$$K_1 = -\frac{a_2}{a_1} K_2 \qquad \text{Eq. (III-31)}$$

From Eq. (4-2):

$$V_m = K_2 - K_1 K_m \qquad \text{Eq. (III-32)}$$

APPENDIX 5

```
FORTRAN.
LOAD LGO.
BMDX85.
-
      SUBROUTINE FUN(F,D,P,X)
      DIMENSION P(10),D(10),X(10),DELT(5),Y(35,5)
C     ESTIMATION OF THE PARAMETERS USING METHOD II
      IF(X(1).EQ.0.0) NN = 1
      IF(X(1).EQ.0.0) CALL DIFF (Y,DELT,P)
      F = Y(NN,5)
      D(1) = (Y(NN,1)-Y(NN,5))/DELT(1)
      D(2) = (Y(NN,2)-Y(NN,5))/DELT(2)
      D(3) = (Y(NN,3)-Y(NN,5))/DELT(3)
      D(4) = (Y(NN,4)-Y(NN,5))/DELT(4)
      NN = NN+1
      RETURN
      END
      SUBROUTINE DIFF (Y,DELT,P)
      DIMENSION Y(35,5),DELT(5),DX(8),P(10),X(10),F(56)
      DELT(1) = 0.01*P(1)
      DELT(2) = 0.01*P(2)
      DELT(3) = 0.01*P(3)
      DELT(4) = 0.01*P(4)
      DELT(5) = 0.0
      P(5) = P(1)
      DO 9 JJ = 1,5
      P(JJ) = P(JJ) + DELT(JJ)
      KK = 1
      N = 1
      DT = 0.5
      TT = 0.0
      X(1) = P(1)
   10 L = 3
      M = 0
   50 CALL RUNGE (TT,DT,N,X,DX,F,L,M,J)
      IF (M-1)75,10,75
   75 GO TO (100,200,999),L
  100 DX(1) = -(P(2)*X(1)+P(3)*X(1)/(P(4)+X(1)))
      GO TO 50
  200 Y(KK,JJ) = X(1)
      KK = KK + 1
      IF (TT.LE.11.0) GO TO 50
      P(JJ) = P(JJ) - DELT(JJ)
    9 CONTINUE
      NN = 1
  999 RETURN
      END
      SUBROUTINE RUNGE(T,DT,N,Y,DY,F,L,M,J)
      DIMENSION DY(8),Y(8),F(56)
        GO TO (100,110,900) ,L
100     GO TO (101,110) ,IG
101     J = 1
        L = 2
        DO 105 K = 1,N
        K1 = K + 3 * N
        K2 = K1 + N
```

```
      K3 = N+K
      F(K1) = Y(K)
      F(K3) = F(K1)
106   F(K2) = DY(K)
      GO TO 406
110   DO 140 K = 1,N
      K1 = K
      K2 = K + 5 * N
      K3 = K2 + N
      K4 = K + N
      GO TO (111,112,113,114),J
111   F(K1) = DY(K) * DT
      Y(K) = F(K4) + .5 * F(K1)
      GO TO 140
112   F(K2) = DY(K) * DT
      GO TO 124
113   F(K3) = DY(K) * DT
      GO TO 134
114   Y(K) = F(K4) + (F(K1) + 2. * (F(K2) + F(K3))+ DY(K) * DT) / 6.
      GO TO 140
124   Y(K) = .5 * F(K2)
      Y(K) = Y(K) + F(K4)
      GO TO 140
134   Y(K) = F(K4) + F(K3)
140   CONTINUE
      GO TO (170,180,170,180),J
170   T = T + .5 * DT
180   J = J + 1
      IF(J -4) 404,404,299
299   M = 1
      GO TO 406
300   IG = 1
      GO TO 405
404   IG = 2
405   L = 1
406   RETURN
      END
```

APPENDIX 6

Derivation of Eq. (III-36): Eq. (III-2) can be written as:

$$t = \frac{K_m}{K_1 K_m + V_m} \ln \frac{C_o}{C} + \frac{V_m}{K_1^2 K_m + K_1 V_m} \ln (C_o K_1 + K_1 K_m + V_m)$$

$$- \frac{V_m}{K_1^2 K_m + K_1 V_m} \ln (C K_1 + K_1 K_m + V_m) \qquad \text{Eq. (6-1)}$$

Partial differentiation of t with respect to K_1 gives:

$$\frac{\partial t}{\partial K_1} = -K_m (K_1 K_m + V_m)^{-2} K_m \ln \frac{C_o}{C_1} + \frac{V_m (C_o + K_m)}{(K_1^2 K_m + K_1 V)(C_o K_1 + K_1 K_m + V_m)}$$

$$- V_m (K_1^2 K_m + K_1 V_m)^{-2} (2K_1 K_m + V_m) \ln (C_o K_1 + K_1 K_m + V_m)$$

$$- \frac{V_m (C + K_m)}{(K_1^2 K_m + K_1 V_m)(C K_1 + K_1 K_m + V_m)}$$

$$+ V_m (K_1^2 K_m + K_1 V_m)^{-2} (2K_1 K_m + V_m) \ln (C K_1 + K_1 K_m + V_m) \qquad \text{Eq. (6-2)}$$

Eq. (6-2) can be simplified as:

$$\frac{\partial t}{\partial K_1} = - \frac{2V_m K_1 K_m + V_m^2}{(K_1^2 K_m + K_1 V_m)^2} \ln \left[\frac{C K_1 + K_1 K_m + V_m}{C_o K_1 + K_1 K_m + V_m} \right] - \frac{K_m^2}{(K_1 K_m + V_m)^2} \ln \frac{C_o}{C_1}$$

$$+ \frac{V_m^2 (C_o - C)}{(K_1^2 K_m + K_1 V_m)(C K_1 + K_1 K_m + V_m)(C_o K_1 + K_1 K_m + V_m)}$$

Eq. (III-36)

Derivation of Eq. (III-37): Partial differention of t (Eq. 6-1) with respect to K_m leads to:

$$\frac{\partial t}{\partial K_m} = -[K_m (K_1 K_m + V_m)^{-2} \cdot K_1 + (K_1 K_m + V_m)^{-1}] \ \ell n \frac{C_o}{C}$$

$$+ \frac{V_m K_1}{(K_1^2 K_m + K_1 V_m)(C_o K_1 + K_1 K_m + V_m)}$$

$$- V_m (K_1^2 K_m + K_1 V_m)^{-2} K_1^2 \ell n (C_o K_1 + K_1 K_m + V_m)$$

$$- \frac{V_m K_1}{(K_1^2 K_m + K_1 V_m)(C K_1 + K_1 K_m + V_m)}$$

$$+ V_m (K_1^2 K_m + K_1 V_m)^{-2} K_1^2 \ell n (C K_1 + K_1 K_m + V_m) \qquad \text{Eq. (6-3)}$$

which can be simplified to:

$$\frac{\partial t}{\partial K_m} = \frac{K_1^2 V_m}{(K_1^2 K_m + K_1 V_m)^2} \ell n \left[\frac{C K_1 + K_1 K_m + V_m}{C_o K_1 + K_1 K_m + V_m} \right] + \frac{V_m}{(K_1 K_m + V_m)^2} \ell n \frac{C_o}{C}$$

$$+ \frac{K_1^2 V_m (C - C_o)}{(K_1^2 K_m + K_1 V_m)(C K_1 + K_1 K_m + V_m)(C_o K_1 + K_1 K_m + V_m)} \qquad \text{Eq. (III-37)}$$

Derivation of Eq. (III-38): Partial differentiation of Eq. (6-1) with respect to V_m yields:

$$\frac{\partial t}{\partial V_m} = - K_m (K_1 K_m + V_m)^{-2} \ln \frac{C_o}{C} + \frac{V_m}{K_1^2 K_m + K_1 V_m)(C_o K_1 + K_1 K_m + V_m)}$$

$$+ [-V_m(K_1^2 K_m + K_1 V_m)^{-2} K_1 + (K_1^2 K_m + K_1 V_m)^{-1} \ln (C_o K_1 K_1 K_m + V_m)$$

$$- \frac{V_m}{(K_1^2 K_m + K_1 V_m)(C K_1 + K_1 K_m + V_m)}$$

$$+ [V_m(K_1^2 K_m + K_1 V_m)^{-2} K_1 - (K_1^2 K_m + K_1 V_m)^{-1}] \ln (C K_1 + K_1 K_m + V_m)$$

Eq. (6-4)

Eq. (6-4) can be simplified and written as:

$$\frac{\partial t}{\partial V_m} = - \frac{K_m}{(K_1 K_m + V_m)^2} \ln \frac{C_o}{C}$$

$$+ \frac{K_1 V_m (C - C_o)}{(K_1^2 K_m + K_1 V_m)(C K_1 + K_1 K_m + V_m)(C_o K_1 + K_1 K_m + V_m)}$$

$$+ \frac{K_1^2 K_m}{(K_1^2 K_m + K_1 V_m)^2} \ln \left[\frac{C_o K_1 + K_1 K_m + V_m}{C K_1 + K_1 K_m + V_m} \right]$$ Eq. (III-38)

Derivation of Eq. (III-39): Partial differentiation of Eq. (6-1) with respect to C_o gives:

$$\frac{\partial t}{\partial C_o} = \frac{K_m}{C_o(K_1 K_m + V_m)} + \frac{K_1 V_m}{(K_1^2 K_m + K_1 V_m)(C_o K_1 + K_1 K_m + V_m)}$$ Eq. (III-39)

APPENDIX 7

```
FORTRAN.
LOAD LGO.
BMDX85.
-
      SUBROUTINE FUN(F,D,P,X)
      DIMENSION P(10),D(10),X(10)
C     ESTIMATION OF THE PARAMETERS USING METHOD III
      V = P(3)
      A = P(2)/(P(1)*P(2)+P(3))
      B = P(2)/(P(1)**2*P(2)+P(1)*P(3))
      C = (P(4)*P(1)+P(1)*P(2)+P(3))/(X(1)*P(1)+P(1)*P(2)+P(2))
      R = (2.0*P(2)*P(1)*P(2)+P(2)**2)/((P(1)**2*P(2)+P(1)*P(2))**2)
      E = P(2)**2*(P(4)-X(1))
      G = (P(1)**2*P(2)+P(1)*P(2))*(X(1)*P(1)+P(1)*P(2) P(2))*(P(4)*P(1)
     1+P(1)*P(2)+P(3))
      H = (P(1)**2*P(2))/(P(1)**2*P(2)+P(1)*P(2))**2
      Q = P(2)/((P(1)*P(2)+P(2))**2)
      F = A*ALOG(P(4)/X(1))+B*ALOG(C)
      D(1) = -R*ALOG(C)-(A**2*ALOG(P(4)/X(1))+E/G
      D(2) = -H*ALOG(C)+Q*ALOG(P(4)/X(1))+(P(1)**2*E/V)/G
      D(3) = -(A**2/P(2))*ALOG(P(4)/X(1))+(P(1)*E/V)/G+((H*P(2)/P(2))*AL
     1OG(C))
      D(4) = A/P(4)+P(1)*B/(P(4)*P(1)+P(1)*P(2)+P(2))
      RETURN
      END
-
```

```
      REQUEST(ALTLIB,DI,VRN=F67)
      FORTRAN.
      USERLIB.
      SETCORE(6000)
LGO.
-
      PROGRAM MAIN(INPUT,OUTPUT,TAPE5=INPUT,TAPE6=OUTPUT)
      DIMENSION X(20),Y(20)
C     NUMERICAL DIFFERENTIATION OF C,T DATA
C     M IS NO. OF DATA POINTS
      M = 8
      READ(5,7)(X(I),Y(I),I=1,M)
    7 FORMAT(2F10.5)
      N = 3
      XOUT = 0.5
      DO 9 I = 1,8
      CALL LAGDIF(X,Y,N,M,XOUT,0.4,YP,IER)
      WRITE(6,7) YP,XOUT
      XOUT = XOUT + 0.5
    9 CONTINUE
      WRITE (6,7)(X(I),Y(I),I = 1,M)
      STOP
      END
-
```

```
      REQUEST(ALTLIB,DI,VRN=F67)
      FORTRAN.
      USERLIB.
      SETCORE(6000)
LGO.
-
      PROGRAM MAIN(INPUT,OUTPUT,TAPE5=INPUT,TAPE6=OUTPUT)
      DIMENSION X(20),Y(20),W(20),SCR(41,6),C(20)
C     LEAST-SQUARES FIT TO A SECOND DEGREE POLYNOMIAL
C     M IS NUMBER OF DATA POINTS
      M = 3
      READ(5,7)(X(I),Y(I),W(I),I = 1,M)
    7 FORMAT (3F10.5)
      MAX = 6
      CALL FLSQFY(M,2,X,Y,W,MAX,SCR,C,IER)
      WRITE(6,8) (C(I),I = 1,3)
    8 FORMAT (3E20.8)
      WRITE(6,7)(X(I),Y(I),W(I),I = 1,M)
      STOP
      END
```

APPENDIX 10

Derivation of Eq. (III-42):

$$\text{Area } 0 \rightarrow \infty = \int_o^\infty C \, dt = \int_o^{C_o} t \, dC \qquad \text{Eq. (10-1)}$$

Eq. (I-2) can be written as:

$$t = \frac{K_m}{K_2} \ell n \, C_o - \frac{K_m}{K_2} \ell n C + \frac{V_m}{K_1 K_2} \ell n \, (C_o K_1 + K_2]$$

$$- \frac{V_m}{K_1 K_2} \ell n \, (CK_1 + K_2) \qquad \text{Eq. (10-2)}$$

Substituting for t in Eq. (10-1) from Eq. (10-2) we get:

$$\int_o^\infty Cdt = \int_o^{C_o} t \, dC = \frac{K_m}{K_2} \int_o^{C_o} \ell n \, C_o \, dC - \frac{K_m}{K_2} \int_o^{C_o} \ell n \, C \, dC$$

$$+ \frac{V_m}{K_1 K_2} \int_o^{C_o} \ell n \, (C_o K_1 + K_2) \, dC$$

$$- \frac{V_m}{K_1 K_2} \int_o^{C_o} \ell n \, (C K_1 + K_2) \, d C \qquad \text{Eq. (10-3)}$$

Integrationof Eq. (10-3) gives:

$$\int_o^\infty C \, dt = [\frac{K_m C}{K_2} \ell n \, C_o - \frac{K_m C}{K_2} \ell n C + \frac{K_m}{K_2} C + \frac{V_m C}{K_1 K_2} \ell n \, (C_o K_1 + K_2)$$

$$- \frac{V_m (K_1 C + K_2)}{K_1^2 K_2} \ell n \, (K_1 C + K_2) + \frac{V_m (K_1 C + K_2)}{K_1^2 K_2}]_o^{C_o} \qquad \text{Eq. (10-4)}$$

Substitution of limits of integration and cancellation of like terms leads to:

$$\int_o^\infty C\,dt = \frac{K_m C_o}{K_2} + \frac{V_m C_o}{K_1 K_2} \ln (C_o K_1 + K_2)$$

$$- \frac{V_m (K_1 C_o + K_2)}{K_1^2 K_2} \ln (K_1 C_o + K_2) + \frac{V_m (K_1 C_o + K_2)}{K_1^2 K_2}$$

$$+ \frac{V_m}{K_1^2} \ln K_2 - \frac{V_m}{K_1^2} \qquad \text{Eq. (10-5)}$$

Eq. (10-5) can be further simplified to:

$$\int_o^\infty C\,dt = \frac{C_o}{K_1} - \frac{V_m}{K_1^2} \ln \left[\frac{K_1 C_o}{K_2} + 1\right] \qquad \text{Eq. (III-42)}$$

APPENDIX II

Derivation of Eqs. (III-58) and (III-59)—Let A_t and A_e be the amounts of drug absorbed and eliminated respectively from time o to t and let A_b be the amount of drug in the "body" at time t. Material balance gives the following equation:

$$A_t = A_b + A_3 \qquad \text{Eq. (11-1)}$$

Differentiation of above equation leads to:

$$\frac{dA_t}{dt} = \frac{dA_b}{dt} + \frac{dA_e}{dt} \qquad \text{Eq. (11-2)}$$

Substitution for A_b (=VC) in Eq. (11-2) results in:

$$\frac{1}{V}\frac{dA_t}{dt} = \frac{dC}{dt} + \frac{1}{V}\frac{dA_e}{dt} \qquad \text{Eq. (11-3)}$$

Substitution for $\frac{1}{V}\frac{dA_e}{dt}$ in Eq. (11-3) from Eq. (III-13) gives:

$$\frac{1}{V}\frac{dA_t}{dt} = \frac{dC}{dt} + \left(K_1 C + \frac{V_m C}{K_m + C}\right) \qquad \text{Eq. (11-4)}$$

Integration of Eq. (11-6) from time o to t gives the following expression:

$$\frac{A_t}{V} = C + \int_o^t \left(K_1 C + \frac{V_m C}{K_m + C}\right) dt \qquad \text{Eq. (11-5)}$$

The maximum value of the right hand side of Eq. (11-5) is:

$$\left[C + \int_o^t \left(K_1 C + \frac{V_m C}{K_m + C}\right) dt \right]_{max.} = \int_o^\infty \left(K_1 C + \frac{V_m C}{K_m + C}\right) dt = \frac{FD}{V}$$

Eq. (11-6)

Hence the percent of the dose absorbed up to time t is;

$$\frac{A_t}{FD} \times 100 = \frac{C + \int_o^t \left(K_1 C + \frac{V_m C}{K_m + C}\right) dt}{\int_o^\infty \left(K_1 C + \frac{V_m C}{K_m + C}\right) dt} \times 100 \qquad \text{Eq. (III-58)}$$

Therefore, the percent remaining to be absorbed, F_t % is given by:

$$F_t \times 100 = \left[1 - \frac{A_t}{FD}\right] \times 100 = \left[1 - \frac{C + \int_o^t \left(K_1 C + \frac{V_m C}{K_m + C}\right) dt}{\int_o^\infty \left(K_1 C + \frac{V_m C}{K_m + C}\right) dt}\right] \times 100$$

Eq. (III-59)

APPENDIX 12

Derivation of Eq. (III-61): The differential Eq. (III-18) can be rearranged and written as:

$$\frac{dC}{dt} = \frac{R_o}{V} \frac{(K_m + C) - (K_1 K_m + V_m + K_1 C)C}{K_m + C} \qquad \text{Eq. (12-1)}$$

Let

$$\frac{R_o}{V} = R \qquad \text{Eq. (12-2)}$$

and

$$K_1 K_m + V_m = K_2 \qquad \text{Eq. (12-3)}$$

Substitution of Eqs. (12-2) and (12-3) in (12-1) and separation of variables of the resulting expression yields:

$$\frac{K_m \, dC}{R K_m + (R-K_2)C - K_1 C^2} + \frac{C \, dC}{R K_m + (R-K_2)C - K_1 C^2} = dt \qquad \text{Eq. (12-4)}$$

Integration of Eq. (12-4) gives:

$$\frac{K_m}{\sqrt{4RK_m K_1 + (R-K_2)^2}} \log \frac{-2K_1 C + (R-K_2) - \sqrt{4RK_m K_1 + (R-K_2)^2}}{-2RK_1 C + (R-K_2) + \sqrt{4RK_m K_1 + (R-K_2)^2}}$$

$$- \frac{1}{2K_1} \log [R K_m + (R-K_2) C - K_1 C^2]$$

$$+ \frac{(R-K_2) K_m}{2K_1 \sqrt{4RK_m K_1 + (R-K_2)^2}} \log \frac{-2K_1 C + (R-K_2) - \sqrt{4RK_m K_1 + (R-K_2)^2}}{-2K_1 C + (R-K_2) + \sqrt{4RK_m K_1 + (R-K_2)^2}}$$

$$= t + K \qquad \text{Eq. (12-5)}$$

Since at $t = 0$, $C = 0$, from Eq. (12-5) we have:

$$K = \frac{K_m}{\sqrt{4RK_mK_1+(R-K_2)^2}} \log \frac{(R-K_2) - \sqrt{4RK_mK_1} + (R-K_2)^2}{(R-K_2) + \sqrt{4RK_mK_1} + (R-K_2)^2}$$

$$- \frac{1}{2K_1} \log (RK_m) + \frac{(R-K_2)K_m}{2K_1\sqrt{4RK_mK_1+(R-K_2)^2}} \log \frac{(R-K_2)-\sqrt{4RK_mK_1+(R-K_2)^2}}{(R-K_2)+\sqrt{4RK_mK_1+(R-K_2)^2}}$$

Eq. (12-6)

Substituting the value of K from Eq. (12-6) in Eq. (12-5) and simplifying the resulting expression:

$$t = \frac{(R-K_2+2K_1K_m)\,K_m}{2K_1\sqrt{4RK_mK_1+(R-K_2)^2}} \log \left\{ \frac{-2K_1C[(R-K_2)+\sqrt{4RK_mK_1+(R-K_2)^2}]+4RK_mK_1}{-2K_1C[(R-K_2)-\sqrt{4RK_mK_1+(R-K_2)^2}]+4RK_mK_1} \right\}$$

$$+ \frac{1}{2K_1} \log \frac{RK_m}{RK_m + (R-K_2)C - K_1C^2} \qquad \text{Eq. (12-7)}$$

which can also be written as:

$$t = \left[\frac{X+2K_1K_m}{2K_1}\right] \frac{K_m}{(\epsilon + X^2)^{\frac{1}{2}}} \log \left[\frac{-2K_1C[X+\sqrt{X^2+\epsilon}] + \epsilon}{-2K_1C[X-\sqrt{X^2+\epsilon}] + \epsilon} \right]$$

$$+ \frac{1}{2K_1} \log \left[\frac{\frac{R_oK_m}{V}}{\frac{R_oK_m}{V} + VC - K_1C^2} \right] \qquad \text{Eq. (III-61)}$$

where $$X = \frac{R_o}{V} - K_1K_m - V_m \qquad \text{Eq. (III-62)}$$

and $$\epsilon = \frac{4R_oK_1K_m}{V} \qquad \text{Eq. (III-63)}$$

Time to reach the steady-state: Eq. (III-66) can be written as:

$$C^* = \frac{X + \sqrt{X^2 + \epsilon}}{2K_1} \qquad \text{Eq. (12-8)}$$

or

$$FC^* = \frac{F}{2K_1} (X + \sqrt{X^2 + \epsilon}) \qquad \text{Eq. (12-9)}$$

where F is the fraction of steady-state. Equation for time (t') to reach the steady state is derived by replacing C in Eq. (III-61) by C^* from Eq. (12-8). Such a substitution yields:

$$t' = \left[\frac{X+2K_1K_m}{2K_1}\right] \frac{4K_m}{(\epsilon+X^2)^{\frac{1}{2}}} \log \left\{ \frac{-[X+(X^2+\epsilon)^{\frac{1}{2}}][X+(X^2+1)^{\frac{1}{2}}]+\epsilon}{-(X^2-X^2+\epsilon)+\epsilon} \right\}$$

$$+ \frac{1}{2K_1} \log \left\{ \frac{\frac{R_oK_m}{V}}{\frac{R_oK_m}{V} + \frac{X}{2K_1}[X+(X^2+C)^{\frac{1}{2}}] - \frac{1}{K_1}[X+(X^2+\epsilon)^{\frac{1}{2}}]^2} \right\} \qquad \text{Eq. (12-10)}$$

In Eq. (12-10), the quantity under the logarithimic sign of the first term is infinity since the quantity in the denominator of that term becomes zero on cancellation of like terms. Therefore, Eq. (12-10) says that for Model II, the steady state is reached at infinity time. Equation for time to reach a certain fraction of the steady state (t'_f) is derived by replacing C in Eq. (III-61) by FC^* from Eq. (12-9). Such a substitution gives:

$$t' = \left[\frac{X+2K_1K_m}{2K_1}\right] \frac{K_m}{(\epsilon + X^2)^{\frac{1}{2}}} \log \left\{\frac{-F\left[X + (X^2+\epsilon)^{\frac{1}{2}}\right]\left[X + (X^2+\epsilon)^{\frac{1}{2}}\right] + \epsilon}{-F\left[X + (X^2+\epsilon)^{\frac{1}{2}}\right]\left[X - (X^2+\epsilon)^{\frac{1}{2}}\right] + \epsilon}\right\}$$

$$+ \frac{1}{2K_1} \log \frac{\frac{R_o K_m}{V}}{\frac{R_o K_m}{V}} + \frac{XF}{2K_1}\left[X+(X^2+\epsilon)^{\frac{1}{2}}\right] - \frac{F^2\left[X+(X^2+\epsilon)^{\frac{1}{2}}\right]^2}{4K_1} \qquad \text{Eq. (12-11)}$$

which can be simplified to:

$$t'_f = \left[\frac{X+2K_1K_m}{2K_1}\right] \frac{K_m}{(\epsilon+X^2)^{\frac{1}{2}}} \log \left\{\frac{-F\left[X+(X^2+\epsilon)^{\frac{1}{2}}\right]^2 + \epsilon}{\epsilon(F+1)}\right\}$$

$$+ \frac{1}{2K_1} \log \left\{\frac{\frac{R_o K_m}{V}}{\frac{R_o K_m}{V} + \frac{F}{2K_1}\left[X+(X^2+\epsilon)^{\frac{1}{2}}\right]}\right\} \Big/ \left\{X - \frac{F}{2}\left(X+(X^2+\epsilon)^{\frac{1}{2}}\right)\right\}$$

Eq. (III-69)

```
FORTRAN.
LGO.
-
      PROGRAM MAIN (INPUT,OUTPUT,TAPE5=INPUT,TAPE6=OUTPUT)
      DIMENSION DX(8),X(8),F(56)
C     FIXED DOSE - FIXED TIME SCHEDULE
      N = 1
      DT = 1.0
      T=0.
C     DOSE = 500.0 MG.
      X(1) = 76.92
   10 L=3
      M=0
   50 CALL RUNGE(T,DT,N,X,DX,F,L,M,J)
      IF(M-1) 75,10,75
   75 GO TO (100,200,999),L
  100 DX(1)=-(0.0156*X(1)+10.46*X(1)/(52.31+X(1)))
      GO TO 50
  200 WRITE(6,800)T,X(1)
  800 FORMAT(5X,2F13.4)
  250 IF(T-99.)260,999,999
  260 GO TO 50
  999 STOP
      END
      SUBROUTINE RUNGE(T,DT,N,Y,DY,F,L,M,J)
      DIMENSION DY(8),Y(8),F(56)
        GO TO (100,110,999) ,L
100     GO TO (101,110) ,IG
101     J = 1
        L = 2
        DO 106 K = 1,N
        K1 = K + 3 * N
        K2 = K1 + N
        K3 = N+K
        F(K1) = Y(K)
        F(K3) = F(K1)
106     F(K2) = DY(K)
        GO TO 406
110     DO 140 K = 1,N
        K1 = K
        K2 = K + 5 * N
        K3 = K2 + N
        K4 = K + N
        GO TO (111,112,113,114),J
111     F(K1) = DY(K) * DT
        Y(K) = F(K4) + .5 * F(K1)
        GO TO 140
112     F(K2) = DY(K) * DT
        GO TO 124
113     F(K3) = DY(K) * DT
        GO TO 134
114     Y(K) = F(K4) + (F(K1) + 2. * (F(K2) + F(K3))+ DY(K) * DT) / 6.
        GO TO 140
124     Y(K) = .5 * F(K2)
        Y(K) = Y(K) + F(K4)
        GO TO 140
```

```
134      Y(K) = F(K4) + F(K3)
140      CONTINUE
       IF(T.EQ.0.0) GO TO 151
C      DOSING INTERVAL IS 8 HOURS
       IF (AMOD(T,8.0).EQ.0.0) Y(K) = Y(K) + 76.92
  151  GO TO (170,180,170,180),J
170    T = T + .5 * DT
180    J = J + 1
       IF(J -4) 404,404,299
299    M = 1
       GO TO 406
300    IG = 1
       GO TO 405
404    IG = 2
405    L = 1
406    RETURN
       END
```

APPENDIX 14

```
FORTRAN.
LGO.
-
      PROGRAM MAIN (INPUT,OUTPUT,TAPE5=INPUT,TAPE6=OUTPUT)
      DIMENSION DX(8),X(8),F(56)
C     PRIMING DOSE - MAINTENANCE DOSE SCHEDULE
      N = 1
      DT = 1.0
      T=0.
C     PRIMING DOSE =  500.0 MG.
      X(1) = 76.92
   10 L=3
      M=0
   50 CALL RUNGE(T,DT,N,X,DX,F,L,M,J)
      IF(M-1) 75,10,75
   75 GO TO (100,200,999),L
  100 DX(1)=-(0.0155*X(1)+10.46*X(1)/(52.31+X(1)))
      GO TO 50
  200 WRITE(6,800)T,X(1)
  800 FORMAT(5X,2E13.4)
  250 IF(T-99.)260,999,999
  260 GO TO 50
  999 STOP
      END
      SUBROUTINE RUNGE(T,DT,N,Y,DY,F,L,M,J)
      DIMENSION DY(8),Y(8),F(56)
        GO TO (100,110,200) ,L
100     GO TO (101,110) ,IG
101     J = 1
        L = 2
        DO 106 K = 1,N
        K1 = K + 3 * N
        K2 = K1 + N
        K3 = N+K
        F(K1) = Y(K)
        F(K3) = F(K1)
106     F(K2) = DY(K)
        GO TO 406
110     DO 140 K = 1,N
        K1 = K
        K2 = K + 5 * N
        K3 = K2 + N
        K4 = K + N
        GO TO (111,112,113,114),J
111     F(K1) = DY(K) * DT
        Y(K) = F(K4) + .5 * F(K1)
        GO TO 140
112     F(K2) = DY(K) * DT
        GO TO 124
113     F(K3) = DY(K) * DT
        GO TO 134
114     Y(K) = F(K4) + (F(K1) + 2. * (F(K2) + F(K3))+ DY(K) * DT) / 6.
        GO TO 140
124     Y(K) = .5 * F(K2)
        Y(K) = Y(K) + F(K4)
        GO TO 140
```

```
134      Y(K) = F(K4) + F(K3)
140      CONTINUE
       IF(T.EQ.0.0) GO TO 151
C      DOSING INTERVAL IS 8 HOURS
C      MAINTENANCE DOSE =  305.8  MG.
       IF (AMOD(T,8.0).EQ.0.0) Y(K) = Y(K) + 47.048
  151  GO TO (170,180,170,180),J
170    T = T + .5 * DT
180    J = J + 1
       IF(J -4) 404,404,299
299    M = 1
       GO TO 406
300    IG = 1
       GO TO 405
404    IG = 2
405    L = 1
406    RETURN
       END
-
```